AFIT/GAE/ENY/92D-07

BEHAVIOR OF A TITANIUM MATRIX COMPOSITE UNDER QUASI-STATIC TENSILE AND COMPRESSIVE LOADING

THESIS

Keith L. Bearden, Captain, USAF

AFIT/GAE/ENY/92D-07

Approved for public release: distribution unlimited

AFIT/GAE/ENY/92D-07

BEHAVIOR OF A TITANIUM MATRIX COMPOSITE UNDER QUASI-STATIC TENSILE AND COMPRESSIVE LOADING

THESIS

Presented to the Faculty of the School of Engineering

of the Air Force Institute of Technology

Air University

In Partial Fulfillment of the

Requirements for the Degree of

Master of Science in Aeronautical Engineering

Keith L. Bearden, B.S.

Captain, USAF

December 1992

Preface

The purpose of this study was to determine the damage mechanisms in a titanium matrix composite, SCS-9/β 21S, when subjected to both tension and compression. There has been a great deal of effort devoted to the tension case on this type of material, by no published data has been accumulated in compression.

Extensive testing of unidirectional laminates was conducted in both tension and compression to determine stress/strain response upon loading and unloading. Test specimens were prepared such that damage and plasticity could be determined and associated with the corresponding part of the stress/strain curve, thereby determining the dominant deformation mechanisms present.

I owe a great debt to a lot of people for the completion of this thesis. Probably the greatest debt goes to my wife for putting up with the long hours at AFIT and at home on my computer. Dr. Mall was key in getting me started on the right track and keeping me headed in the right direction. I need to thank LTC Hansen, my sponsor in NIC, for supplying material, names, contacts and most importantly for advice and insight. I would also like to express my appreciation for the technicians in the AFIT Model Shop for quickly sectioning my specimens and for fabricating my IITRI compression fixture.

Table of Contents

List of Figures

List of Tables

List of Symbols

E	Young's Modulus of stiffness
E1	Stiffness of lamina in the fiber direction
E2	Stiffness of lamina transverse to the fibers
Ef	Stiffness of the fibers
Em	Stiffness of the matrix
G	Shear modulus
G12	Shear modulus of a lamina
Ti	Titanium
Vf	Volume fraction for the fiber
Vm	Volume fraction for the matrix
υ	Poisson's Ratio
υf	Poisson's Ration for the fiber
υm	Poisson's Ration for the matrix
$\upsilon 12$	Poisson's Ration of a lamina
ξ	Fiber reinforcement measure in Halpin-Tsai
σ	Stress
ε	Strain

Abstract

Quasi-Static tensile and compressive testing was performed on a unidirectional, zero and ninety degree, titanium matrix composite. The specific material was SCS-9/β 21S. The initial tensile and compressive modulus for both laminates was the same. The ninety degree laminate had a tensile and compressive modulus of 115.89 GPa. The zero degree laminate had a tensile and compressive modulus of 197.51 GPa. The ninety degree laminate exhibited a three stage stress/strain response in tension. The first stage is completely linearly elastic, however, partial debonding of the fiber from the matrix was observed. This partial debond did not effect the stress/strain response. The second stage is due to the complete debond of the fiber from the matrix. The ninety degree laminate in compression had a two stage stress/strain response, and the zero degree laminate had a two stage stress/strain response in tension and compression. Plasticity and damage were the main causes of deformation. Plasticity involved deformation of the matrix between the fibers and Poisson's contraction of the matrix from the fibers. Damage involved fiber matrix debond, matrix cracking and fiber cracking. All of these mechanisms were present, and they were related to the appropriate stress/strain characteristics.

Behavior of a Titanium Matrix Composite under Quasi-Static Tensile and Compressive Loading

I. Introduction

Titanium Matrix Composites (TMC) are of great importance to the aerospace industry because of their low density to strength and their ability to maintain strength at elevated temperatures. This composite is of particular interest to the aerospace industry which will use this material for structural elements and surface skins. There is so much interest that Textron Specialty Materials dedicated the world's first plant for the sole production of titanium matrix composites on May 22, 1992 (Brown, 1992: 66).

The titanium matrix composite used in this investigation is SCS-9/β 21S. SCS-9 is silicon carbide fiber with a nominal diameter of 81 μm. β 21S is a beta phase titanium alloy. There is no previous work available concerning the tensile or the compressive properties of this composite.

The purpose of this report is to investigate systematically and characterize the behavior of SCS-9/β 21S Titanium Matrix Composite under quasi-static tensile and compressive loading. This material is very similar to SCS-6/β 21S. SCS-6/β 21S has been fully characterized in tension but little work has been done on SCS-9/β 21S. The main difference is that the SCS-6 fiber is almost twice as large in diameter as an SCS-9 fiber. The advantage of the SCS-9 fiber, therefore, is that there is little sacrifice in strength between composites made of these fibers but the SCS-9 fiber composite will have about half the thickness. It has been observed by McDonnel Douglas that there is a significant difference between the strengths of this material in tension and compression

(Hansen, 1992). The modulus in tension and compression may differ as well. This discrepancy makes it difficult for designers to make proper decisions. The modulus and strength discrepancies, as reported, can contribute to the premature failure of test sections. The problem the designer faces is which modulus to input into the finite element code chosen to analyze the actual part. If the wrong value is chosen, the finite element model will not accurately simulate the part. This thesis work will focus on the unidirectional composite, both the zero degree and the ninety degree. Testing of this material will yield in tension and compression Young's Modulus parallel to the fiber direction, E_1, and perpindicular to the fiber, E_2, and Poisson's Ratio with respect to the 1-2 plane, υ_{12} and with respect to the 2-1 plane, υ_{21}. Through the use of metallography, acetate edge replicas, optical and scanning electron microscopes, the damage progression and modes will be investigated systematically. This information can then be used by the designer. This type of work has not been accomplished to date. There is some tensile data for SCS-9/β 21S, but there is no compression data. No one has yet attempted to characterize the deformation mechanisms in either tension or compression for this material, and relate this microscopic information with the macroscopic response of this composite material.

II. Discussion and Summary of Previous Work

2.1 Predictions of Material Properties

These calculations involve the prediction of composite properties based upon the properties of the fiber and the matrix individually. Specifically, E_1, E_2, G_{12} and υ_{12}. Both E_1 and υ_{12} use the rule of mixtures for their calculation (Jones, 1975: 91).

$$E_1 = E_f V_f + E_m V_m \qquad (1)$$

Where:

E_f = Young's Modulus of the fiber

V_f = Volume fraction of fibers

E_m = Young's Modulus of the matrix

V_m = Volume fraction of matrix

Poisson's Ratio, υ_{12} is calculated the same way replacing E with υ. It has been shown that the rule of mixtures does not yield good results for E_2 or G_{12} (Agarwal, 1990: 76). The Halpin-Tsai equation will be used for the determination of these two quantities. The Halpin-Tsai equation is an empirical relationship used to determine the off-axis properties.

$$\frac{M}{M_m} = \frac{1 + \xi \eta V_f}{1 - \eta V_f} \qquad (2)$$

where:

$$\eta = \frac{(M_f/M_m) - 1}{(M_f/M_m) + \xi} \qquad (3)$$

where:

M = Composite modulus E_2, G_{12}

M_f = Fiber modulus E_f, G_f

M_m = Matrix modulus E_m, G_m

For the determination of E_2, $\xi = 2$ and for the determination of G_{12}, $\xi = 1$. (Jones, 1975: 114-115)

The area method was used to determine the fiber and matrix volume fraction. A photograph was taken of the cross section of several 90 degree specimens and the number of fibers in a given total area was used to determine the fiber volume fraction. The fiber volume fraction results were between 38 and 42 percent. For all calculations, the average value of 40 percent was used for the fiber volume fraction. Fiber properties are provided directly by McDonnel Douglas (Hansen, 1992). Matrix properties are taken from an Ad Tech Systems Research, Inc. briefing presented at a NIC meeting on January 28-29, 1992 (Ahmad, 1992: 7). The following results were obtained:

$$E_1 = 196.62 GPa$$
$$E_2 = 173.24 GPA$$
$$\nu_{12} = .2656$$
$$G_{12} = 65.14 GPa$$

All calculations are shown in Appendix A.

For the compression tests, a buckling analysis of the material had to be performed. For simplicity, the Euler buckling equation was used. The constraint condition for the IITRI fixture is fixed/fixed. Therefore, the equation used to determine the length of the test section to avoid buckling is:

$$L=\left[\frac{4\pi^2 E_1 I}{P_{crit}}\right]^{1/2} \qquad (5)$$

P_{crit} is calculated using the rule of mixtures and the maximum stress for the fiber and the matrix. A fiber bundle strength of .82 was also used . The result of this calculation is:

$$L = .061 \text{ m}$$

This calculation is also shown in Appendix A. For the ninety compression tests a gage length of .0254 m was used and for the zero compression tests a gage length of .0127 m was used

2.2 Current Research

2.2.1 Tensile Experiments. Currently there is a great deal of work being performed on TMC's in tension. Newaz and Majumdar at the Batelle Memorial Institute concentrate on SCS-6/Ti 15-3 (Newaz, 1991: 1). This material is very similar to SCS-9/β 21S. Table 1 shows the comparison of fiber and matrix properties.

TABLE 1

FIBER MATRIX COMPARISON

MATERIAL	YOUNG'S MODULUS GPa	FIBER DIAMETER m
SCS-6	399.91	$142.24*10^{-6}$
SCS-9	324.07	$81.28*10^{-6}$
Ti 15-3	92.4	
β 21S	111.7	

The work done by Majumdar and Newaz showed the damage progression and plasticity that occurred in a $[0]_8$ and a $[90]_8$. For the $[0]_8$, they showed that the main deformation mode is plasticity of the matrix; they also concluded that the contribution of damage to the overall deformation response was low (Newaz, 1991: 16). The zero degree specimen had a two stage stress/strain response, that is, it displayed one linear response followed by one non-linear response prior to failure. The ninety degree specimen, however, exhibited a three-stage stress/strain response. Figure 1 depicts this type of response. Where Stage I and Stage II are basically linear and Stage III is non-linear.

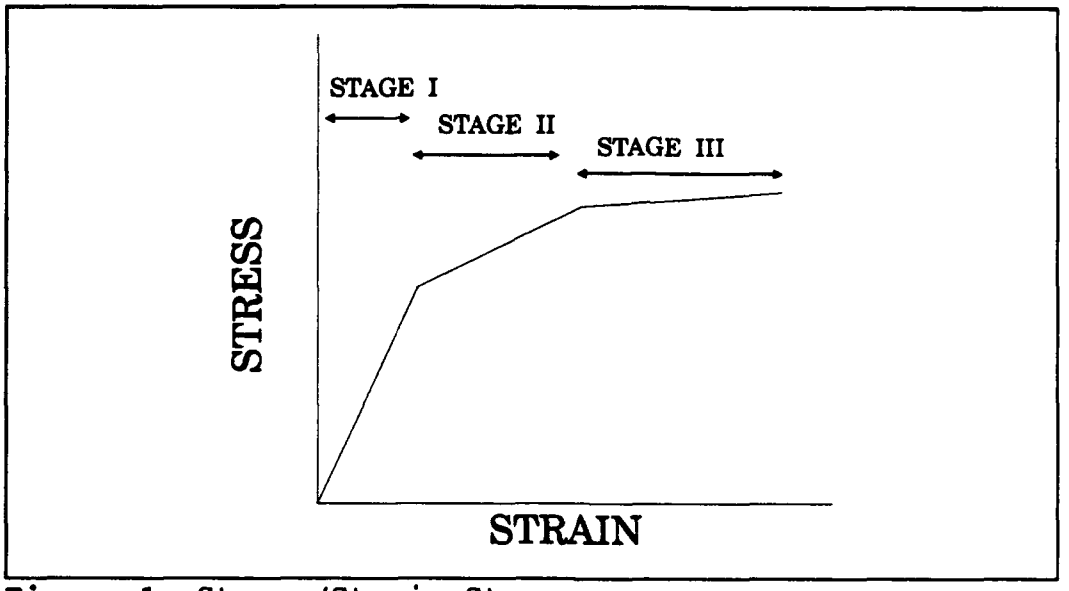

Figure 1 Stress/Strain Stages

Stage I behaves like a linearly-elastic solid. The strain is fully recoverable upon unloading. Stage II is dominated by damage with some plasticity. Stage III is controlled by plasticity and damage, but plasticity plays the major role (Newaz, 1991: 10).

The responses detailed by Newaz and Majumdar are in agreement with the results obtained by Kenaga, et al, at Purdue University using a Boron/Aluminum composite. Their zero degree specimen exhibited no plasticity before failure, but the ninety degree specimen did exhibit plasticity with damage (Kenaga, 1986: 520).

Newaz and Majumdar used instantaneous Poisson's Ratio to distinguish between damage and plasticity. Poisson's Ratio increased from about .3 to .5 during a plastic state of deformation, but Poisson's Ratio decreased when damage was occurring (Majumdar, 1991: 4). Figure 2 shows how Poisson's Ratio may be used to distinguish between

damage and plasticity.

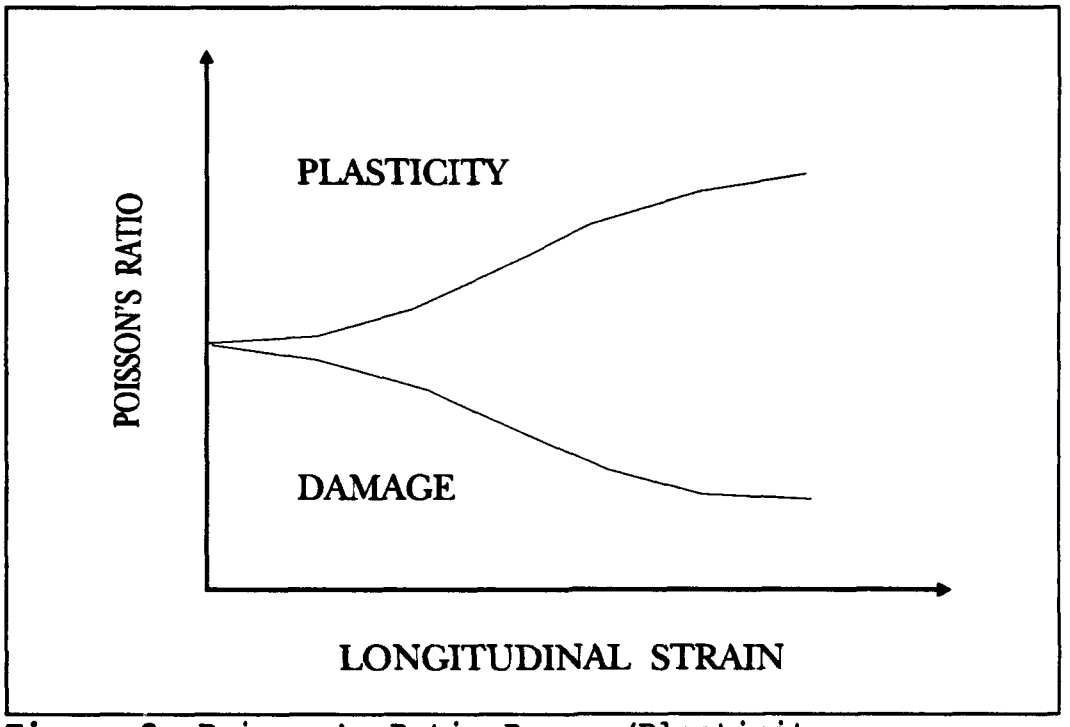

Figure 2 Poisson's Ratio Damage/Plasticity

Damage and plasticity can also be distinguished from observations on the specimen. Damage can be seen as cracks and debonds, while plasticity can be observed as slip bands and permanent deforamtion of the matrix (Newaz, 1991: 5).

The determination of whether plasticity or damage was dominant can also be observed by loading a specimen into each stage and unloading. Plasticity will be seen as a residual strain in the specimen after unloading, damage can be seen as "yielding" of the material without residual strain after unloading, and a combination of plasticity and

damage. Figure 3 depicts the three possibilities (Neweaz, 1991: 8).

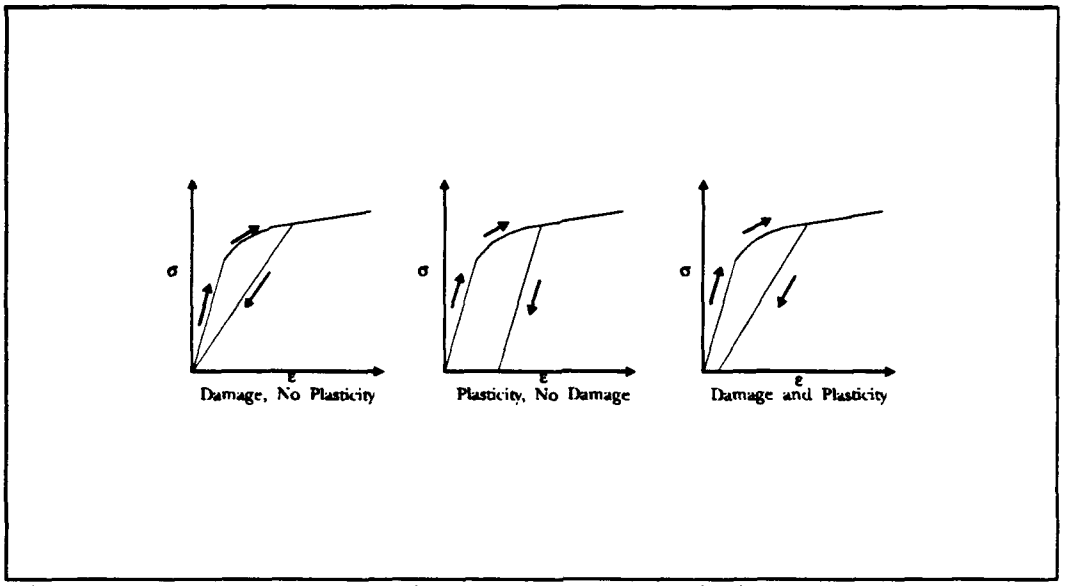

Figure 3 Stress/Strain Damage/Plasticity

The theories and work performed by Newaz and Majumdar will be the basis for the tensile work performed in this report.

2.2.2 Compression Experiments. To date there has been no published work concerning compression testing of Titanium Matrix Composites. The experimental procedure used for this report is based upon the Consortium Testing Specification which calls for compression testing using an IITRI compression fixture (CTS 2.3). Since there has been no published data in this area, the same assumptions made for tension will be made for compression. McDonnell Douglas provides certain compression results (Hansen, 1992). These results show only an initial modulus. Therefore, in compression the zero degree and the ninety degree laminates have a stress/strain response similar to

an isotropic material. There is a linear-elastic section, followed by a nonlinear plastic response. There is one other significant difference between the compression and the tensile stress/strain curves. For the zero degree laminate, the initial modulus differs by 18 percent (compression is stiffer than tension) and the ultimate strength in compression is more than twice that of tension. For the ninety degree laminate, however, the initial modulus only differs by 5 percent, but the ultimate strength in compression is still twice that of tension (Hansen, 1992). In an unpublished report by Newaz and Majumdar, they present the same conclusions for a ninety degree laminate only (Newaz, 1992: 3).

2.2.3 Damage and Deformation Expectations.

2.2.3.1 Damage. There are two main types of damage expected during this investigation: 1) Fiber/Matrix debonding and 2) Broken fibers. Figures 4 and 5 illustrate an untested $[90]_{16}$ and an untested $[0]_{16}$ laminate. It is clear from these figures that there is no fiber/matrix debond. During loading of the ninety degree composite in tension or compression the fiber and matrix will debond differently. During tension, the matrix will debond above and below the fiber. During compression, the matrix will debond on the sides of the fiber. This is illustrated in Figure 6.

2.2.3.2 Deformation. For the ninety degree laminate, there are two ways to observe permanent deformation. One is if the debond shown in Figure 6 does not close up. This will show permanent plastic deformation of the matrix around the fiber. Another way to observe permanent deformation in the ninety degree laminate is by showing Poisson's effect of matrix contraction. This is seen by the fibers protruding from the matrix after the specimen has been unloaded. It is clear from Figure 4 that the fibers

do not protrude from the matrix prior to loading. There is no real way to observe deformation in the zero degree laminate, except through the residual strain after unloading.

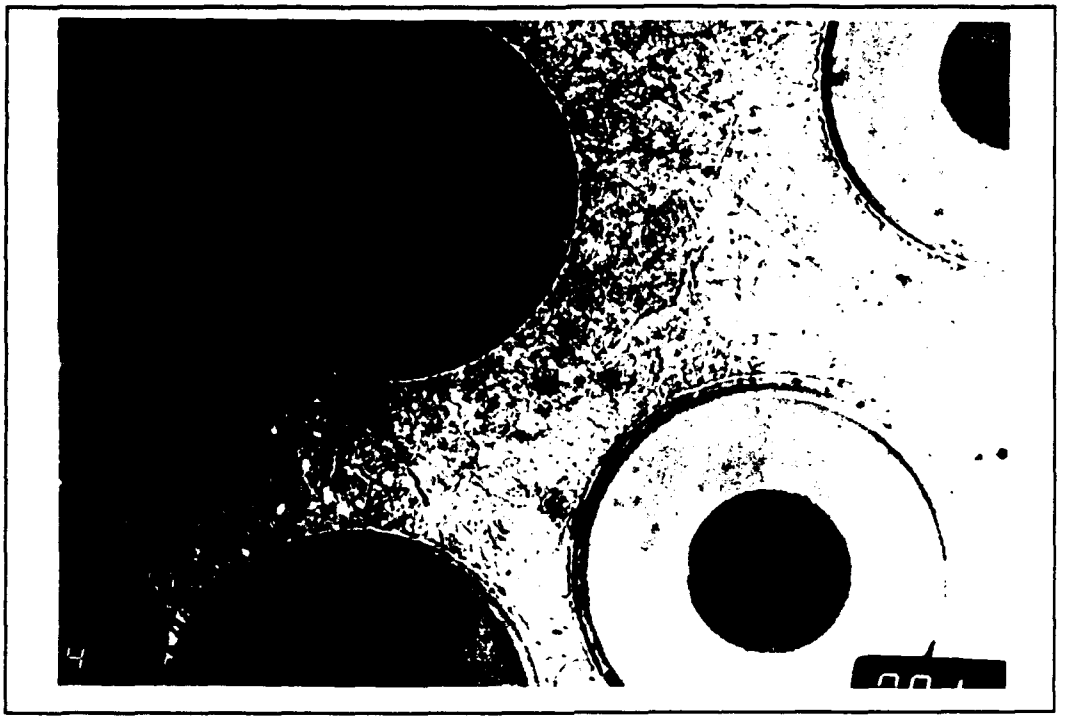

Figure 4 Untested [90]

Figure 5 Untested [0]

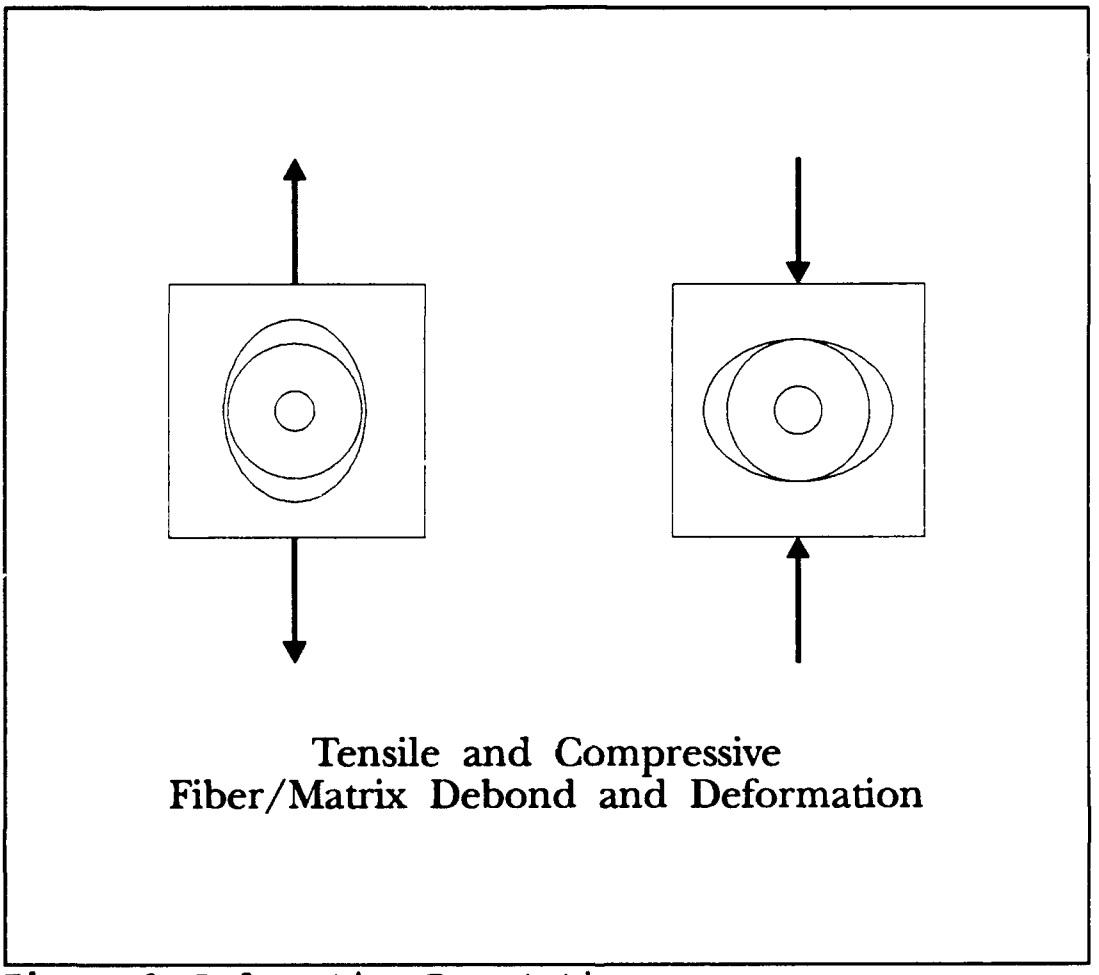

Figure 6 Deformation Expectations

III. Experimental Setup

3.1 Specimen Preparation.

All test coupons were cut from a .305 x .61 m panel of SCS-9/β21S Titanium Metal Matrix Composite, panel number B9105967. The panel was fabricated and C-Scanned by McDonnell Douglas Corporation and delivered to the Materials Behavior Branch of Wright Laboratories. The C-Scan confirmed that the panel was correctly fabricated. The panel was then cut using a diamond wafering saw by the technicians at the AFIT Model Shop according to Figure 7. The nominal dimensions of each specimen are 1.27 W x .178 T x 15.24 L cm.

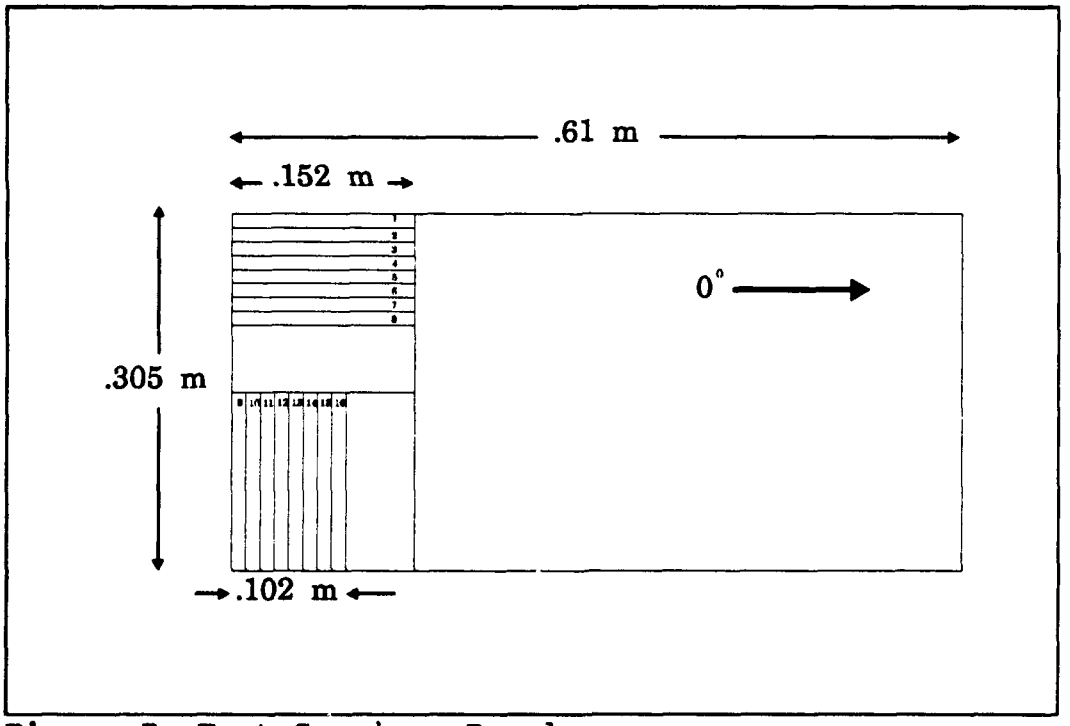

Figure 7 Test Specimen Panel

The specimens were heat treated at 427 °C under a vacuum for 24 hours and then polished to facilitate acetate edge replication. Polishing was performed at the Metallography Lab of the Wright Materials Lab using the Buehler Metlap Polisher. A specimen polishing fixture was used to polish three specimens at once. The following polishing technique was used: 1) With the Metlap #8 platen, specimens were polished using 45, 15 and 6 micron diamond suspension fluid. Each grade of diamond suspension was used until scratches visible under a microscope all appeared to be uniform and in the same direction. 2) The specimens were polished with the 45 micron perf pad and 45 micron diamond suspension until all scratches again appeared to be uniform. 3) The specimens were polished with the 15 micron perf pad and the 15 micron diamond suspension until all scratches are uniform. 4) Repeat the process with the 6 micron perf pad. 5) A nylon pad on an aluminum platen and the 1 micron diamond suspension were used to polish the specimens until all scratches are eliminated. It requires approximately three and half hours to polish three specimens to 1 micron.

One of the goals of this experiment was to witness the development and growth of plasticity in the matrix. According to Majumdar, the best method for showing the development and progression of slip bands and plasticity in this type of material is by first polishing the specimen to 1 micron, then etching with a Kroll's Etch for 15 seconds, and then testing the specimen, taking acetate replicas at the desired increments (Majumdar,1992). The edge of the specimen was etched with Kroll's Etch applied with a cotton swab. It was necessary to insure that sodium bicarbonate was readily available to prevent over etching the specimen.

The final dimensions of the specimens are contained in Table 2.

TABLE 2

TEST SPECIMENS

Specimen ID #	Layup	Length (m)	Width (m)	Thickness (m)
B910596-1	$[0]_{16}$	$152.4*10^{-3}$	$12.76*10^{-3}$	$1.792*10^{-3}$
B910596-2	$[0]_{16}$	$152.4*10^{-3}$	$12.57*10^{-3}$	$1.758*10^{-3}$
B910596-3	$[0]_{16}$	$152.4*10^{-3}$	$12.58*10^{-3}$	$1.763*10^{-3}$
B910596-4	$[0]_{16}$	$152.4*10^{-3}$	$12.40*10^{-3}$	$1.757*10^{-3}$
B910596-5	$[0]_{16}$	$152.4*10^{-3}$	$12.67*10^{-3}$	$1.753*10^{-3}$
B910596-6	$[0]_{16}$	$152.4*10^{-3}$	$12.67*10^{-3}$	$1.753*10^{-3}$
B910596-7	$[0]_{16}$	$152.4*10^{-3}$	$12.67*10^{-3}$	$1.753*10^{-3}$
B910596-8	$[0]_{16}$	$152.4*10^{-3}$	$12.67*10^{-3}$	$1.753*10^{-3}$
B910596-9	$[90]_{16}$	$152.4*10^{-3}$	$12.68*10^{-3}$	$1.753*10^{-3}$
B910596-10	$[90]_{16}$	$152.4*10^{-3}$	$12.65*10^{-3}$	$1.750*10^{-3}$
B910596-11	$[90]_{16}$	$152.4*10^{-3}$	$12.62*10^{-3}$	$1.756*10^{-3}$
B910596-12	$[90]_{16}$	$152.4*10^{-3}$	$12.63*10^{-3}$	$1.765*10^{-3}$
B910596-13	$[90]_{16}$	$152.4*10^{-3}$	$12.72*10^{-3}$	$1.755*10^{-3}$
B910596-14	$[90]_{16}$	$152.4*10^{-3}$	$12.67*10^{-3}$	$1.757*10^{-3}$
B910596-15	$[90]_{16}$	$152.4*10^{-3}$	$12.65*10^{-3}$	$1.757*10^{-3}$
B910596-16	$[90]_{16}$	$152.4*10^{-3}$	$12.63*10^{-3}$	$1.762*10^{-3}$

These are the dimensions and layups of the as tested specimens.

The test specimens used for tensile and compressive tests had fiberglass tabs mounted to them. The fiberglass material consisted of continuous glass fibers in a

phenolic sheet. The fiberglass was cut into 3.81 x 1.27 cm samples for the tension tests and 6.99 x 1.27 cm for the compression tests and the ends were tapered with a file to make the tabs. These tabs were mounted to the test specimens with an epoxy/resin and baked at 68.33 °C for one hour to speed up the curing of the epoxy.

Strain gages were used on the specimens tested to failure to measure Poisson's Ratio for both the tensile and compressive tests. Strain gages were used on all of the compressive tests to prevent crushing of the extensometer after failure of the specimen.

3.2 Test Equipment

All experiments were performed on an MTS 810 110 Kip Material Test System. The test machine was controlled by an MTS 458.20 Miroconsole, with three controllers and a microprofiler. For those experiments requiring a strain gage, a Measurements Group 2310 Signal Conditioning Amplifier was used and Micro-Measurements 350 ohm strain gages were used. An MTS 1.27 cm Extensometer was also used to measure strain for the tension tests. A Zenith 286 Personal Computer with a math coprocessor was used to receive and process all data from the MTS 810 and store the strain and load data into a file. Figure 8 shows the equipment used to perform the experiments.

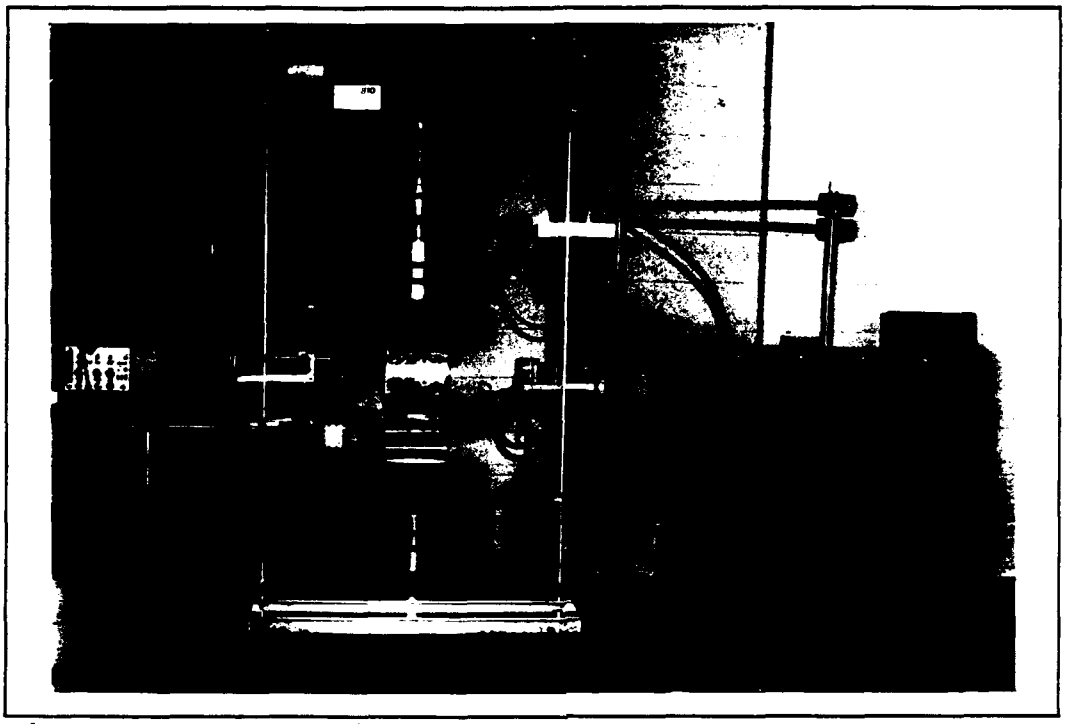

Figure 8 Test Equipment

3.3 Experimental Procedure

3.3.1 Tensile Test Procedure. The first step in the experiment was to program the microprofiler on the MTS 458.20 Microconsole to load the specimen. All tensile tests were run under load control. Programming the microconsole involved breaking the loading desired into segments, based on the percentage of the load card and the rate to load the specimen. All tensile experiments were loaded at 44.48 N/s. The specimen was then loaded into the test machine, the computer was programmed to store the data into a particular file, and the test was begun. Once the test was completed, the resulting data

was imported into a spread sheet for data reduction and analysis. See Figure 5 for a photograph of the tensile test setup.

At certain loads of interest, edge replicas would be taken of the specimen to look for debonds, cracks, and plasticity. Taking an effective edge replica was a very "touchy" procedure. There will be some detail here for the future use of students. The specimens have all ready been polished to 1 micron and etched with Kroll's Etch according to *Specimen Preparation*. At the desired load, the MTS 810 is 'put on hold'. It will hold the specimen at the set load until the *Resume* button is depressed. The acetate has been cut before hand into 1.27 x 2.54 cm pieces and tape attached to the top. Secure the acetate to the side of the specimen with the tape, centering the acetate on the middle of the specimen. Thoroughly soak a cotton swab in acetone. Lift up the un-taped portion of the acetate, and in a single motion coat the specimen with acetone and press the acetate onto the specimen. Then using either the stick on the cotton swab or a steel rod, roll the acetate against the specimen. Roll the acetate only once, this prevents the formation of ghost images on the acetate. Wait approximately 45 seconds and then remove the acetate. This will produce a good replica better than 50 percent of the time.

3.3.1.1 Verification of Test Machine. To verify that the extensometer and strain gages all reported the same data, a dummy specimen was prepared using a strain gage on both sides. The purpose of putting a strain gage on both sides was to insure that the MTS 810 did not induce bending during the loading of a specimen. The results of this test showed the strain gages to be in complete agreement with the extensometer indicating that no bending had occurred.

3.3.2 Compression Test Procedure. The compression test procedure is very similar to the tensile procedure. The only major difference involves the use of the IITRI (Illinois Institute of Technology Research Institute) Compression Fixture. This fixture was designed in accordance with ASTM D 3410-87 (ASTM, 1987: 5) as called out by the Consortium Testing Specification 2.3. The fixture used for these experiments appears in Figure 6. The fixture was fabricated by the AFIT Model Shop according to the drawings provided. The main blocks are made of titanium, the alignment pins of stainless steel and the grips and wedges of D2 tool steel. The grips and wedges are replaceable to facilitate separate applications and different dimensions of test specimens. All compression experiments were loaded at 55.6 N/s.

Edge replicas were not taken on compression tests due to the setup of the IITRI fixture. The zero degree specimens are predicted to fail at above 62 KN, with a gage length of a little over 1.27 cm. This is too great a load in too small an area to perform hands-on-work. For this reason, deformation data will be determined from different specimens loaded into the specific regions of the stress/strain curve. The actual specimen will be examined under optical and/or scanning electron microscope. The only event this method may miss is the debond that closes up in a ninety degree specimen that is loaded into either Stage I or into Stage II (Newaz, 1991: 19). There is no guarantee that what happened in tension will also happen in compression.

3.3.2.1 Verification of IITRI Fixture. Since this test fixture was designed purely from the ASTM standard, it was deemed necessary to validate the results it would provide. Two steel coupons, the same size as test specimens, were cut from a single

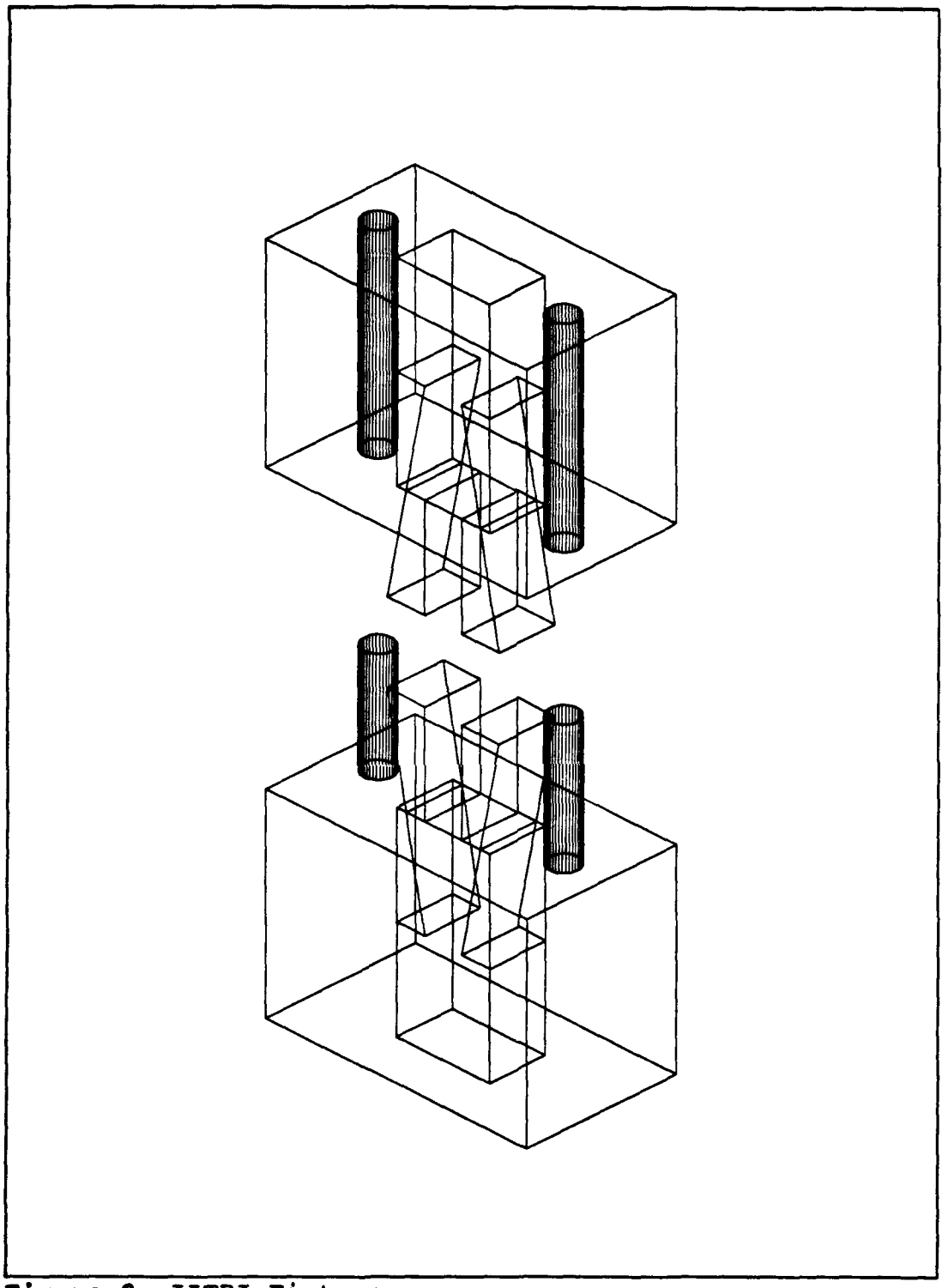

Figure 9 IITRI Fixture

blank. Mild steel was used. Strain gages were attached to each specimen according to *Specimen Preparation*. One steel specimen was tested in tension to 2.22 KN and the data recorded. The other steel specimen was placed in the IITRI fixture and tested to -2.22 KN and the data recorded. The modulus was extracted from both curves and compared. For the linear section the moduli differed by less than 3 percent. This falls well within the acceptable criteria according to ASTM standard of 10 percent (ASTM, 1987: 5).

IV. Results

4.1 Tensile Experiments. The stress/strain results of all tensile experiments are contained in this section. Table 3 condenses the results of all tensile experiments.

TABLE 3

RESULTS OF TENSILE EXPERIMENTS

Spec ID Number	Layup	Test Type	Load Rate (N/s)	Initial Modulus (GPa)	Unload Modulus (GPa)
9	$[90]_{16}$	FAILURE	44.48	116.87	N/A
10	$[90]_{16}$	STAGE I	44.48	117.56	117.56
12	$[90]_{16}$	STAGE II	44.48	121.28	74.46
13	$[90]_{16}$	STAGE III	44.48	119.56	61.72
4	$[0]_{16}$	FAILURE	44.48	193.3	N/A
1	$[0]_{16}$	STAGE I	44.48	202.64	202.64
2	$[0]_{16}$	STAGE II	44.48	204.84	202.53

4.1.1 $[90]_{16}$ Tensile Experiments. The ninety degree laminate exhibited the three stage stress/strain response as proposed by Newaz and Majumdar (Newaz, 1991: 16). Four tensile experiments were performed on the ninety degree laminate. One of these

specimens (number 9) was loaded to failure, during which longitudinal and lateral strain data were collected. The stress/strain curve is illustrated in Figure 10. This curve clearly depicts the three stages of the ninety degree laminate. The initial modulus, Stage I, for this specimen (number 9) is 116.87 GPa. The modulus in Stage II is 95 GPa, and the modulus in Stage III is approximately zero. Using the data from this curve, three variations of the original test were chosen to show the effect of decreasing the load on a specimen which was loaded into each stage to understand and document the damage growth mechanisms. The second specimen (number 10) was loaded into Stage I and then unloaded. The third specimen (number 12) was loaded into Stage II and unloaded, and the fourth specimen (number 13) was loaded into Stage III and unloaded. The average initial modulus for all of the four experiments is 118.80 GPa and the standard deviation was only 2 GPa. These results agree with those obtained by the McDonnell Douglas Corp. McDonnell Douglas reports the average initial modulus for the ninety degree laminate in tension to be 117.10 GPa with a standard deviation of 4.4 GPa (Hansen, 1992). The repeatability of these test is extremely high. The stress/strain curves for specimens 10, 12 and 13 are illustrated in Figures 11 - 13. The plot of longitudinal versus transverse strain is presented in Figure 14. The plot of instantaneous Poisson's ratio verses longitudinal strain for this specimen is presented in Figure 15.

4.1.2 $[0]_{16}$ Tensile Experiments. The zero degree laminate exhibited only a two stage stress/strain curve as shown in Figure 16. The first experiment loaded a specimen (number 4) to failure. Both longitudinal and lateral strain data was gathered throughout the experiment. The initial modulus for this specimen was 193.3 GPa. The two stage

stress/strain response is in agreement with the work performed by Newaz and Majumdar (Newaz, 1991: 16). Since the zero degree laminate exhibited only a two stage stress/strain response, only two other experiments were necessary to understand its complete behavior. The second specimen (number 1) was loaded into Stage I and unloaded and the third specimen (number 2) was loaded into Stage II and unloaded. However, an additional test was conducted to insure that the failure data collected from specimen number 4 was valid since this specimen failed in the grips. The fourth specimen (number 3) was loaded in tension to failure. The fourth specimen (number 3) failed at approximately the same load as the first specimen (number 4). Therefore, the failure data from the first specimen (number 4) is valid. The average initial modulus for all four experiments was 204.19 GPa with a standard deviation of 9.31 GPa. Again, this data is in direct agreement with the data obtained by the McDonnell Douglas Corp. McDonnell Douglas reports an average initial modulus of 202.60 GPa with a standard deviation of 6.71 GPa (Hansen, 1992). The stress/strain curves for specimen numbers 1, 2 and 4 are in Figures 16 - 18, the plot of longitudinal versus transverse strain is in Figure 19 and the plot of instantaneous Poisson's Ratio verses longitudinal strain for specimen number 4 is in Figure 20.

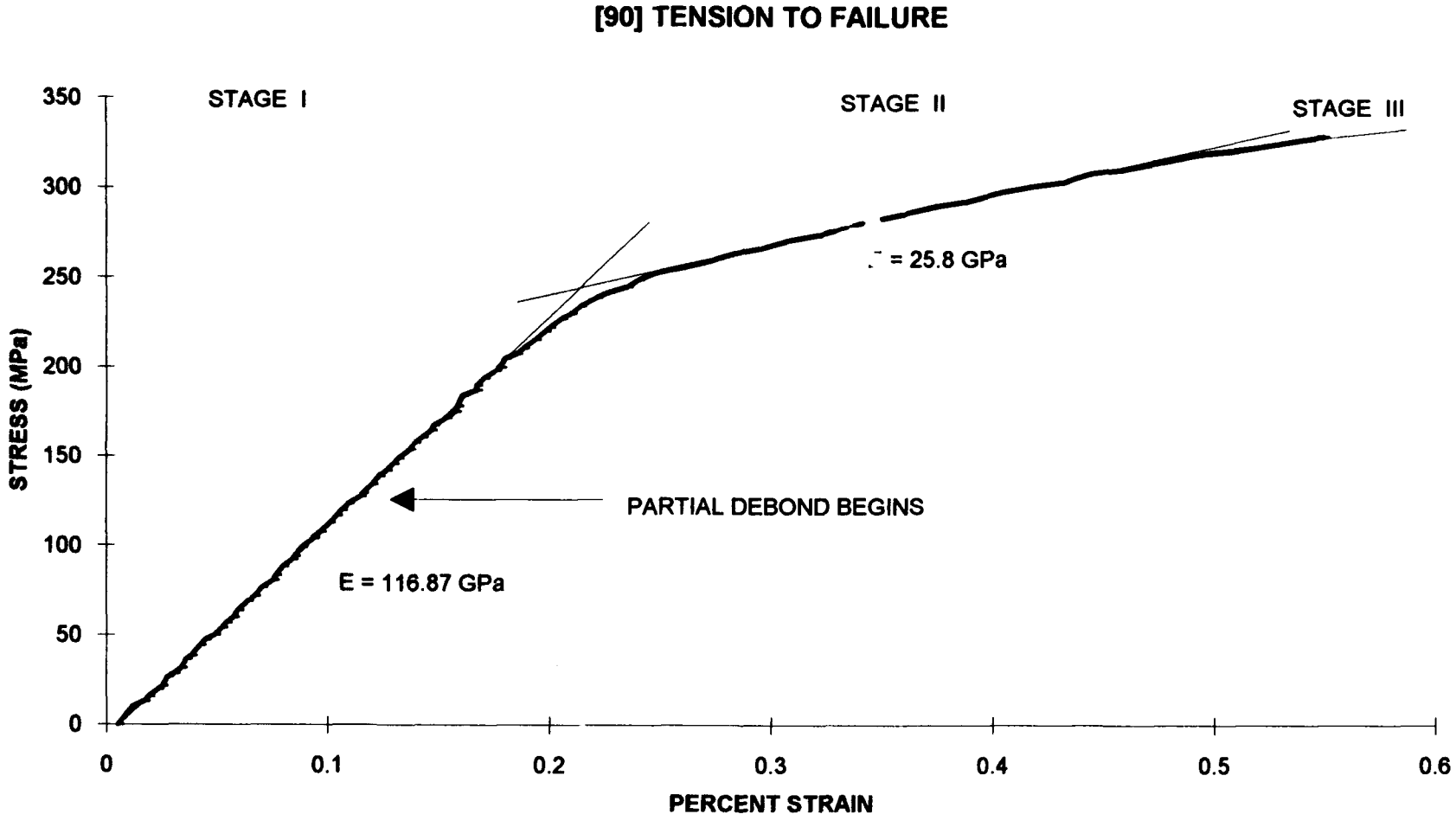
[90] TENSION TO FAILURE
STAGE I
STAGE II
STAGE III
350
300
250
200
150
100
50
0
STRESS (MPa)
= 25.8 GPa
PARTIAL DEBOND BEGINS
E = 116.87 GPa
0
0.1
0.2
0.3
0.4
0.5
0.6
PERCENT STRAIN

Figure 10

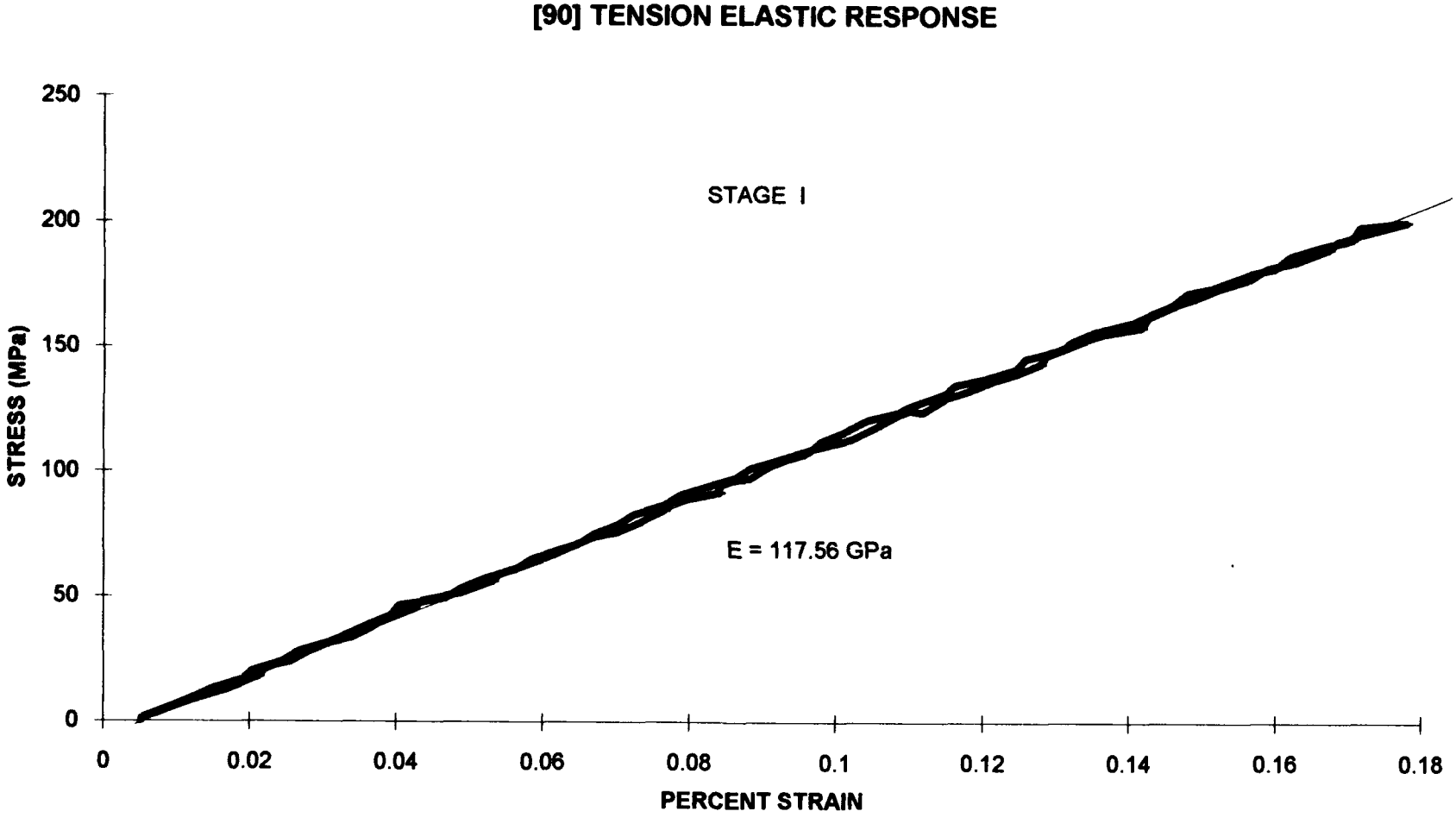
[90] TENSION ELASTIC RESPONSE
STAGE I
E = 117.56 GPa
STRESS (MPa)
PERCENT STRAIN
250
200
150
100
50
0
0
0.02
0.04
0.06
0.08
0.1
0.12
0.14
0.16
0.18

Figure 11

[90] TENSION FIRST PLASTIC RESPONSE

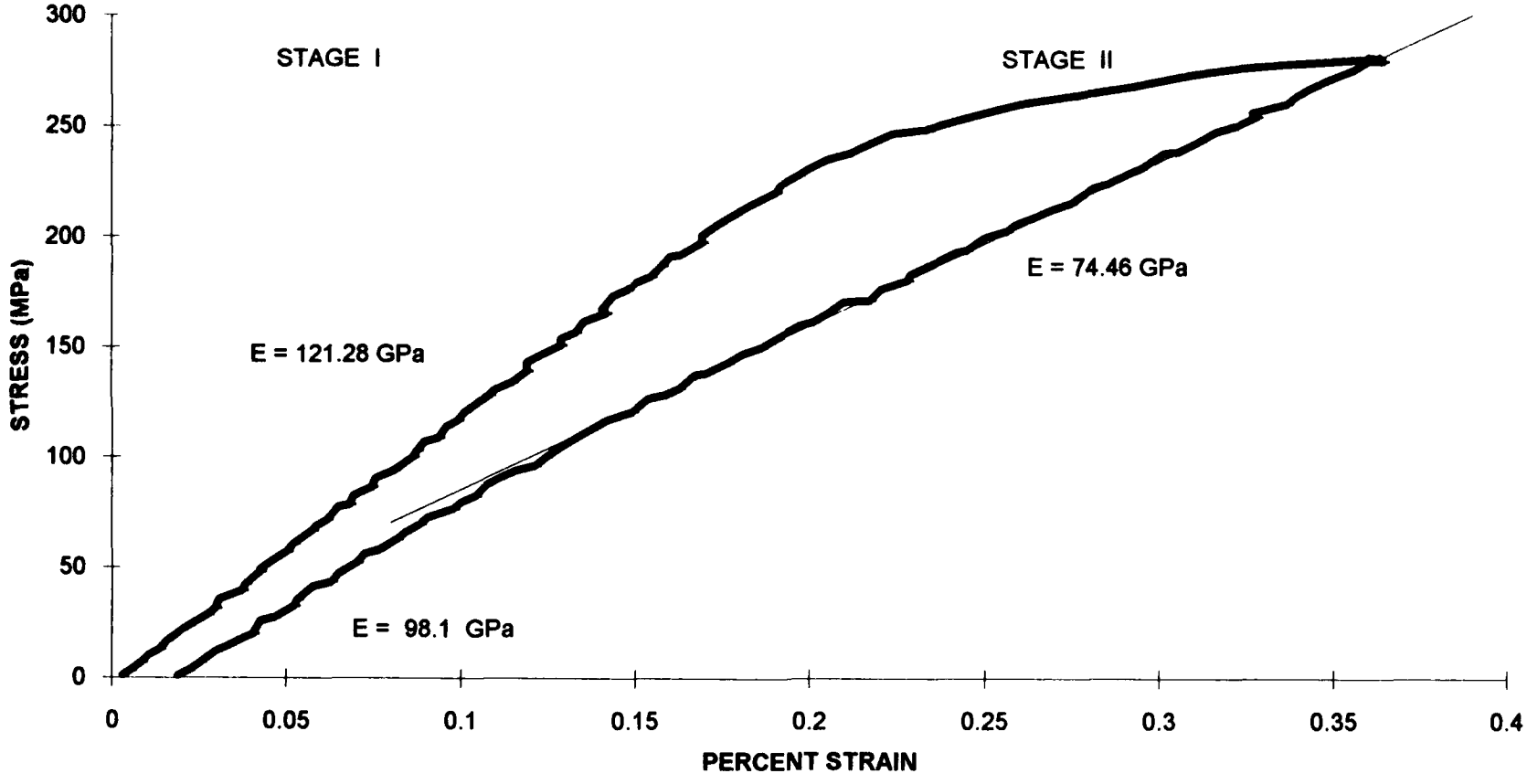

Figure 12

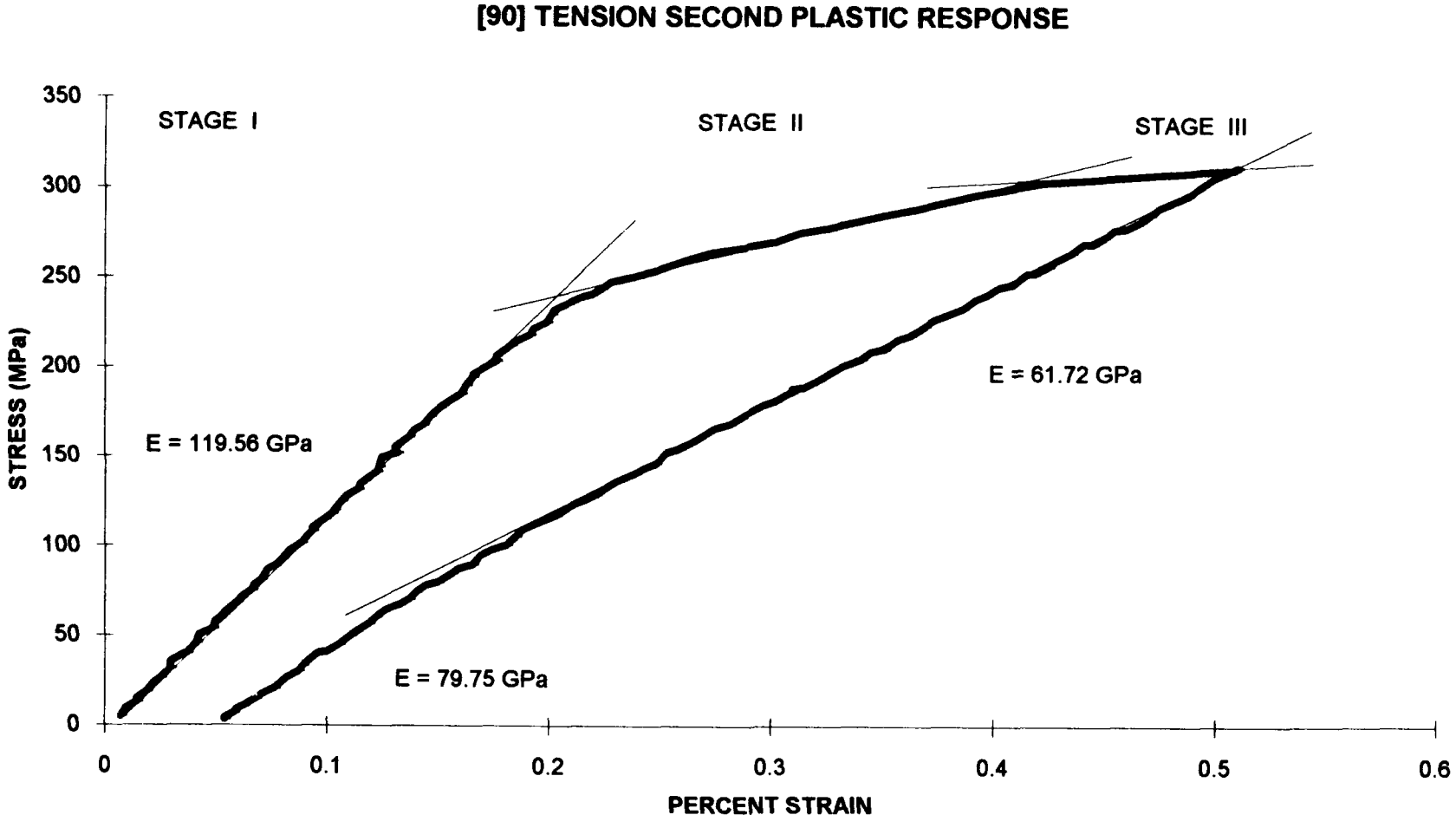
[90] TENSION SECOND PLASTIC RESPONSE
STAGE I
STAGE II
STAGE III
E = 119.56 GPa
E = 79.75 GPa
E = 61.72 GPa
STRESS (MPa)
PERCENT STRAIN
350
300
250
200
150
100
50
0
0
0.1
0.2
0.3
0.4
0.5
0.6

Figure 13

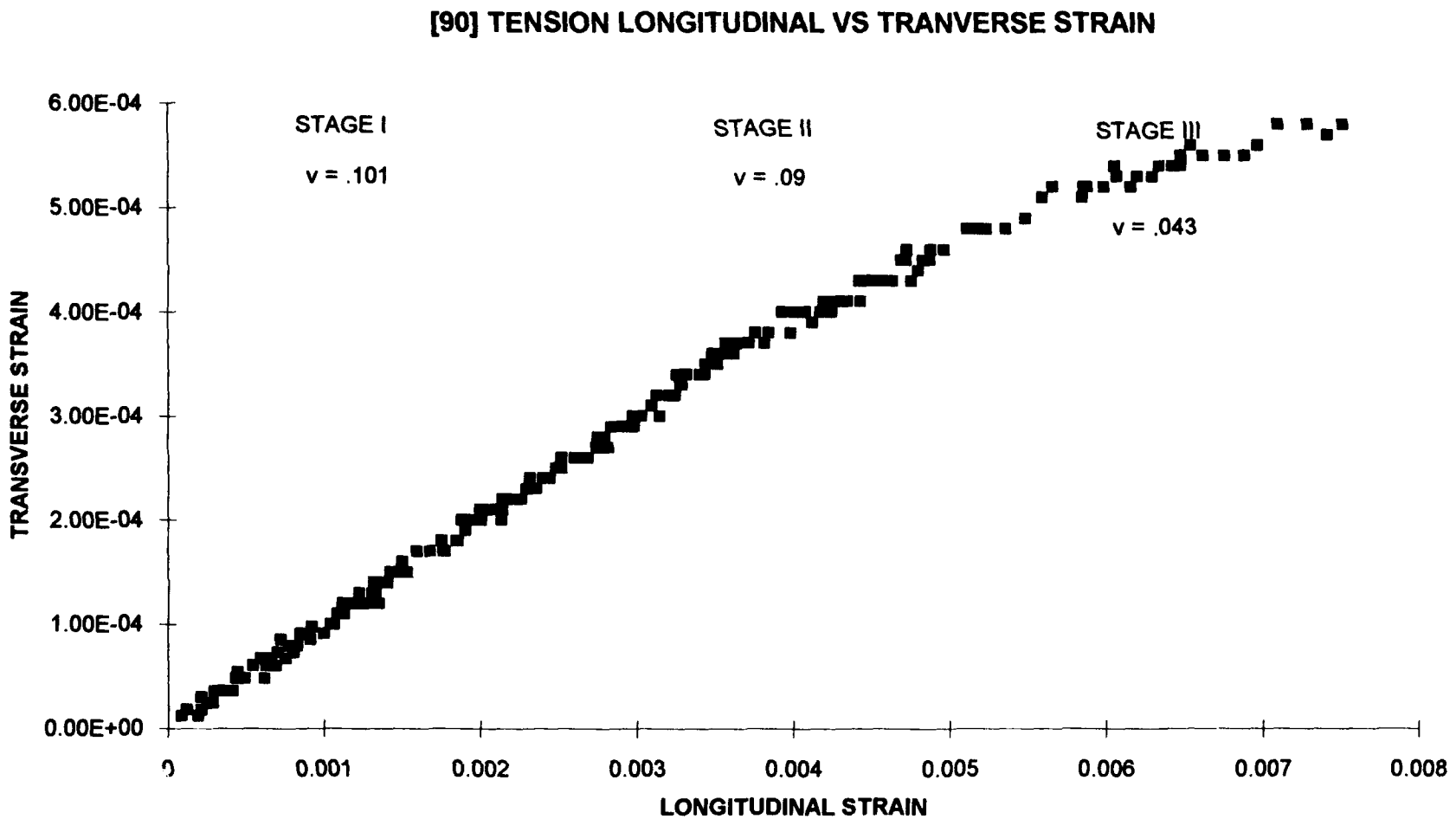
[90] TENSION LONGITUDINAL VS TRANVERSE STRAIN
STAGE I
v = .101
STAGE II
v = .09
STAGE III
v = .043
TRANSVERSE STRAIN
6.00E-04
5.00E-04
4.00E-04
3.00E-04
2.00E-04
1.00E-04
0.00E+00
0
0.001
0.002
0.003
0.004
0.005
0.006
0.007
0.008
LONGITUDINAL STRAIN

Figure 14

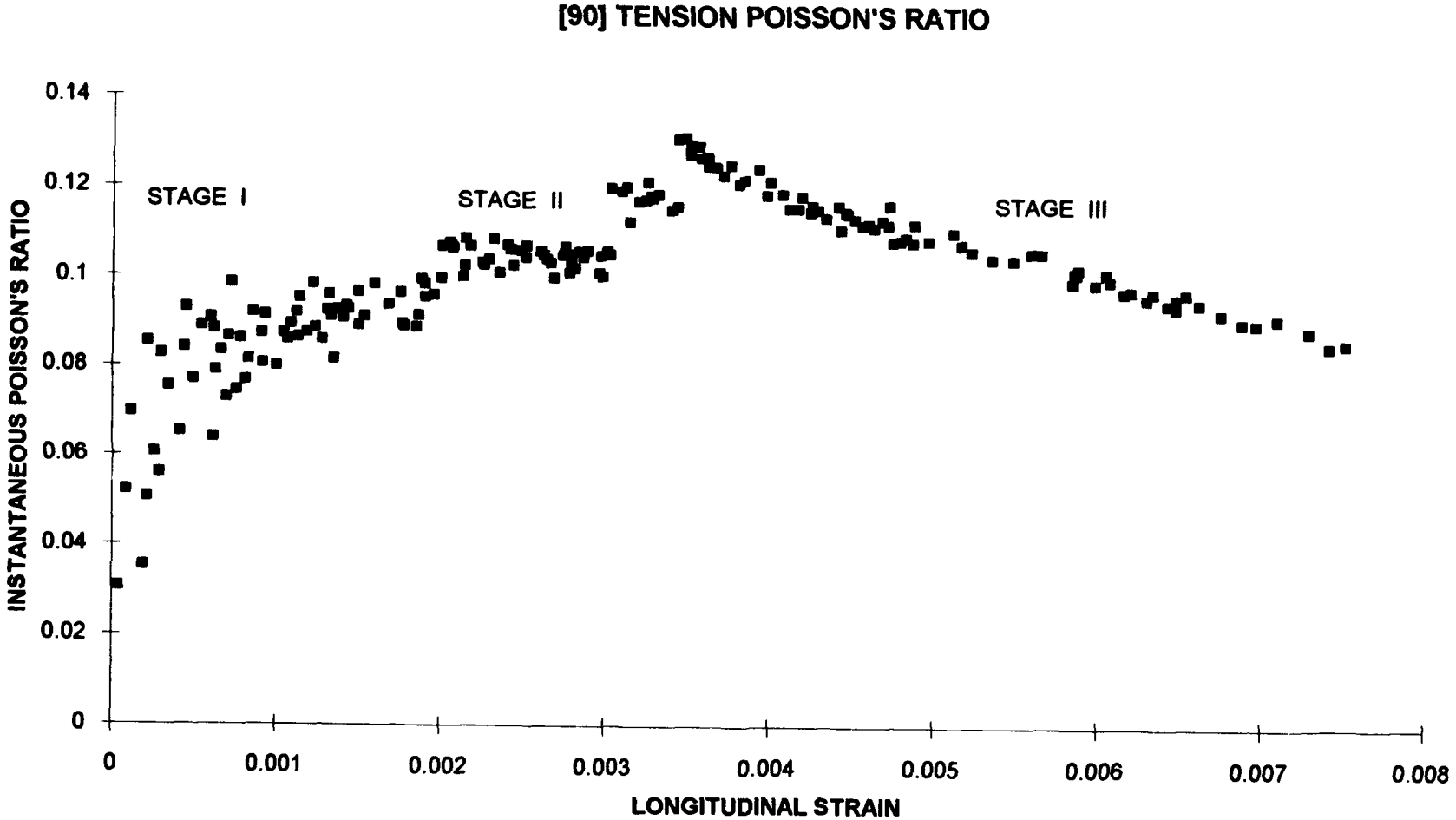
[90] TENSION POISSON'S RATIO
INSTANTANEOUS POISSON'S RATIO
0.14
0.12
0.1
0.08
0.06
0.04
0.02
0
STAGE I
STAGE II
STAGE III
0
0.001
0.002
0.003
0.004
0.005
0.006
0.007
0.008
LONGITUDINAL STRAIN

Figure 15

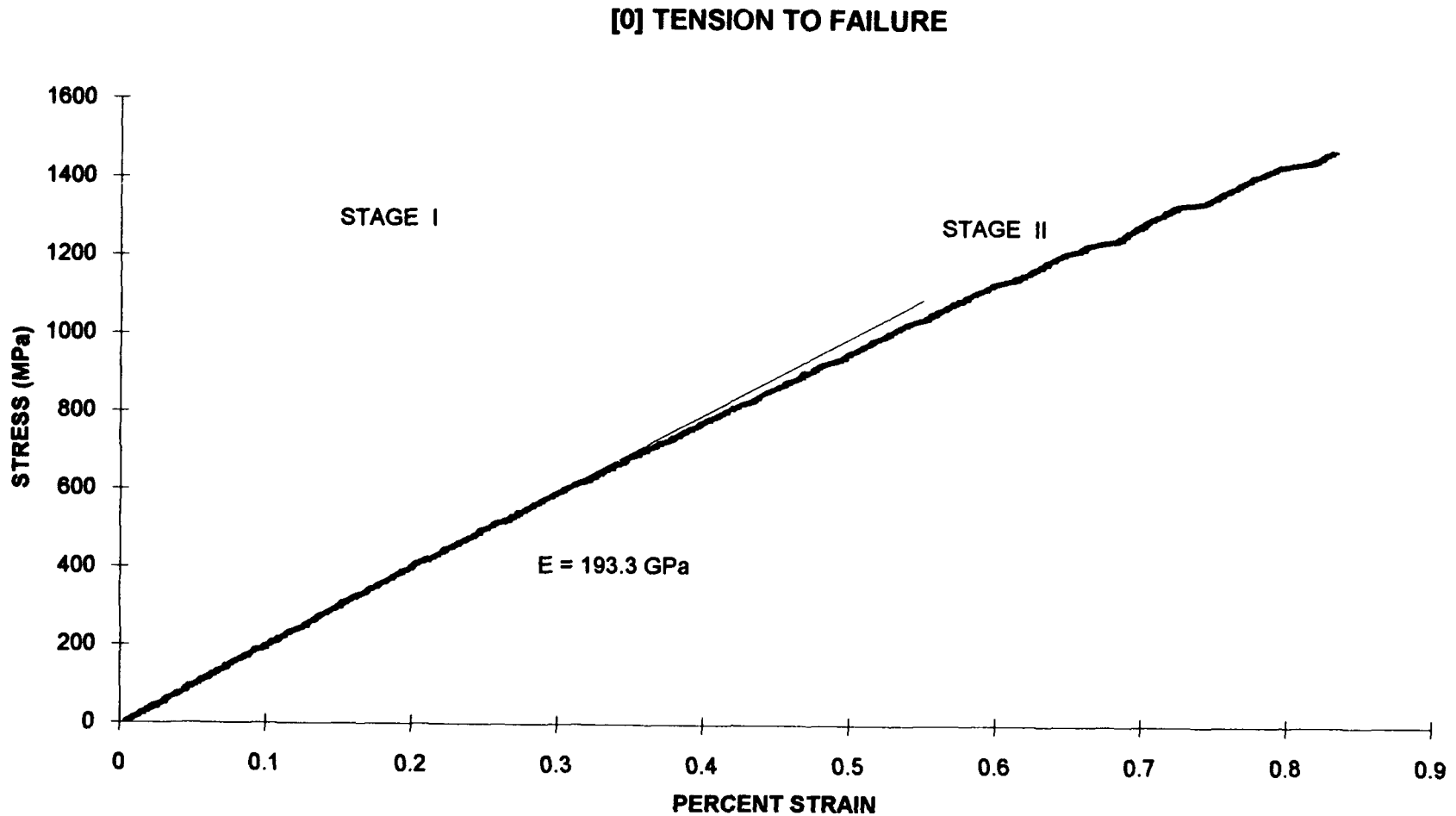
[0] TENSION TO FAILURE
STAGE I
STAGE II
E = 193.3 GPa
STRESS (MPa)
1600
1400
1200
1000
800
600
400
200
0
0
0.1
0.2
0.3
0.4
0.5
0.6
0.7
0.8
0.9
PERCENT STRAIN

Figure 16

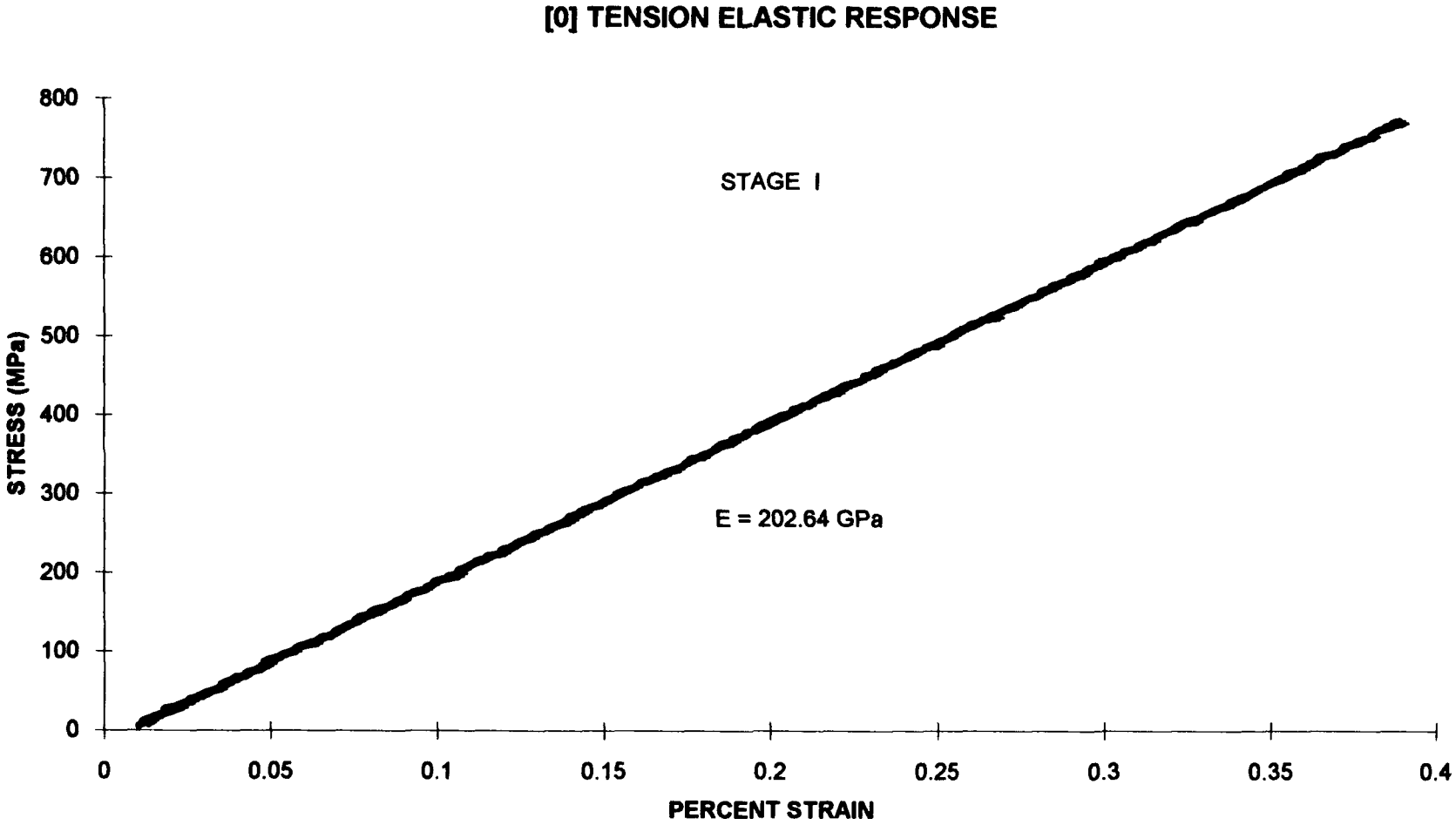
[0] TENSION ELASTIC RESPONSE
STAGE I
E = 202.64 GPa
STRESS (MPa)
800
700
600
500
400
300
200
100
0
0
0.05
0.1
0.15
0.2
0.25
0.3
0.35
0.4
PERCENT STRAIN

Figure 17

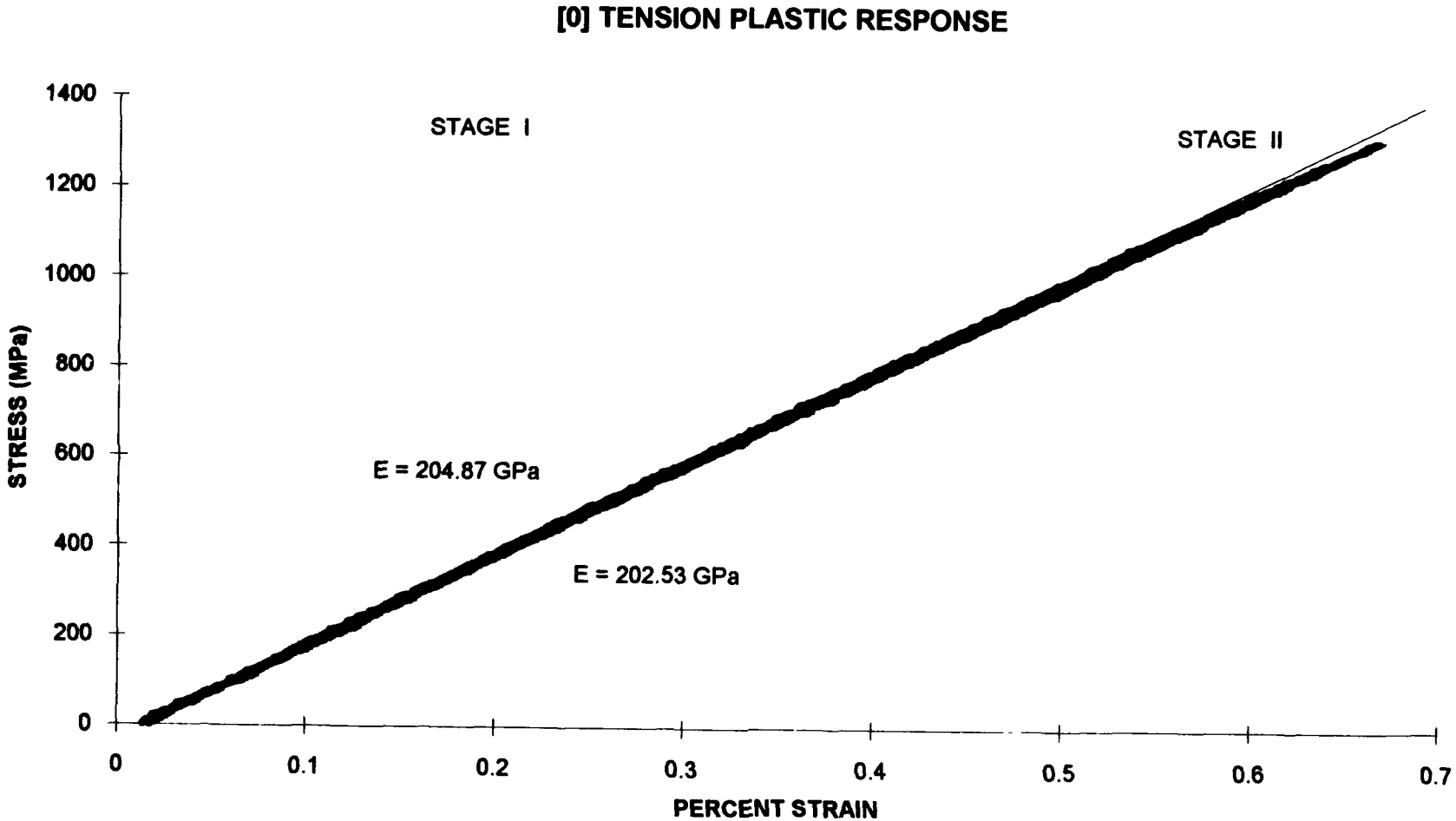
[0] TENSION PLASTIC RESPONSE
STAGE I
STAGE II
E = 204.87 GPa
E = 202.53 GPa
STRESS (MPa)
PERCENT STRAIN
1400
1200
1000
800
600
400
200
0
0
0.1
0.2
0.3
0.4
0.5
0.6
0.7

Figure 18

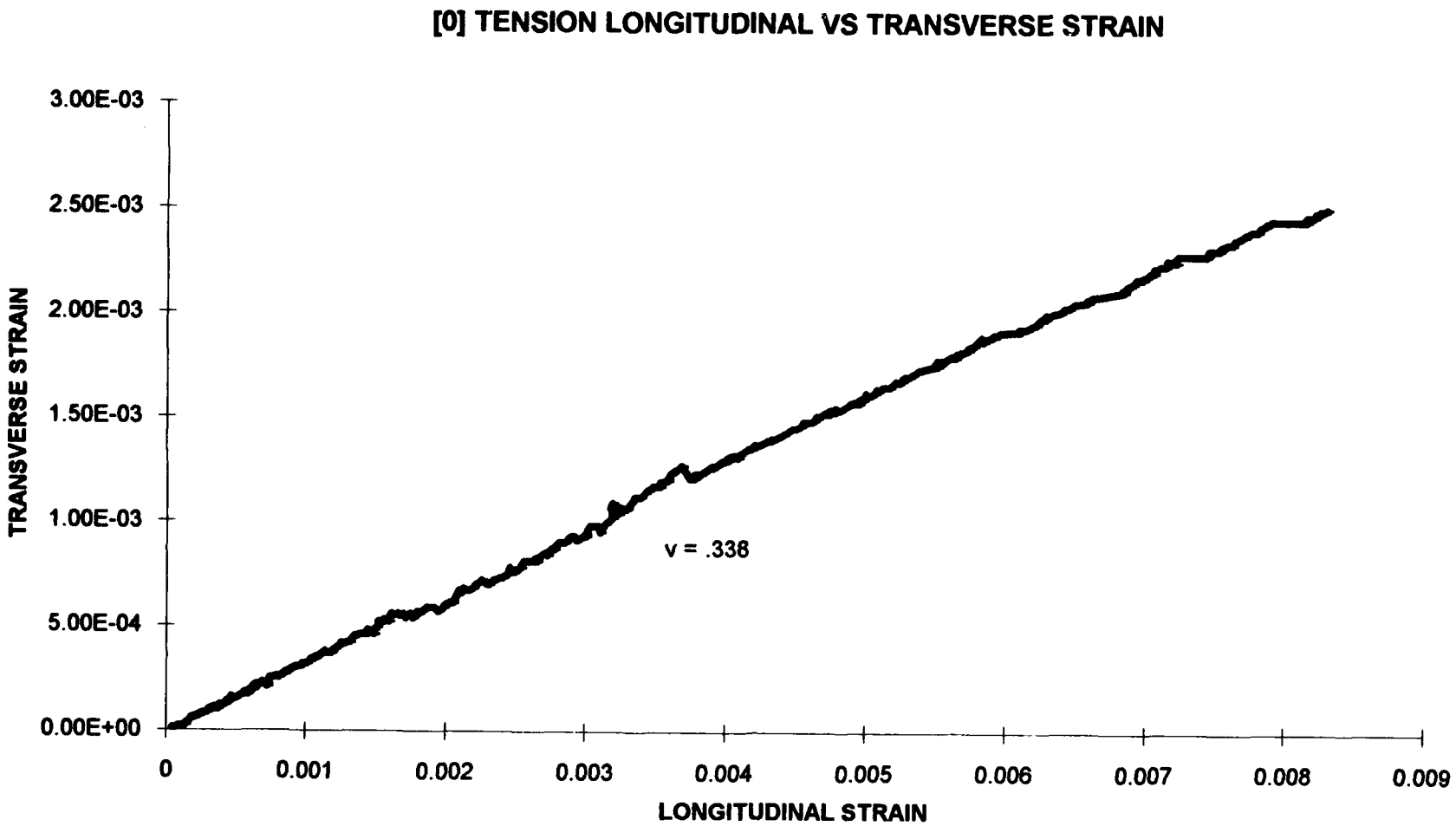
[0] TENSION LONGITUDINAL VS TRANSVERSE STRAIN
TRANSVERSE STRAIN
3.00E-03
2.50E-03
2.00E-03
1.50E-03
1.00E-03
5.00E-04
0.00E+00
v = .338
0
0.001
0.002
0.003
0.004
0.005
0.006
0.007
0.008
0.009
LONGITUDINAL STRAIN

Figure 19

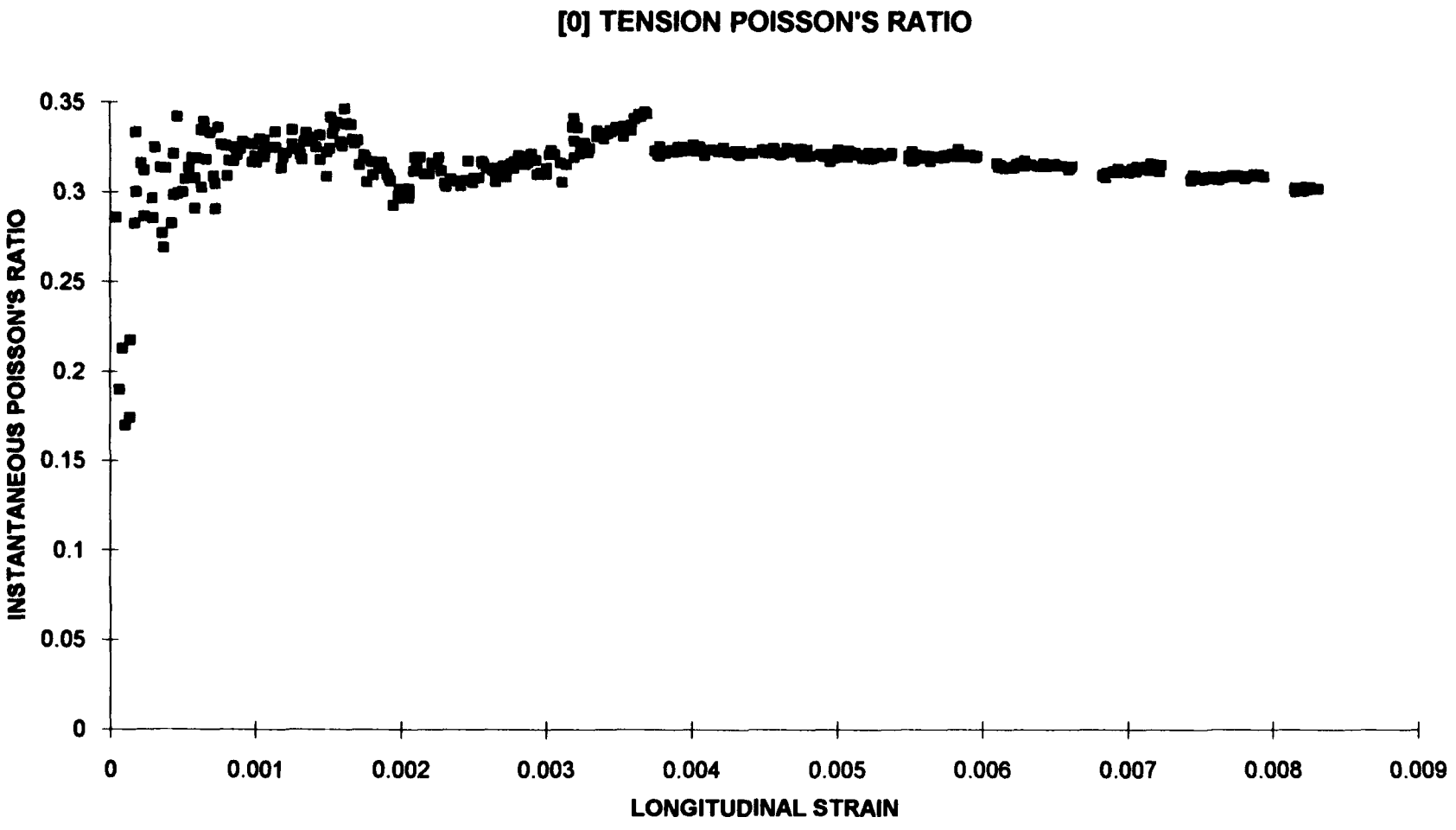
[0] TENSION POISSON'S RATIO
INSTANTANEOUS POISSON'S RATIO
0.35
0.3
0.25
0.2
0.15
0.1
0.05
0
0
0.001
0.002
0.003
0.004
0.005
0.006
0.007
0.008
0.009
LONGITUDINAL STRAIN

Figure 20

4.2 Compressive Experiments. The results and stress/strain curves for all compressive tests are contained in this section. Table 4 shows the results of all compressive experiments.

TABLE 4

RESULTS OF COMPRESSIVE EXPERIMENTS

Spec ID Number	Layup	Test Type	Load Rate (N/s)	Initial Modulus (GPa)	Unload Modulus (GPa)
15	$[90]_{16}$	FAILURE	55.6	116.87	N/A
16	$[90]_{16}$	STAGE I	55.6	109.07	109.07
14	$[90]_{16}$	STAGE II	55.6	109.99	107.40
6	$[0]_{16}$	FAILURE	55.6	197.2	N/A
7	$[0]_{16}$	STAGE I	55.6	197.67	197.67
8	$[0]_{16}$	STAGE II	55.6	189.40	120.91

4.2.1 $[90]_{16}$ Compressive Experiments. The ninety degree laminate reacted as expected during the compression tests. A gage length of approximately 2.54 cm was used with complete success; buckling, a common compression experimental difficulty was not encountered. A unidirectional specimen will generally fail due to matrix shear, with the

possibility of fiber debonding and fiber crushing (Agarwal, 1990: 99). The first specimen, (number 15) was tested in compression to failure, and failed in shear as illustrated in Figure 21, unless otherwise noted, all photographs are loaded horizontal to the page. Longitudinal and lateral strain data was accumulated from this specimen while under compression.

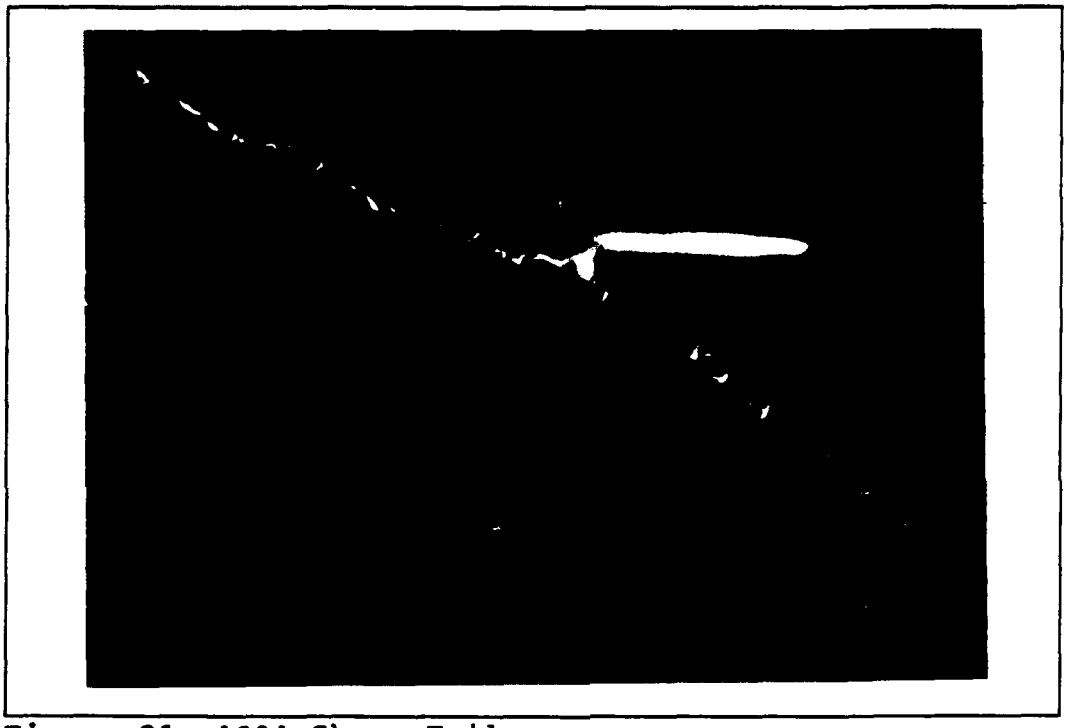

Figure 21 [90] Shear Failure

The stress/strain curve for the ninety degree laminate in compression exhibited only a two stage response. The initial modulus for the first specimen (number 15) was 116.87 GPa, identical to the value for tension. The compression tests for the ninety degree laminate were also very repeatable. Due to having a two stage response, only two further tests were conducted for the ninety degree laminate in compression. The second

specimen (number 16) was loaded into Stage I and unloaded, and the third specimen (number 14) was loaded into Stage II and unloaded. The average initial modulus for these three experiments was 111.95 GPa with a standard deviation of 4.28 GPa. Previous studies have not presented any compression data for unidirectional SCS-9/β 21S, only data for SCS-6/β 21S are available, so no comparison can be made. The stress/strain curves for all three ninety degree specimens, the longitudinal versus transverse strain curves and the instantaneous Poisson's Ratio versus longitudinal strain curve, are shown in Figures 23 - 27.

4.2.2 $[0]_{16}$ Compressive Experiments. These compression tests presented some difficulty. Due to the extremely high load levels needed to achieve failure (2.4 GPa), fiberglass tabs had to be affixed to the specimen in order to prevent slipping. With the addition of the fiberglass tabs, the first specimen (number 6) failed in shear with an initial modulus of 197.2 GPa, see Figure 22. The zero degree laminate in compression also exhibited a two stage stress strain response; therefore, only two other test were required to understand its' complete behavior, the second specimen (number 7) was loaded into Stage I and unloaded, and the third specimen (number 8) was loaded into Stage II and unloaded. Longitudinal and lateral strain data were collected from specimen number 8. Only longitudinal strain data was collected from specimen number 7, because Poisson's Ratio data was satisfied by specimen number 8. The results of the zero degree laminate were also very repeatable. The average initial modulus for all three tests was 194.76 GPa with a standard deviation of 4.65 GPa. The initial modulus for tension and compression are virtually the same.

In the initial zero degree laminate compression to failure test, the strain gage on specimen number 6 debonded before failure, at a strain of 1.5%. Therefore, this stress/strain curve will not be presented. Figure 28 depicts the failed specimen with extrapolated strain data to show the failure point. The load at failure was determined from this test. The stress/strain curves for specimens 7 and 8, the longitudinal versus transverse strain curve and the instantaneous Poisson's Ratio versus longitudinal strain curves are contained in Figures 29 - 32.

Figure 22 [0] Compression Shear Failure

[90] COMPRESSION TO FAILURE

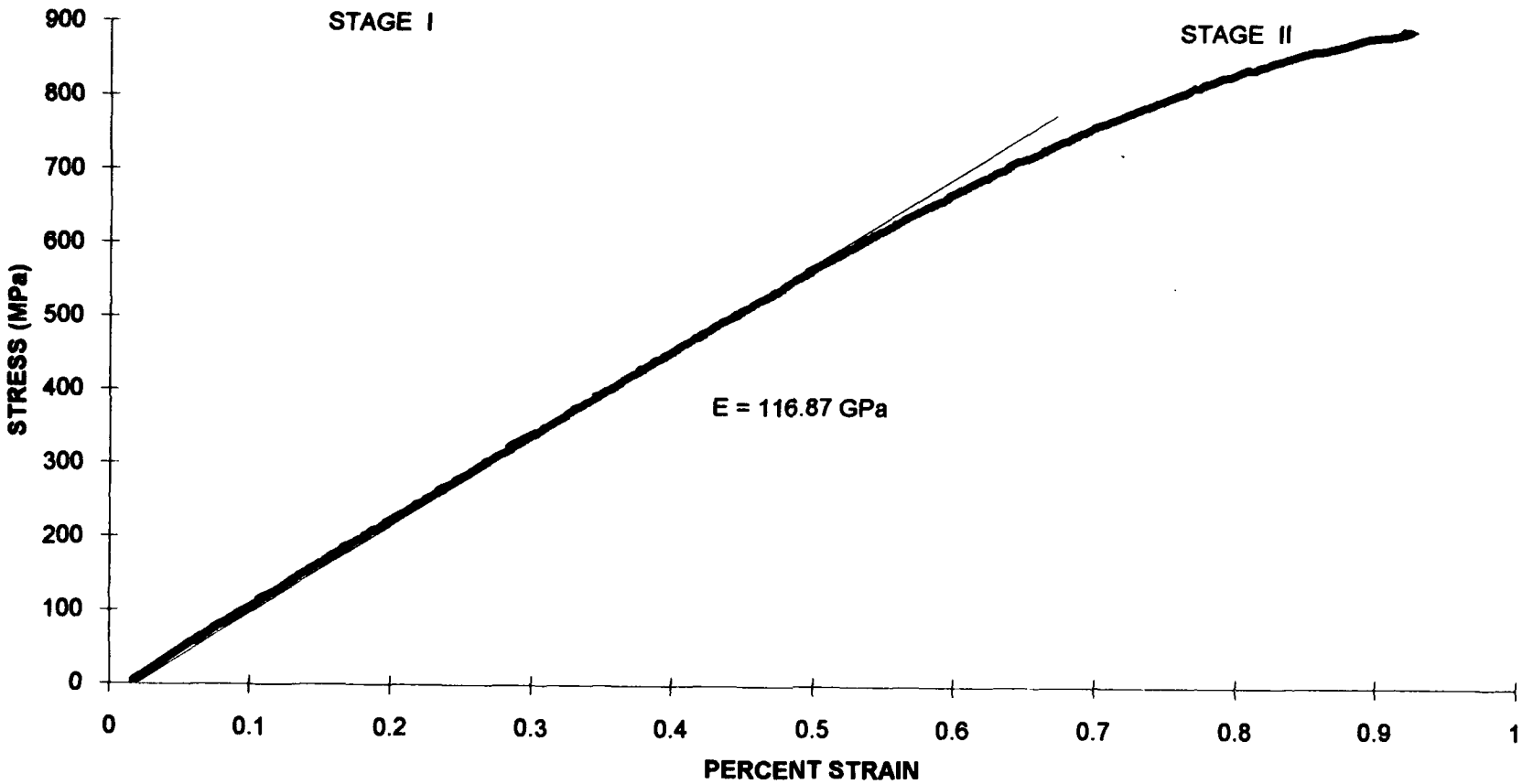

Figure 23

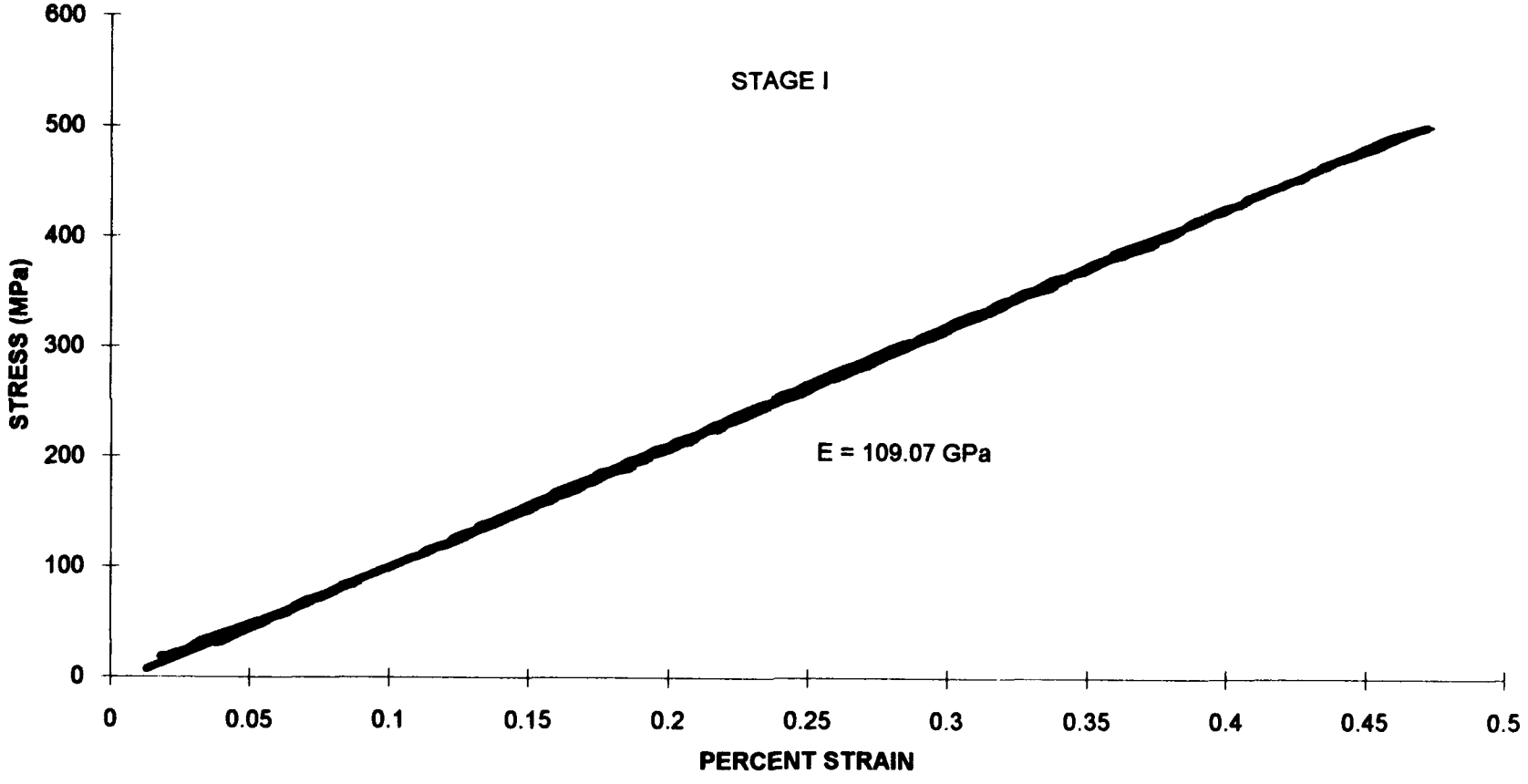
[90] COMPRESSION ELASTIC RESPONSE
STAGE I
E = 109.07 GPa
STRESS (MPa)
600
500
400
300
200
100
0
0
0.05
0.1
0.15
0.2
0.25
0.3
0.35
0.4
0.45
0.5
PERCENT STRAIN

Figure 24

[90] COMPRESSION PLASTIC RESPONSE

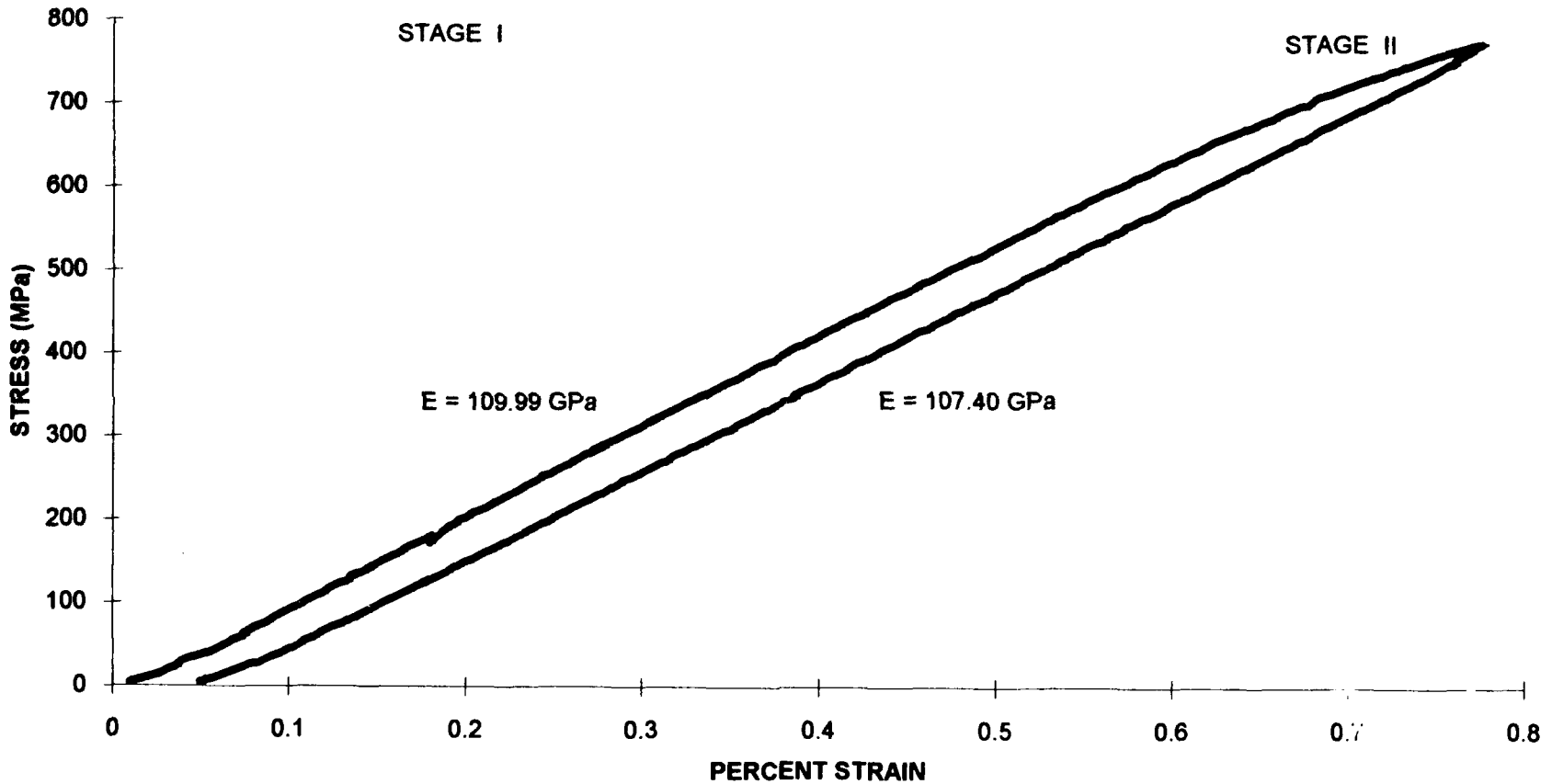

Figure 25

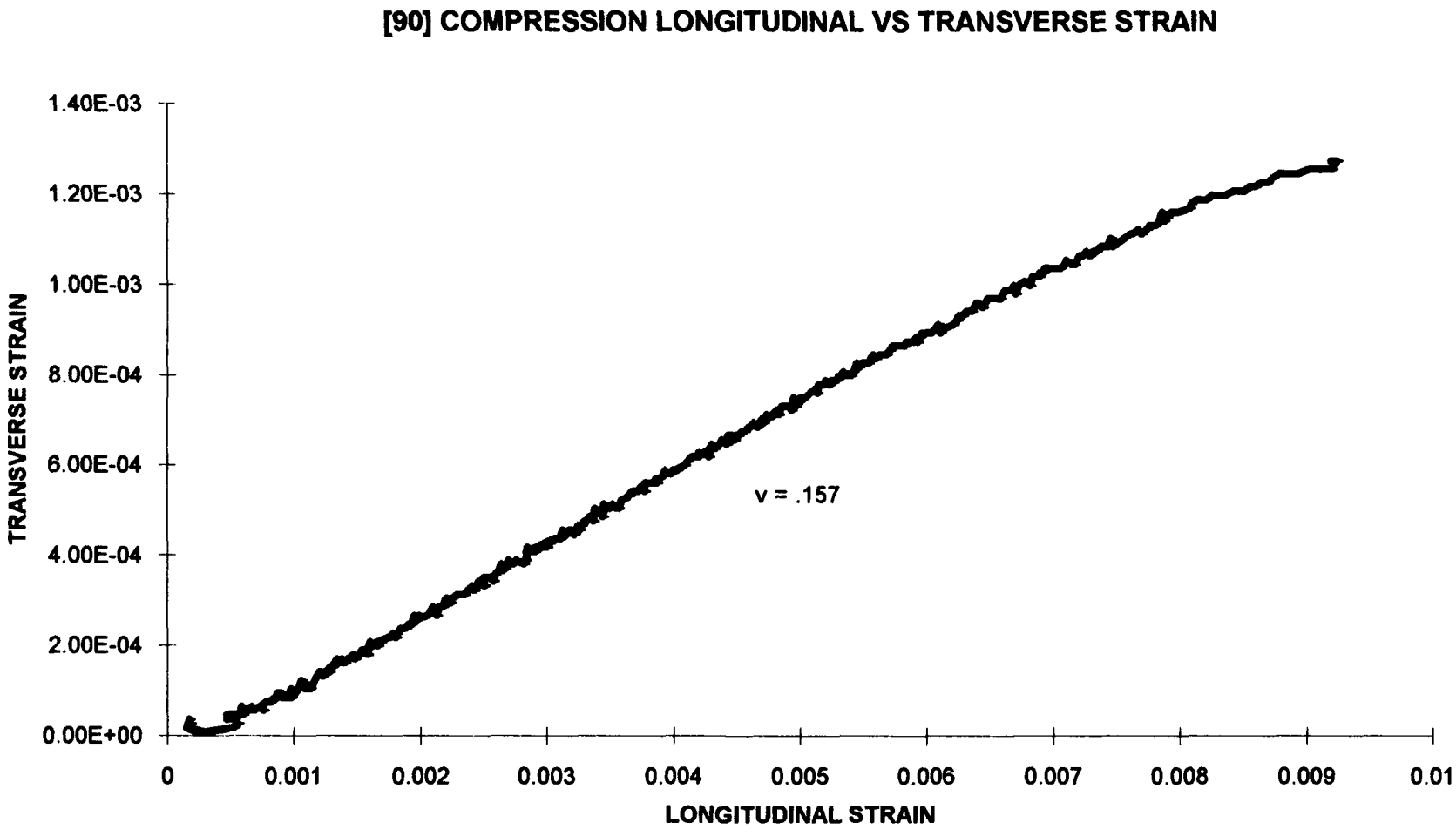
[90] COMPRESSION LONGITUDINAL VS TRANSVERSE STRAIN
TRANSVERSE STRAIN
1.40E-03
1.20E-03
1.00E-03
8.00E-04
6.00E-04
4.00E-04
2.00E-04
0.00E+00
v = .157
0
0.001
0.002
0.003
0.004
0.005
0.006
0.007
0.008
0.009
0.01
LONGITUDINAL STRAIN

Figure 26

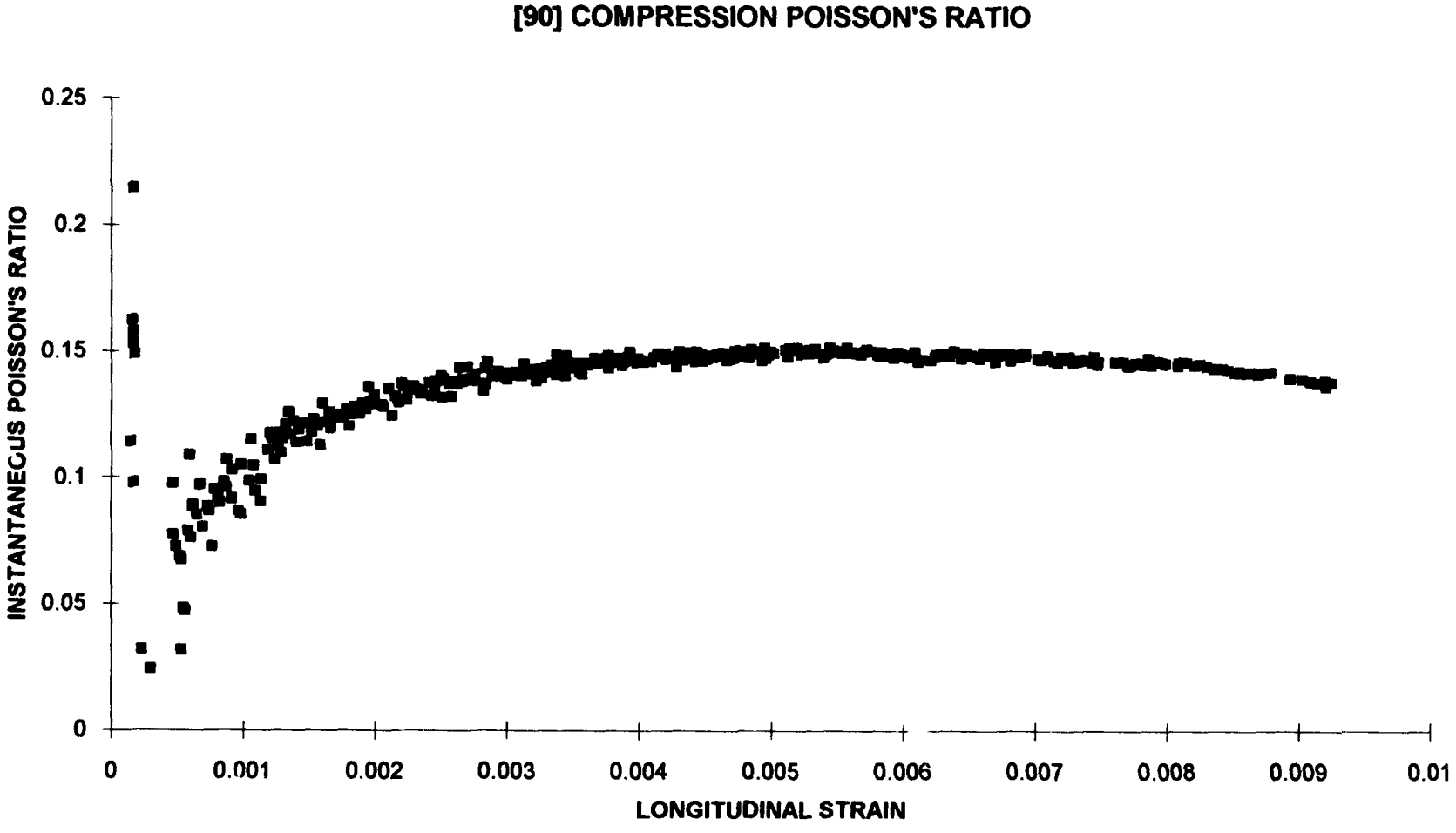
[90] COMPRESSION POISSON'S RATIO
INSTANTANECUS POISSON'S RATIO
0.25
0.2
0.15
0.1
0.05
0
0
0.001
0.002
0.003
0.004
0.005
0.006
0.007
0.008
0.009
0.01
LONGITUDINAL STRAIN

Figure 27

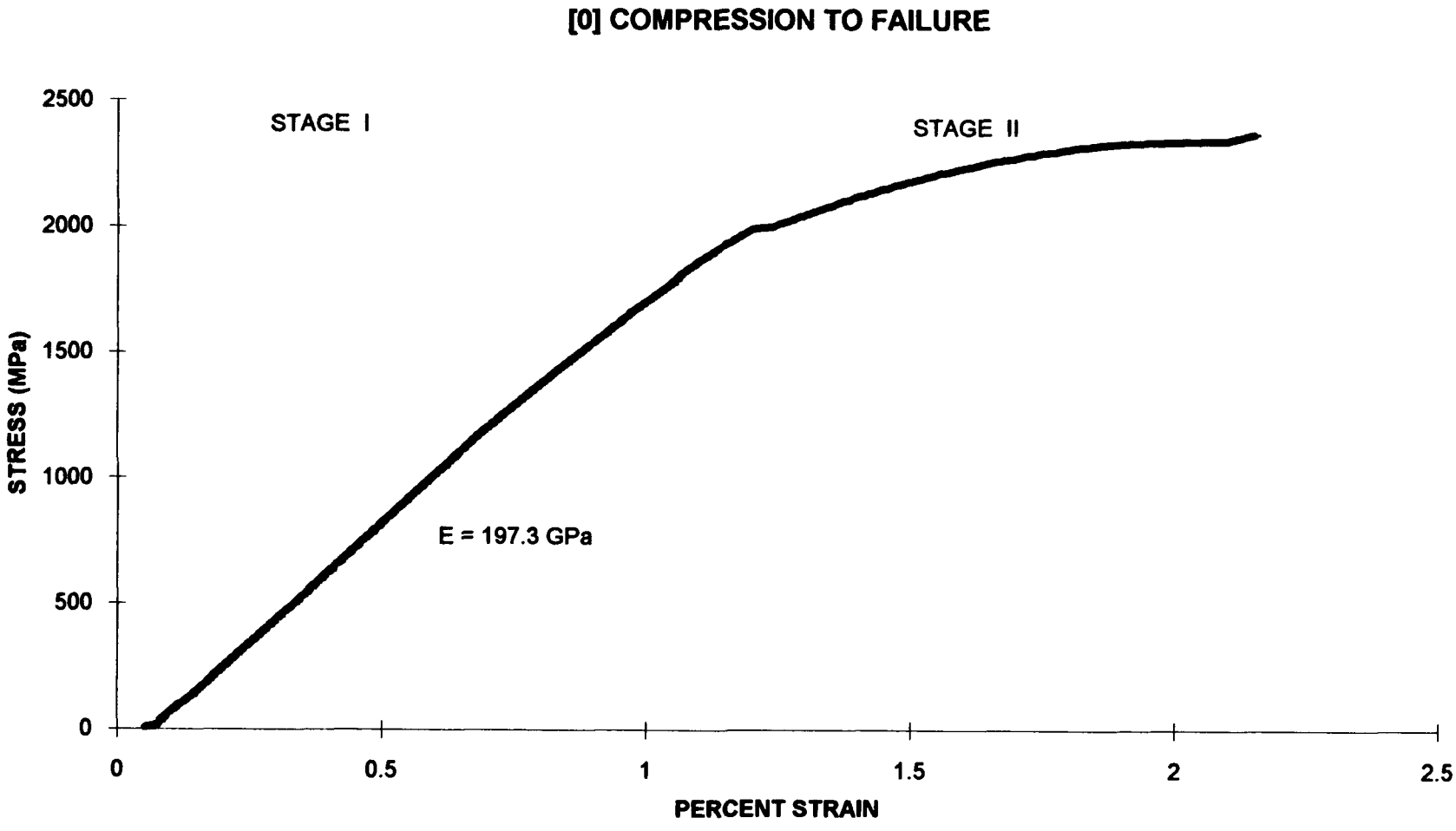
[0] COMPRESSION TO FAILURE
STAGE I
STAGE II
E = 197.3 GPa
STRESS (MPa)
2500
2000
1500
1000
500
0
0
0.5
1
1.5
2
2.5
PERCENT STRAIN

Figure 28

[0] COMPRESSION ELASTIC RESPONSE

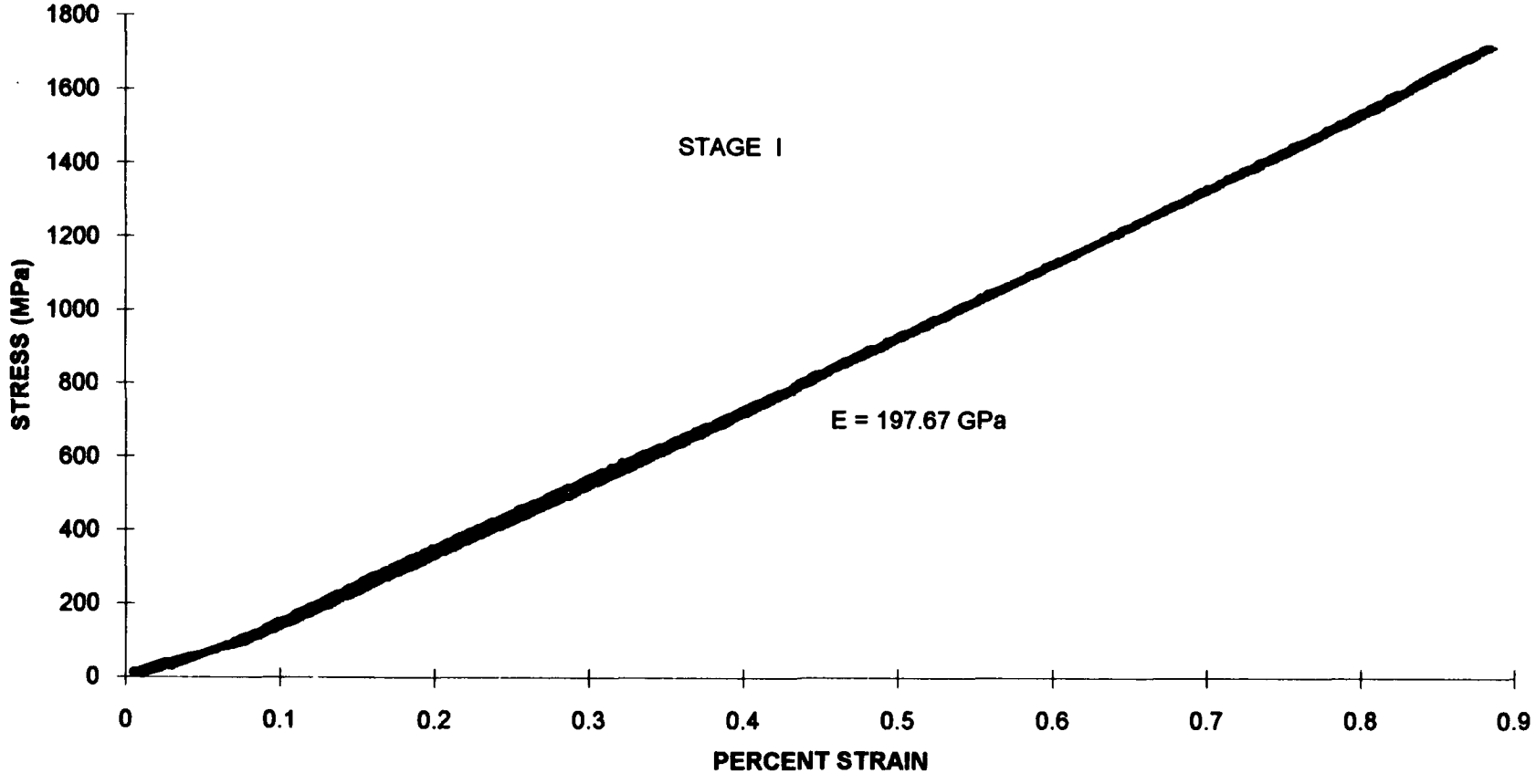

Figure 29

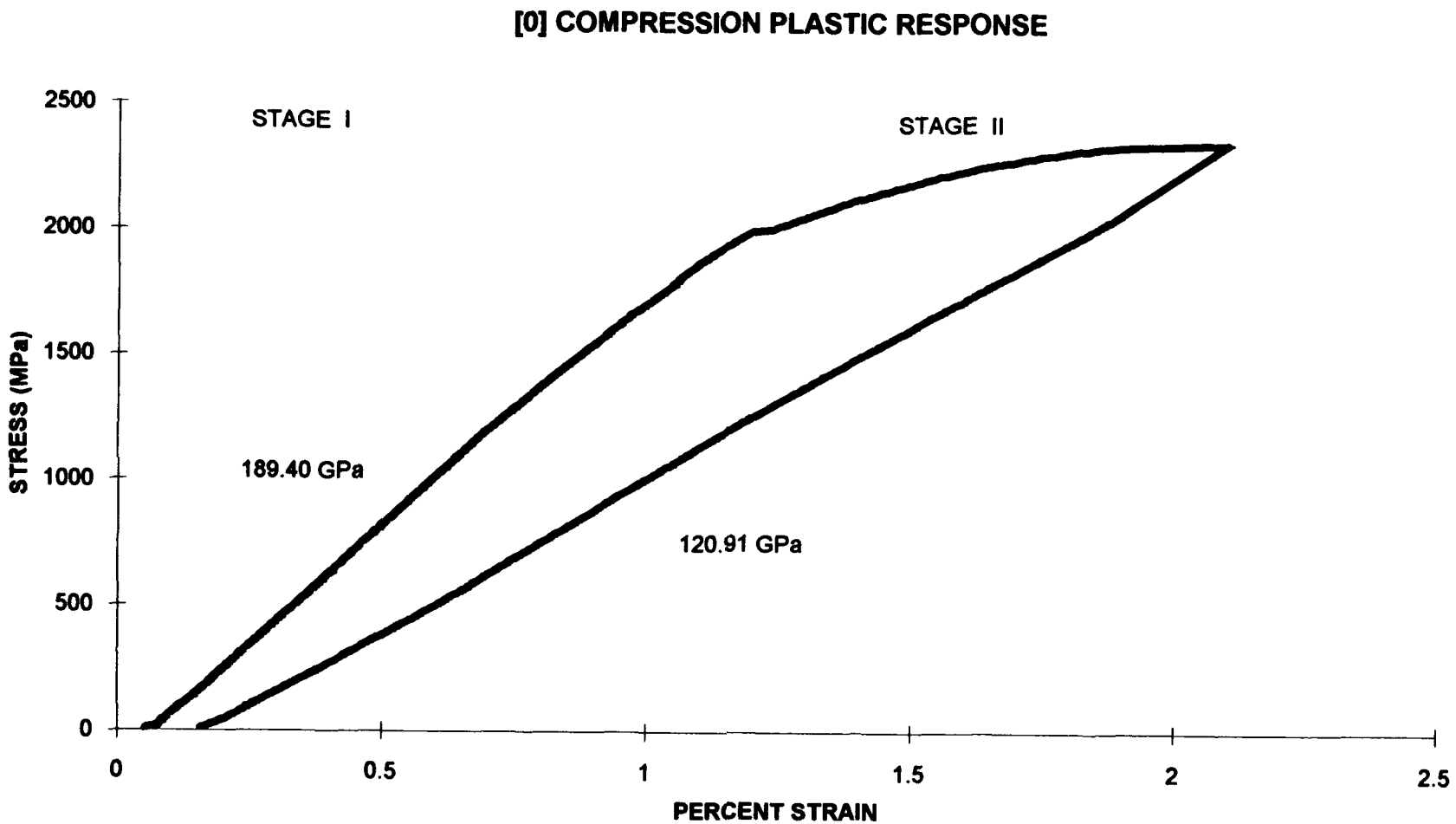
[0] COMPRESSION PLASTIC RESPONSE
STAGE I
STAGE II
189.40 GPa
120.91 GPa
STRESS (MPa)
2500
2000
1500
1000
500
0
0
0.5
1
1.5
2
2.5
PERCENT STRAIN

Figure 30

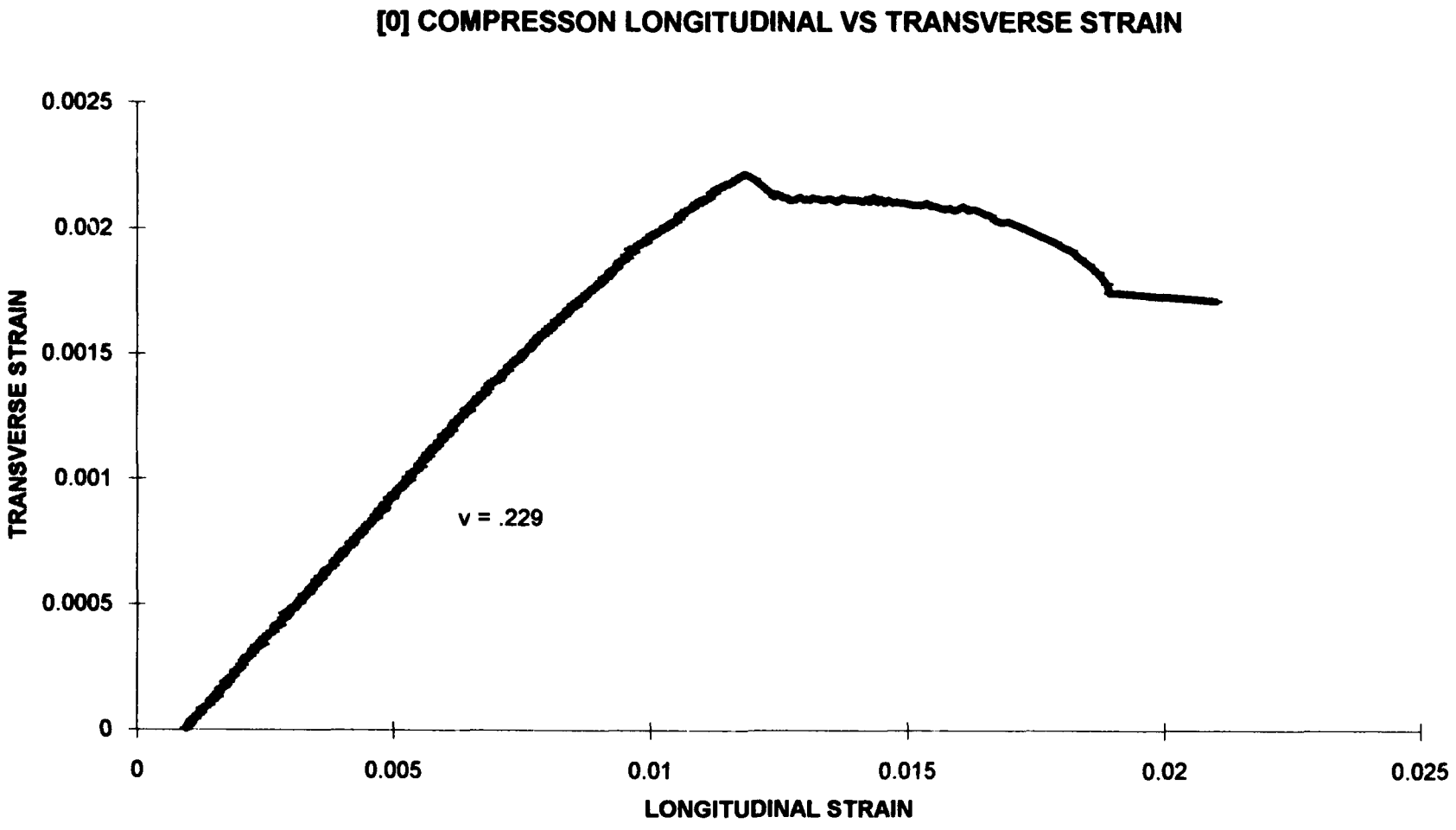
[0] COMPRESSON LONGITUDINAL VS TRANSVERSE STRAIN
TRANSVERSE STRAIN
0.0025
0.002
0.0015
0.001
0.0005
0
v = .229
0
0.005
0.01
0.015
0.02
0.025
LONGITUDINAL STRAIN

Figure 31

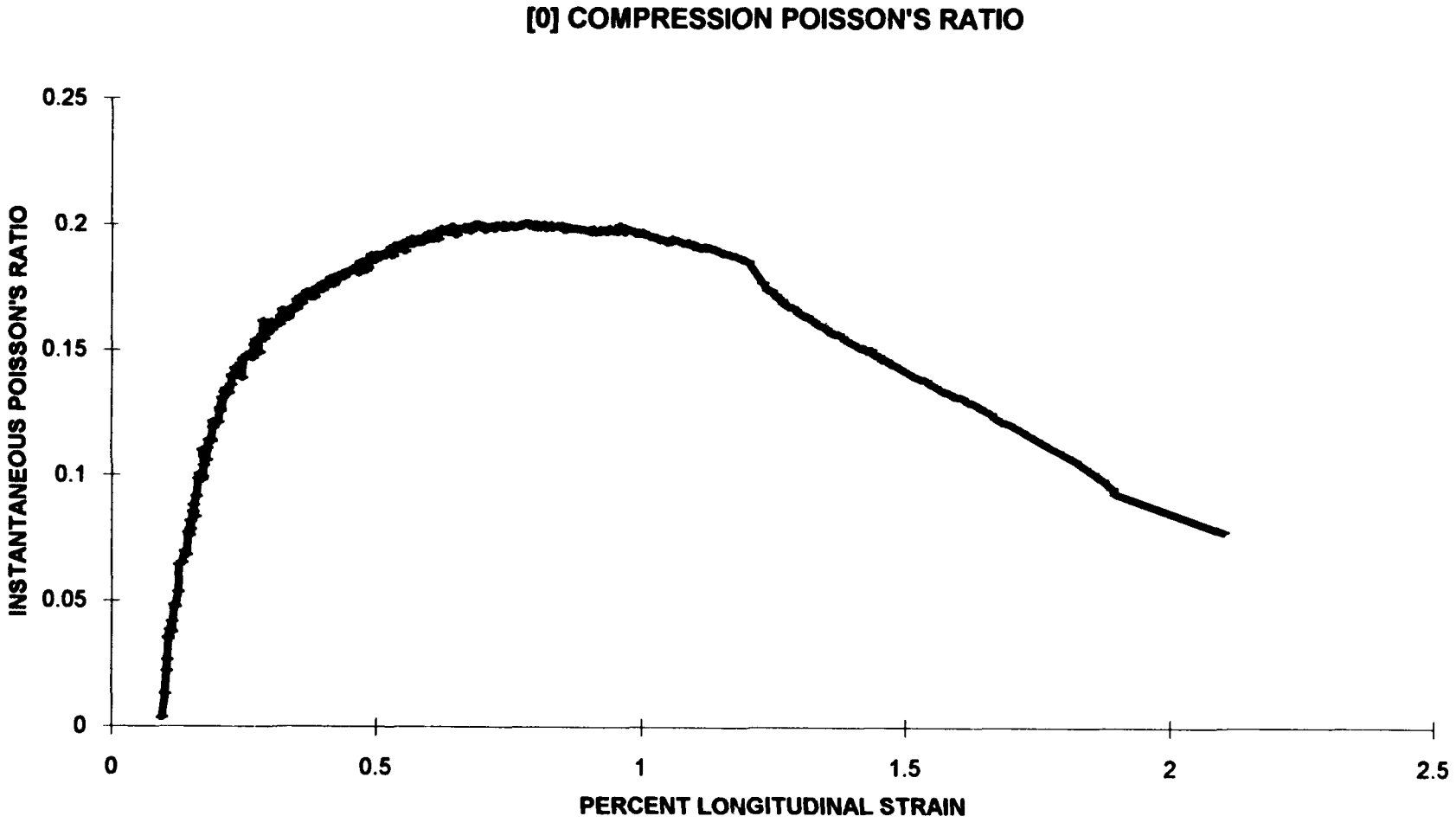
[0] COMPRESSION POISSON'S RATIO
INSTANTANEOUS POISSON'S RATIO
0.25
0.2
0.15
0.1
0.05
0
0
0.5
1
1.5
2
2.5
PERCENT LONGITUDINAL STRAIN

Figure 32

V. Discussion

5.1 Tensile Microstructure. The microstructure and failure mechanisms of the tensile experiments are contained in this section.

5.1.1 $[90]_{16}$ Tensile Microstructure. The ninety degree laminate exhibited a three stage stress/strain response in the first test to failure. This is shown in Figure 10 of the Results section. Three additional tests were conducted to investigate the damage mechanisms during each stage of the stress/strain curve. Poisson's Ratio data were also collected to determine whether plasticity or damage was the dominant deformation mechanism. During plastic deformation, Poisson's Ratio increases; during damage progression Poisson's Ratio decreases, but if both damage and plasticity are occurring Poisson's Ratio may not change.

5.1.1.1$[90]_{16}$ Tensile Failure. The first specimen (number 11) was loaded to failure, while longitudinal and lateral strain data were collected. Acetate replicas were taken every 40 MPa, to monitor the deformation progression. The failed specimen exhibited both plastic deformation and debonding of the fiber from the matrix. The debond is depicted by the gap seen between the fiber and the matrix. The debond is shown in Figure 37. Slip bands were not observed in the matrix of the failed specimen. There was, however, permanent plastic deformation of the matrix. According to Majumdar, slip bands are most easily observed by heat treating the material before testing to the solutionizing temperature and then quenching it. This heat treatment will prevent the formation of alpha particles of titanium. These alpha particles are very large and prevent dislocation pile ups, making observation of slip bands very difficult (Majumdar,

1992). The permanent plastic deformation can be seen as the fiber protruding from the matrix due to Poisson's effect. The protruding fibers are shown in Figure 41.

5.1.1.2 $[90]_{16}$ Tensile Stage I Unload. The second specimen (number 10) was loaded into Stage I and then unloaded. The modulus for the specimen was 117.56 GPa upon loading and unloading. The material behaved as a linear-elastic solid. This behavior was predicted by the results of Newaz and Majumdar (Newaz, 1991: 10). During this stage, however, partial debonding did occur at approximately 120 MPa. This debonding is illustrated in Figure 34. Upon unloading, the debond shown in Figure 34 did not close up. "Closing up" was observed by Newaz and Majumdar (Newaz, 1991: 18). Figure 33 depicts this specimen (number 10) after the experiment was performed. This figure clearly shows that the partial debond between the fiber and matrix is still present. This partial debond, however, did not effect the stress/strain response. Figure 38 shows that there is no permanent deformation. The fibers are not protruding from the matrix. The partial debond does not allow for a permanent contraction, due to Poisson's effect.

The plot of instantaneous Poisson's ratio versus longitudinal strain, illustrated in Figure 15 of Results, shows that Poisson's ratio is virtually constant during Stage I. From this it can be inferred that the partial debond that occurs has little effect upon the stress/strain response of this material. The plot of longitudinal versus transverse strain also shows that Poisson's ratio is constant between zero strain and .002 strain. The value for Poisson's Ratio during Stage I is .01.

5.1.1.3 $[90]_{16}$ Tensile Stage II Unload. The third specimen (number 12)

was loaded into Stage II and then unloaded. The initial modulus for this experiment was 121.28 GPa. The unload section of the stress/strain curve had a bilinear response. The bilinear unload section is a result of the residual compressive stresses on the fibers. The fibers debond in Stage II while damage is occurring, while unloading, there is a Poisson's effect that eventually reclamps the matrix and the fiber and therefore, stiffens the composite. As the amount of damage increases, eventually, Poisson's contraction will not be able to reclamp the fiber and the matrix, and there will not be a bilinear response. The initial modulus for the unload was 74.46 GPa and the final modulus for unloading was 98.1 GPa. The initial decrease in modulus was 38.6 percent. This type of result was predicted by Newaz and Majumdar, although their material exhibited a larger percentage decrease of 43 percent (Newaz, 1991: 10). During Stage II, the debond between the fiber and matrix continued to propagate. The debond became complete around the fiber in Stage II, even after the completely unloading the specimen; the complete debond is shown in Figure 35. Cracks also began to appear between closely adjacent fibers in the direction parallel to loading. These longitudinal cracks first appeared at approximately 200 MPa. They are shown in Figure 42. Such cracks were predicted by Marshall et al., who showed that longitudinal cracks will develop before lateral cracks especially when fibers are closely packed together (Marshall, 1992: 11). These cracks were only seen when fibers were closely packed together in these early stages of the stress/strain curve. They did show up in fibers with more separation at higher loads. These longitudinal cracks are clearly visible in Figure 42. Transverse cracks were not observed except at the failure surface, which are atributed to the failure. Transverse cracks did not show up at any load

level in the other specimens.

Instantaneous Poisson's ratio during Stage II was increasing as illustrated in Figure 15 of Results, between approximately .002 and .004 strain. This increase indicates that plasticity is present during Stage II. The plot of longitudinal versus transverse strain shows a decrease in overall Poisson's Ratio. This trend of longitudinal versus transverse strain was also witnessed by Newaz and Majumdar (Newaz, 1991: 10). This indicates that both plasticity and damage were occurring during Stage II. Plasticity was observed as permanent deformation due to Poisson's effect. This permanent deformation is illustrated in Figure 39. The stress/strain curve for this specimen shows only a small amount of residual strain upon unloading, indicating that damage was the primary deformation mechanism during Stage II with plasticity being present.

5.1.1.4 $[90]_{16}$ Tensile Stage III Unload. The fourth specimen (number 13) was loaded into Stage III and then unloaded. The response of this specimen is shown in Figure 13 of the Results section. This experiment yielded basically the same results on loading as did the first specimen (number 11) loaded to failure. The response upon unloading, however, was the reason for performing this experiment. Upon unloading, the stress/strain response had a modulus of 61.72 GPa. This is a 48.38 percent decrease in stiffness from the original loading response. This decrease was also predicted by Newaz and Majumdar, although their results exhibited a greater decrease in stiffness of 56 percent (Newaz, 1991: 10). However, the general trend of stiffness decreasing signficantly remains the same. This stage also exhibited longitudinal cracks, fiber debonding, plastic deformation and fiber damage. The fiber debonding is illustrated in Figure 36, while the

permanent deformation due to Poisson's effect is illustrated in Figure 40.

During Stage III, Poisson's Ratio was constantly decreasing which indicates that damage was also occurring during this stage. Longitudinal versus transverse strain also showed a significant decrease in Poisson's Ratio indicating damage occurring. The stress/strain curve shows that a considerable amount of residual strain is left in the specimen after unloading. This large amount of residual strain indicates that plasticity was the primary deformation mechanism in Stage III with some damage occurring. Figures are shown in order of progression for fiber debond and for deformation.

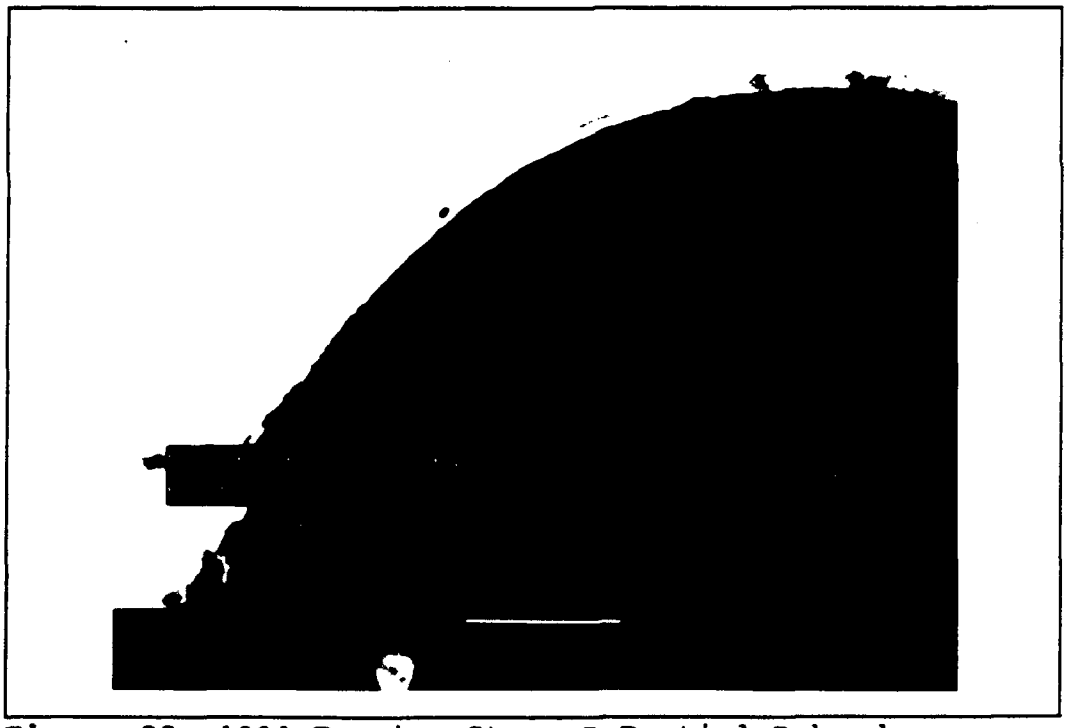

Figure 33 [90] Tension Stage I Partial Debond

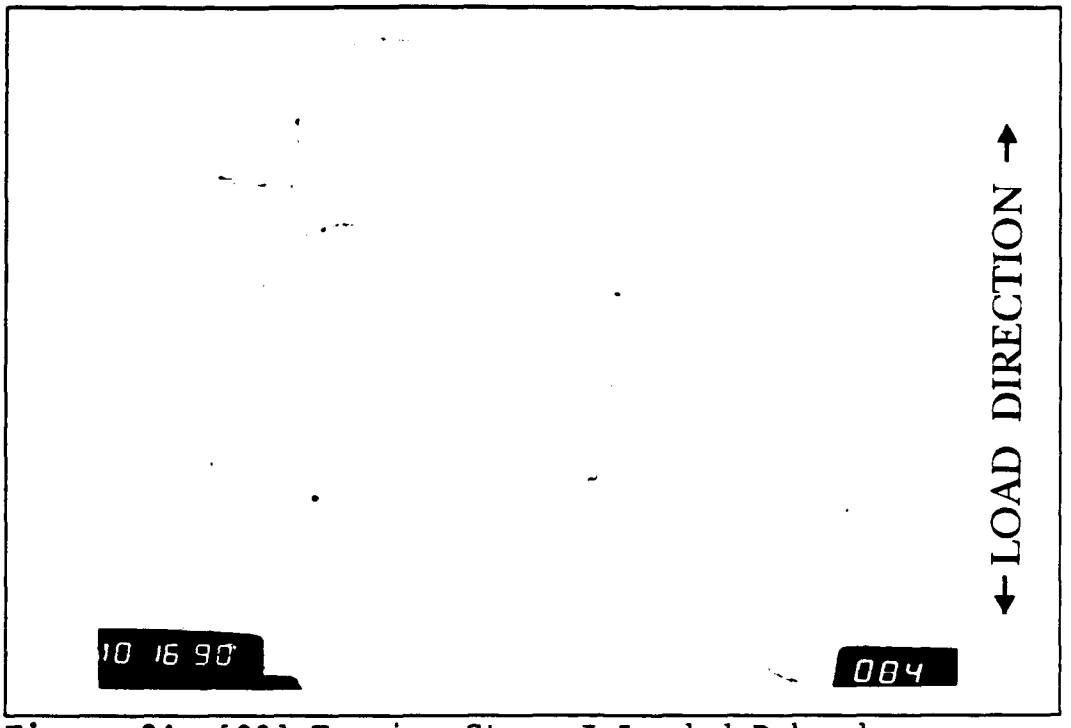

Figure 34 [90] Tension Stage I Loaded Debond

Figure 35 [90] Tension Stage II Complete Debond

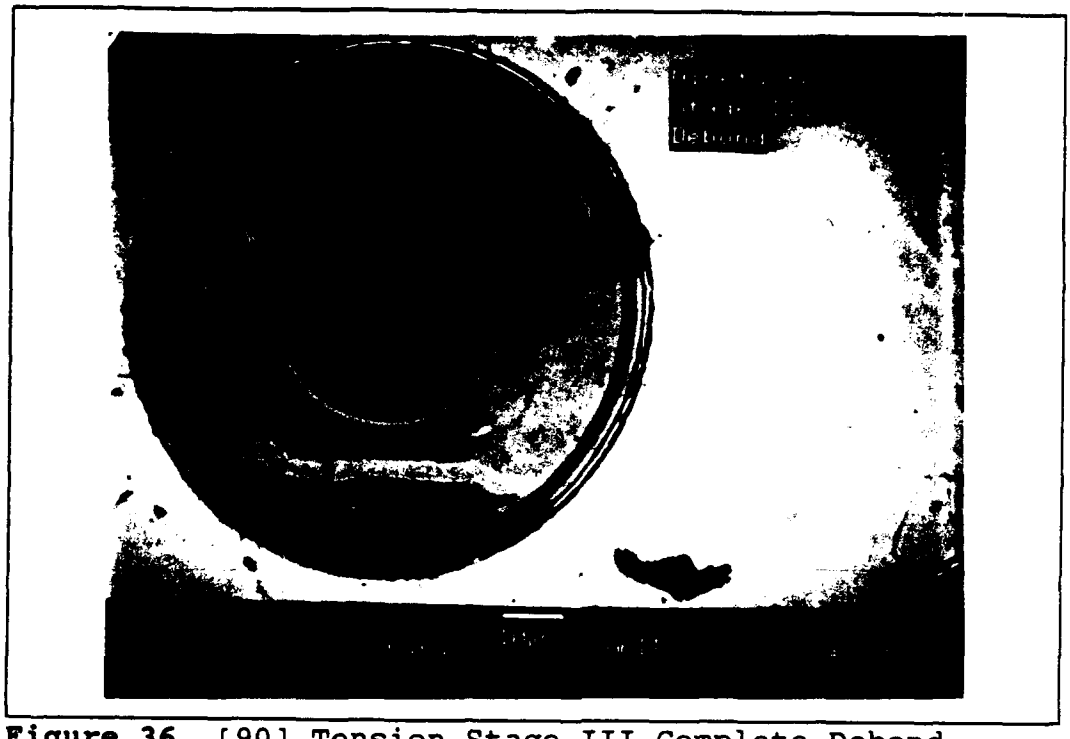

Figure 36 [90] Tension Stage III Complete Debond

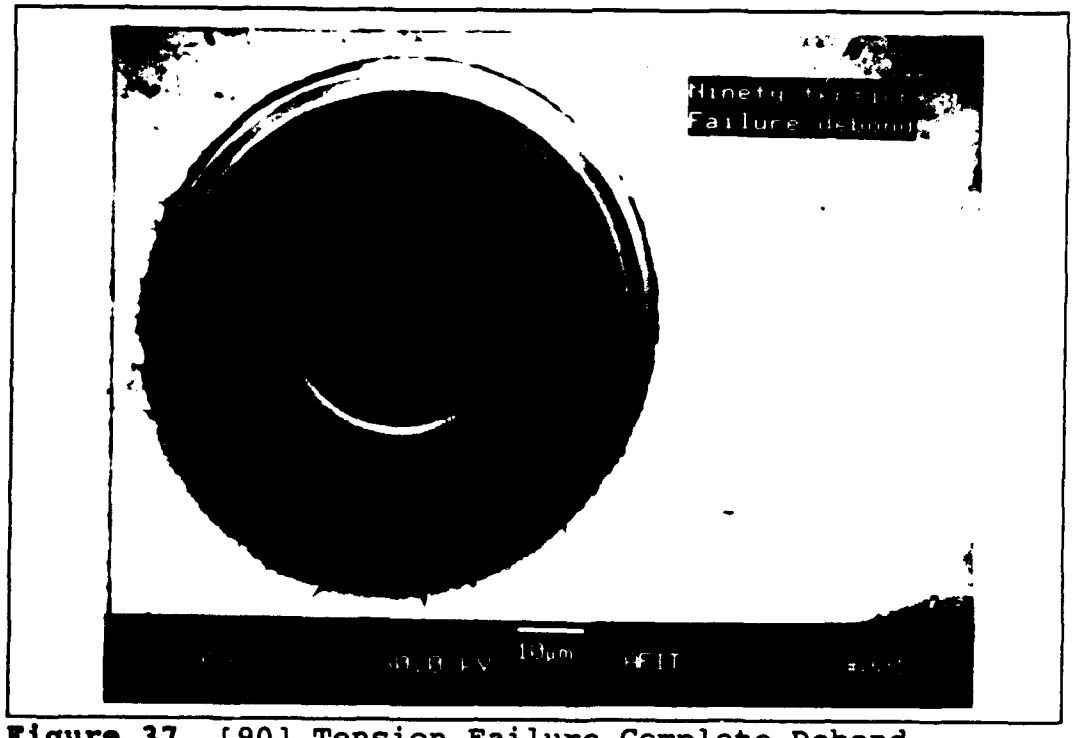

Figure 37 [90] Tension Failure Complete Debond

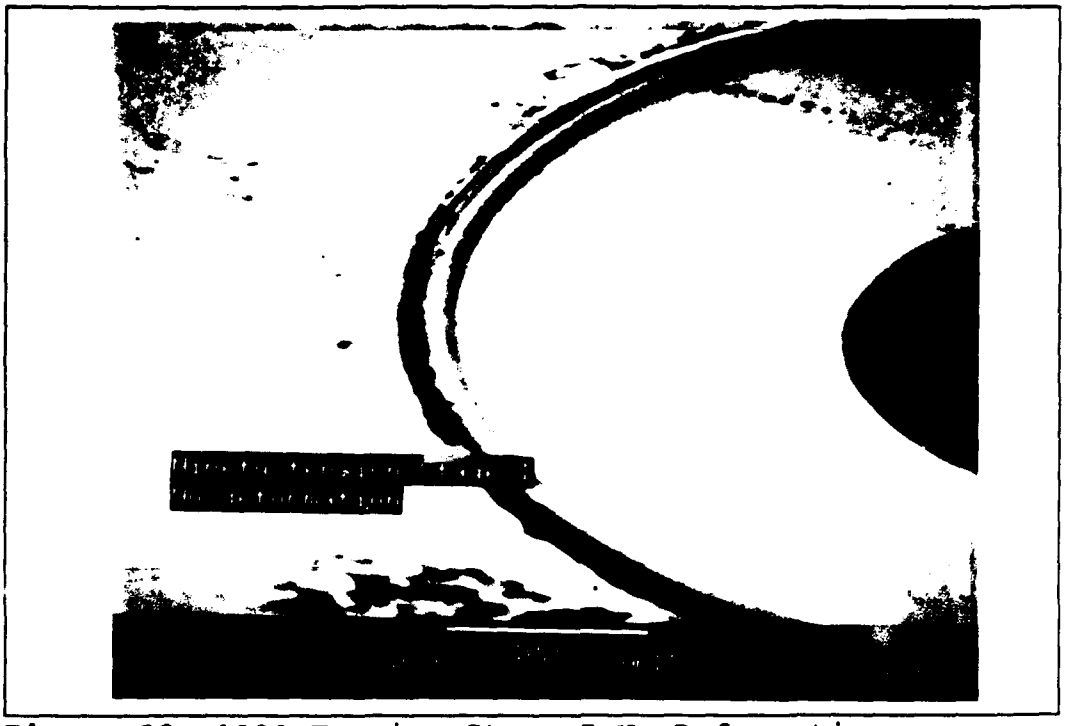

Figure 38 [90] Tension Stage I No Deformation

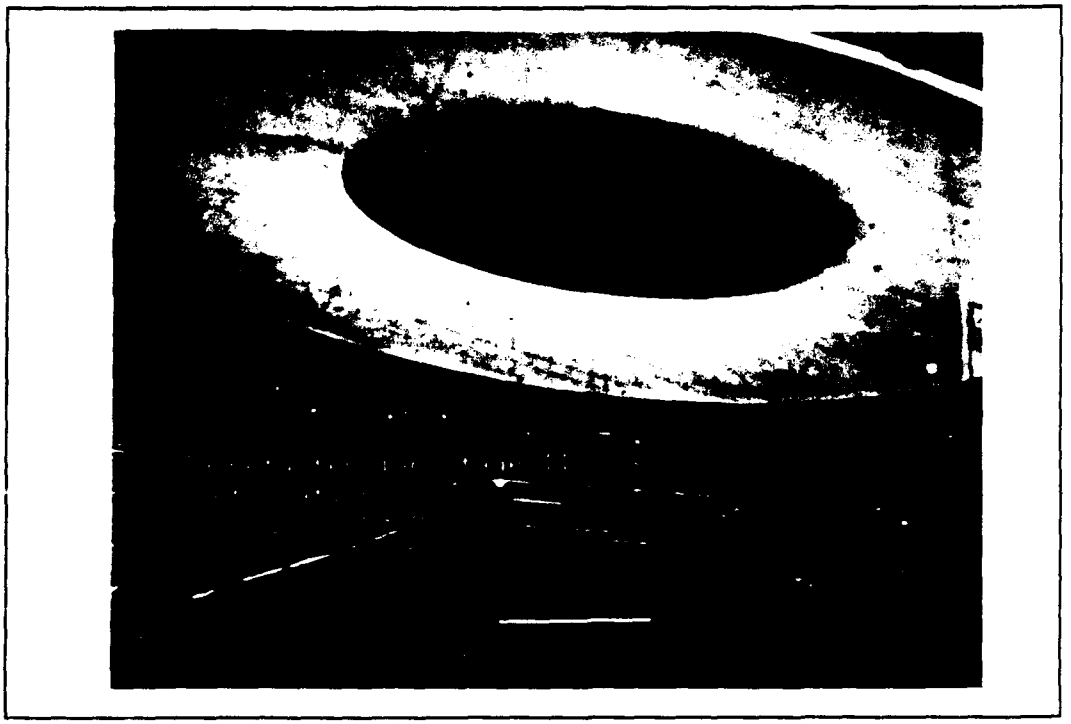

Figure 39 [90] Tension Stage II Deformation

Figure 40 [90] Tension Stage III Deformation

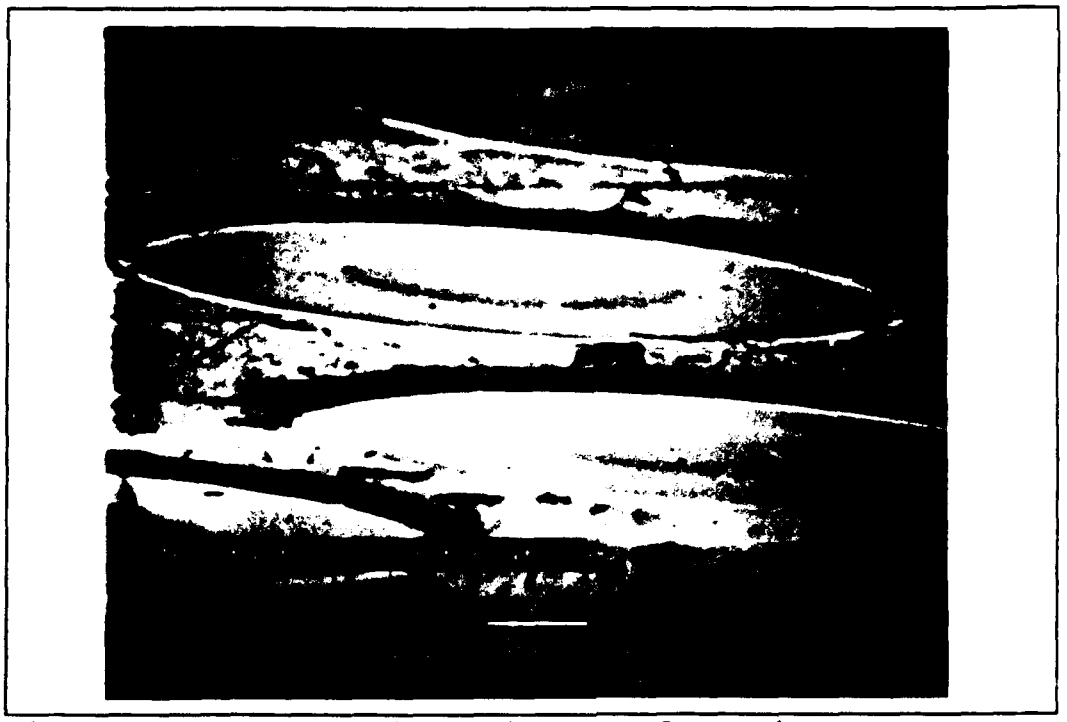

Figure 41 [90] Tension Failure Deformation

Figure 42 [90] Tension Longitudinal Cracks

5.1.2 $[0]_{16}$ Tensile Microstructure. The zero degree laminate exhibited only a two stage stress/strain response. Stage I was completely linear while Stage II was non-linear.

5.1.2.1 $[0]_{16}$ Tensile to Failure. Specimens number 4 and 5 were loaded to failure. The stress/strain curve for specimen number 4 is illustrated in Figure 16 of the Results section. The failed specimen showed both cracked fibers and debonded fibers. Plastic deformation was not observable. The failed specimen exhibited only a small amount of nonlinearity in the stress/strain curve, and Poisson's effect is not observable in the zero degree laminate. Figure 45 shows the cracked and debonded fibers at failure.

The plot of Instantaneous Poisson's Ratio versus longitudinal strain shown in Figure 20 of the Results section shows that Poisson's Ratio stays basically constant until

immediately prior to failure when it decreases rapidly. The plot of longitudinal versus transverse strain, Figure 19, also shows Poisson's ratio to be constant until prior to failure where it begins to drop off.

5.1.2.2 $[0]_{16}$ Tensile Stage I Unload. The second specimen (number 1) was loaded into Stage I and then unloaded. All the strain was completely recoverable, as illustrated in Figure 17 of the Results section. During Stage I, only damage to the fibers was occurring. The fibers were cracking at loads as low as 400 MPa, even though the stress/strain curve remained linear, indicating that the damage in this stage has no affect on the stress/strain response. The cracks in these fibers were not present in the untested specimens. Although, a lot of fibers are broken in this material prior to testing, the fibers that are broken are almost always broken at the molybenum ribbon. The broken fibers illustrated in Figure 43 do not occurr at a molydenum ribbon.. Poisson's Ratio during Stage I remained basically constant to further indicate no change in the properties of the material occurred during Stage I.

5.1.2.3 $[0]_{16}$ Tensile Stage II Unload. The third specimen (number 2) was loaded into Stage II and then unloaded. The stress/strain curve is illustrated in Figure 18 of the Results section. During Stage II, fibers continued to break and the debond of the fibers continued. Poisson's Ratio increased only slightly during Stage II and then just before failure it began to drop off. Stage II deformation was dominated by plasticity. The stress/strain curve shows the load and unload portions of the curve to have nearly the same modulus, 1.14 percent difference, with a small amount of residual strain after unloading. This was the same result as that determined by Newaz and Majumdar (Newaz,

1991: 9). Broken and debonded fibers are shown in Figure 44.

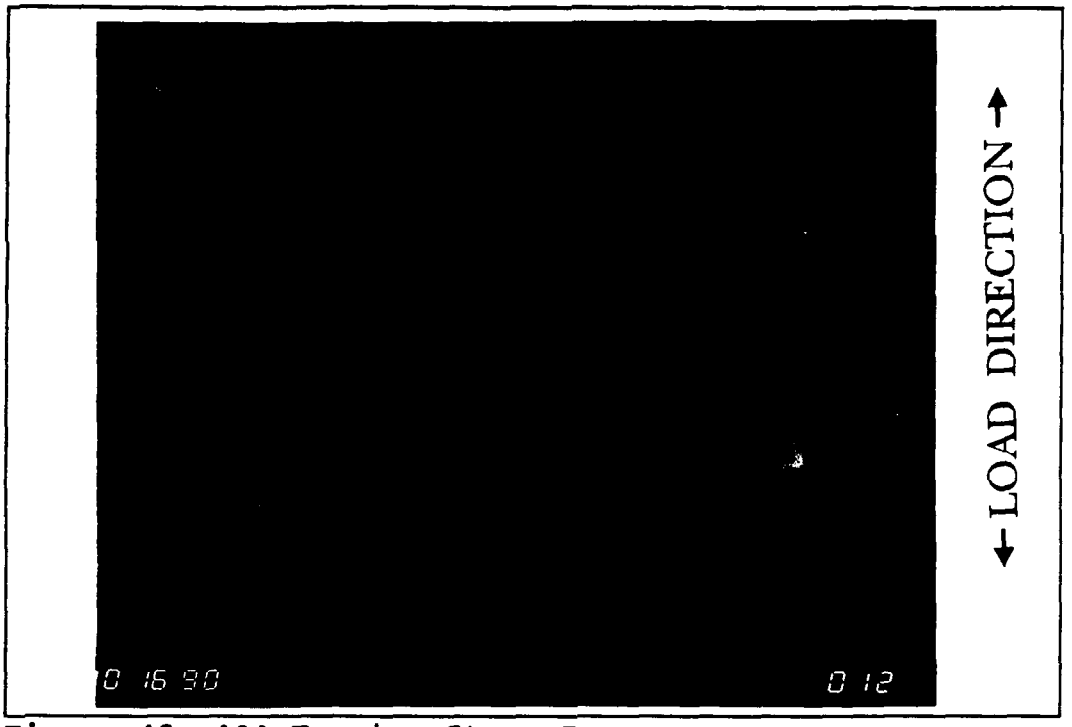

Figure 43 [0] Tension Stage I

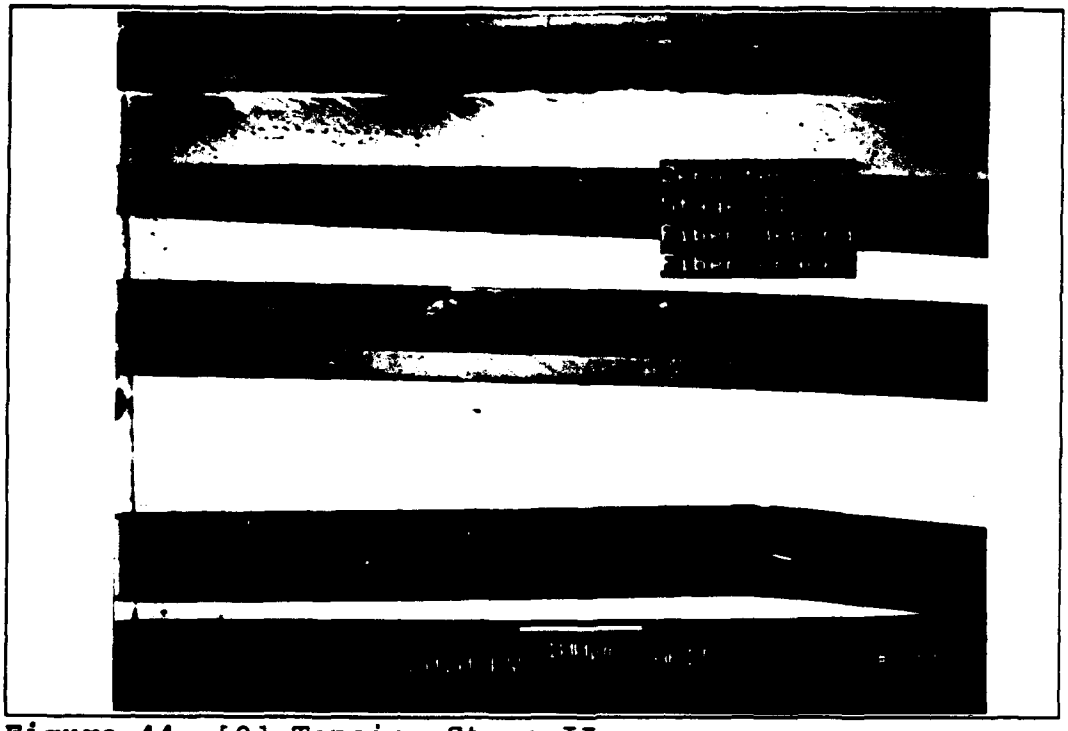

Figure 44 [0] Tension Stage II

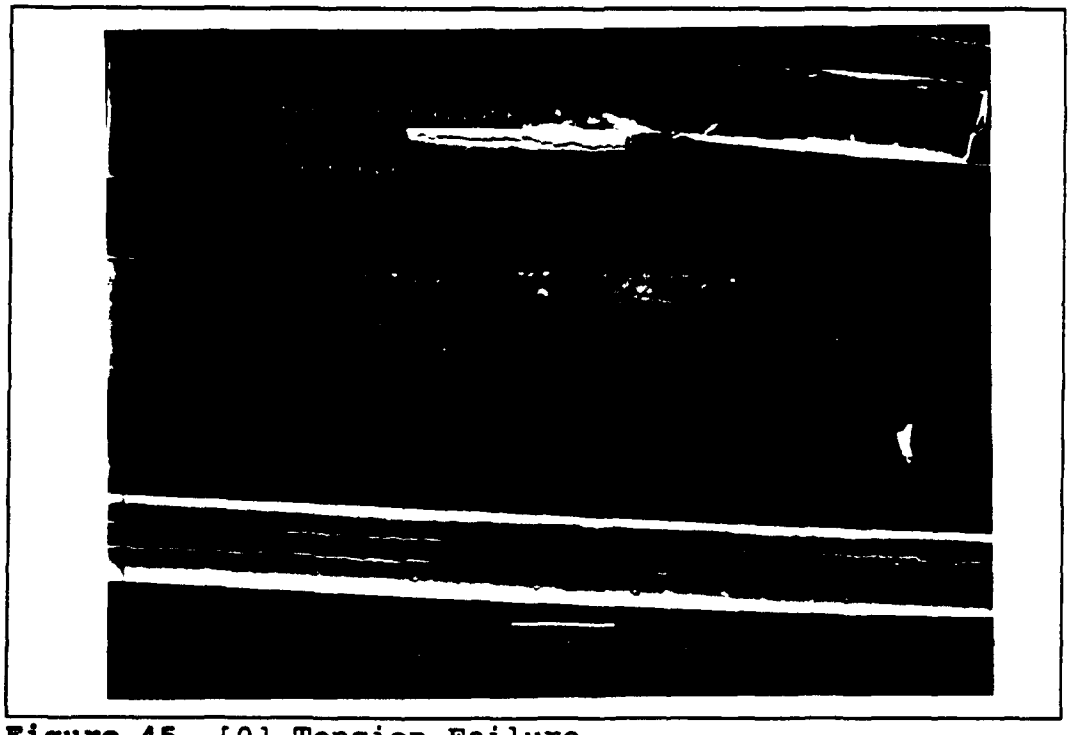

Figure 45 [0] Tension Failure

5.2 Compressive Microstructure. The microstructure and deformation mechanisms of the ninety and zero degree laminates are discussed in this section.

5.2.1 $[90]_{16}$ Compressive Microstructure. The ninety degree laminate exhibited a two stage stress/strain response in compression as shown by Figure 23 of the Results section.

5.2.1.1 $[90]_{16}$ Compression to Failure. The first specimen (number 15) was loaded to failure. The stress/strain curve, the instantaneous Poisson's Ratio versus longitudinal strain, and the longitudinal versus transverse strain curves are illustrated in Figures 23 - 27 of the Results section. Fiber debonding, matrix cracking, permanent plastic deformation and fiber breaking are all apparent in this specimen (number 15). These characteristics are illustrated in Figure 48.

5.2.1.2 $[90]_{16}$ Compression Stage I Unload. The second specimen (number 16) was loaded into Stage I and then unloaded. The stress/strain curve is shown in Figure 24 of the Results section. All strain is fully recoverable upon unloading. Unlike tension, any debond that may have occurred during compression, did close up. The lack of permanent fiber debond is illustrated in Figure 46.

Poisson's Ratio remains basically constant during Stage I, indicating that there is no real change in material properties. This curve is shown in Figure 27 of the Results section. The longitudinal versus transverse strain curve, Figure 26, further documents that Poisson's Ratio is not changing.

5.2.1.3 $[90]_{16}$ Compression Stage II Unload. The third specimen (number 14) was loaded into Stage II and then unloaded. The stress/strain curve for this specimen

is shown in Figure 25 of the Results section. The initial modulus is 109.99 GPa and the modulus upon unloading is 107.1 GPa. This is a decrease of only 2.6 percent. This small decrease indicates that the dominant deformation mechanism in Stage II is plasticity with some damage. The damage is seen as fiber debonding. The plastic deformation is seen as the elongation of the matrix around the fiber perpindicular to the load direction. These are illustrated in Figure 47.

Poisson's Ratio during Stage II leveled off and then decreased toward failure. Longitudinal strain versus transverse strain also showed this result. Unloading of the specimen showed there to be a large amount of residual strain. The residual strain indicates that plasticity was present during Stage II and the decrease in Poisson's Ratio with the decrease in modulus on unloading both indicate that damage was present during Stage II.

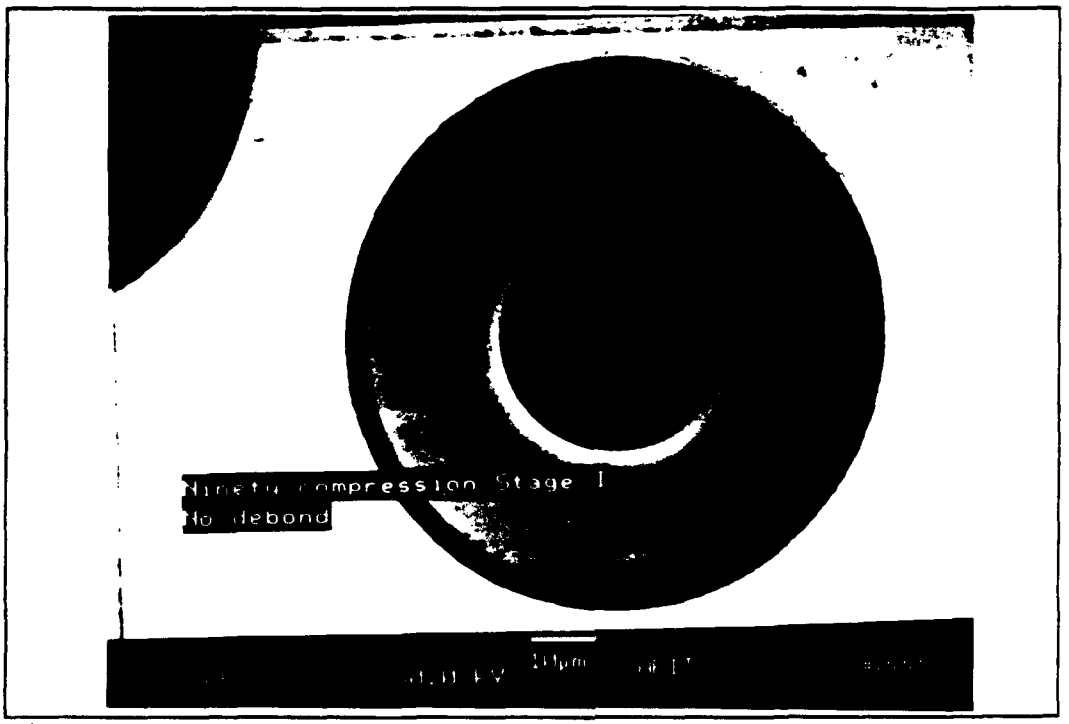

Figure 46 [90] Compression Stage I

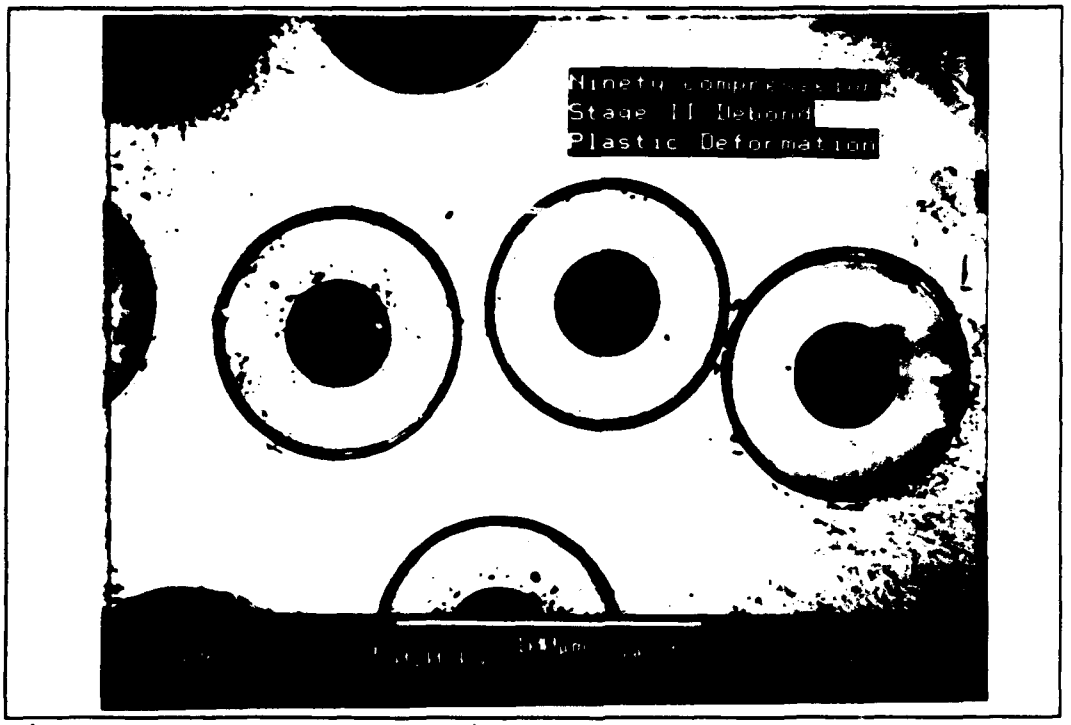

Figure 47 [90] Compression Stage II

Figure 48 [90] Compression Failure

5.2.2 $[0]_{16}$ Compressive Microstructure. The zero degree laminate exhibited a two stage stress/strain response in compression. This response is illustrated in Figure 28 of Results. Due to the problems associated with such high loads and high strains, complete zero degree compression failure data will not be presented. The test was run (specimen number 6), however, and the failure load and initial modulus was collected. These data were used to determine Stage I and Stage II. Data was extrapolated from the point of strain gage debond to create Figure 28 of the Results section. Figure 51 shows the debond between fiber and matrix of the failed specimen.

5.2.2.1 $[0]_{16}$ Compression Stage I Unload. The second specimen (number 7) was loaded into Stage I and then unloaded. The modulus was 197.67 GPa. The strain was fully recoverable. The stress/strain curve is shown in Figure 29 of the Results section. Poisson's ratio data were collected from specimen number 8. Instantaneous Poisson's ratio versus longitudinal strain is shown in Figure 32 of the Results section. During Stage I, Poisson's Ratio increases and then levels off, just as it did in the ninety degree laminate. Longitudinal versus transverse strain behaved just as it did in the ninety degree laminate. There was no apparent fiber debonding or damage of any kind visible on this specimen. This can be seen in Figure 49.

5.2.2.2 $[0]_{16}$ Compression Stage II Unload. The third specimen (number 8) was loaded into Stage II and then unloaded. The stress/strain curve for this specimen is shown in Figure 30 of the Results section. The initial modulus was 189.5 GPa and the modulus upon unloading was 120.9 GPa. This is a 36.2 percent decrease in stiffness, indicating that damage is present. During Stage II, Poisson's Ratio stays constant and

then begins to drop off rapidly, further indicating the presence of damage. This result was also observed by the longitudinal versus transverse strain curve. There is also a considerable amount of residual strain after unloading. These three factors indicate that plasitcity and damage are both occurring during Stage II. Due to the amount of residual strain and the slight decrease in Poisson's Ratio, plasticity is probably the dominent deformation mechanism during Stage II, but damage also had to play a major role due to the large decrease in stiffness. Figure 50 shows the damage to the fibers and the debond of the fibers. Plasticity was present because of the residual strain, but there was no way to observe the plastic deformation.

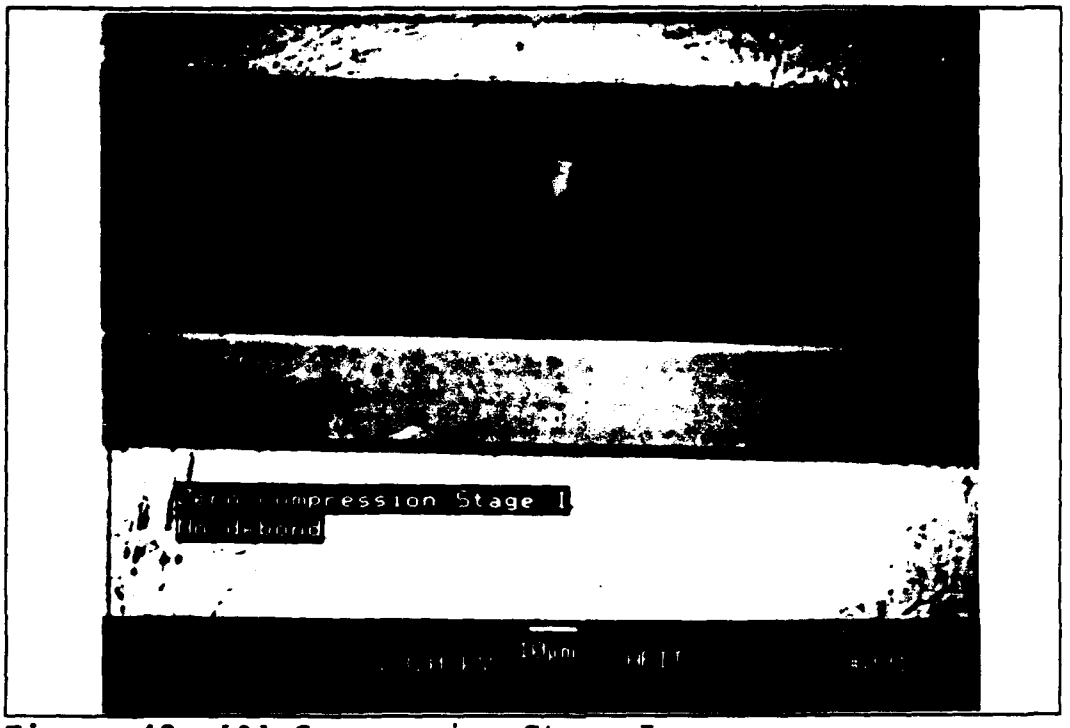

Figure 49 [0] Compression Stage I

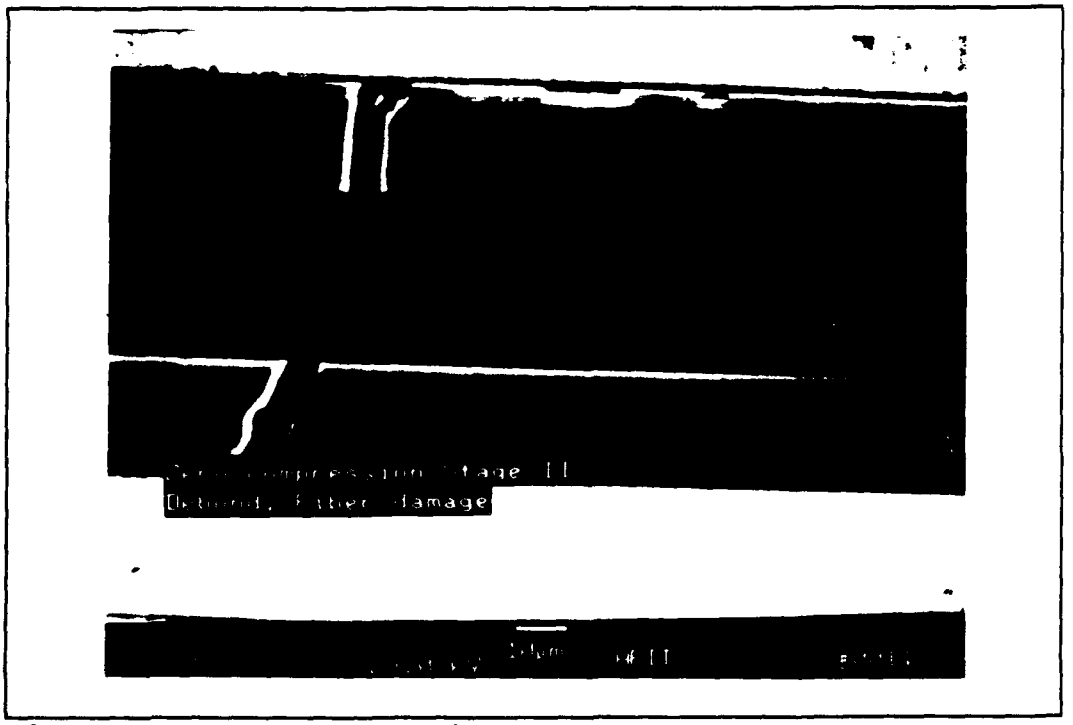

Figure 50 [0] Compression Stage II

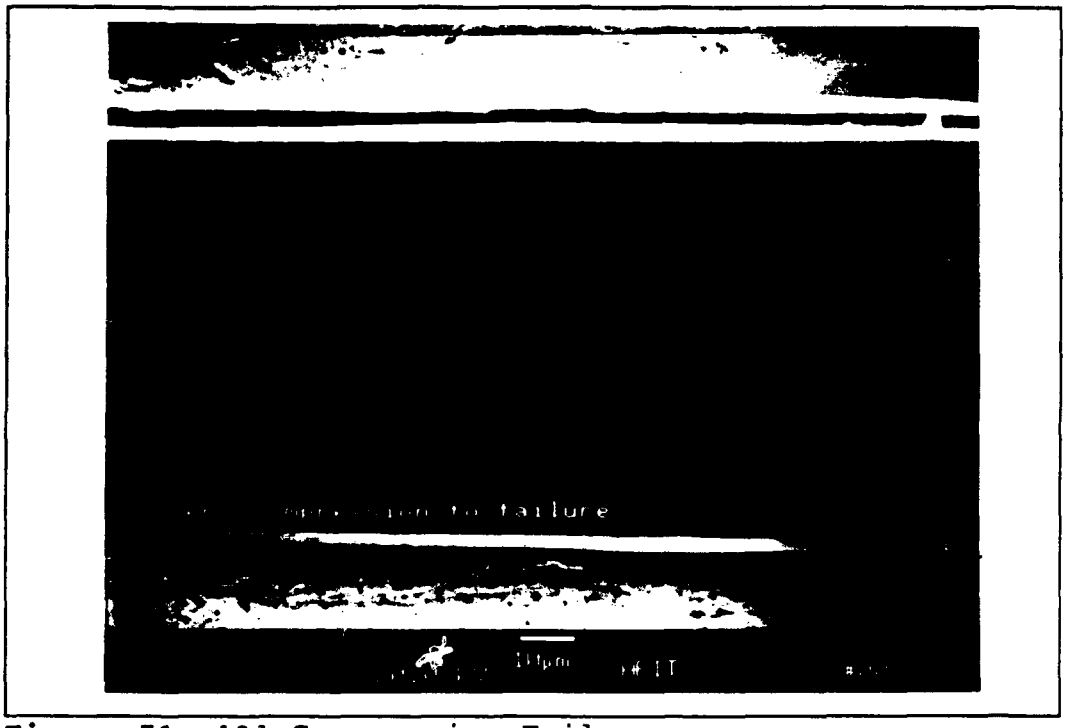

Figure 51 [0] Compression Failure

5.3 Tensile/Compression Comparison. This section will compare the tensile and compressive results.

5.3.1 $[90]_{16}$ Tensile and Compression. The ninety degree laminate exhibited the same initial modulus in both tension and compression. It had a three stage stress/strain response in tension, but only a two stage stress/strain response in compression.

In tension, damage played a major role in the stress/strain response. In Stage II, damage was the dominant deformation mechanism, but damage was still present during Stage III. The damage encountered during Stage II was fiber debonding and longitudinal cracking of the matrix. This behavior has been attributed to the first change in slope of the stress/strain curve illustrated in Figure 10 of the Results section (Rattray, 1991: 62). In compression, however, plasticity played the dominant role with damage being present but not influential in the stress/strain response. Since the compression curve did not exhibit an early debond like tension, compression did not have a three stage stress/strain response. The two stage stress/strain response of the ninety degree laminate in compression and the lack of a fiber debond, give more credence to the theory that the fiber debond in tension causes the first non-linear response.

It is very interesting to note the failure strengths of tension and compression. The ninety degree laminate failed at 328 MPa in tension and 893 MPa in compression. The ninety degree laminate is **2.7** times as strong in compression as it is in tension. The failure stress/strain curves for the ninety degreee laminate in tension and compression is illustrated in Figure 52.

5.3.2 $[0]_{16}$ Tensile and Compression. The zero degree laminate exhibited a two

stage stress/strain response in both tension and compression. The zero degree laminate also exhibited the same modulus in tension and compression.

In tension, plasticity was the main deformation mechanism, but in compression, damage also played a substantial role. This could be due to the high amount of strain, 2 percent, that is seen in compression as opposed to .8 percent seen in tension.

The ultimate strength in tension and compression for the zero degree laminate were also substantially different. The zero degree laminate failed at 1.4 GPa in tension and at 2.4 GPa in compression. Therefore, the zero degree laminate is 1.7 times stronger in compression as it is tension. The failure stress/strain curves for the zero degree laminate in tension and compression is illustrated in Figure 53.

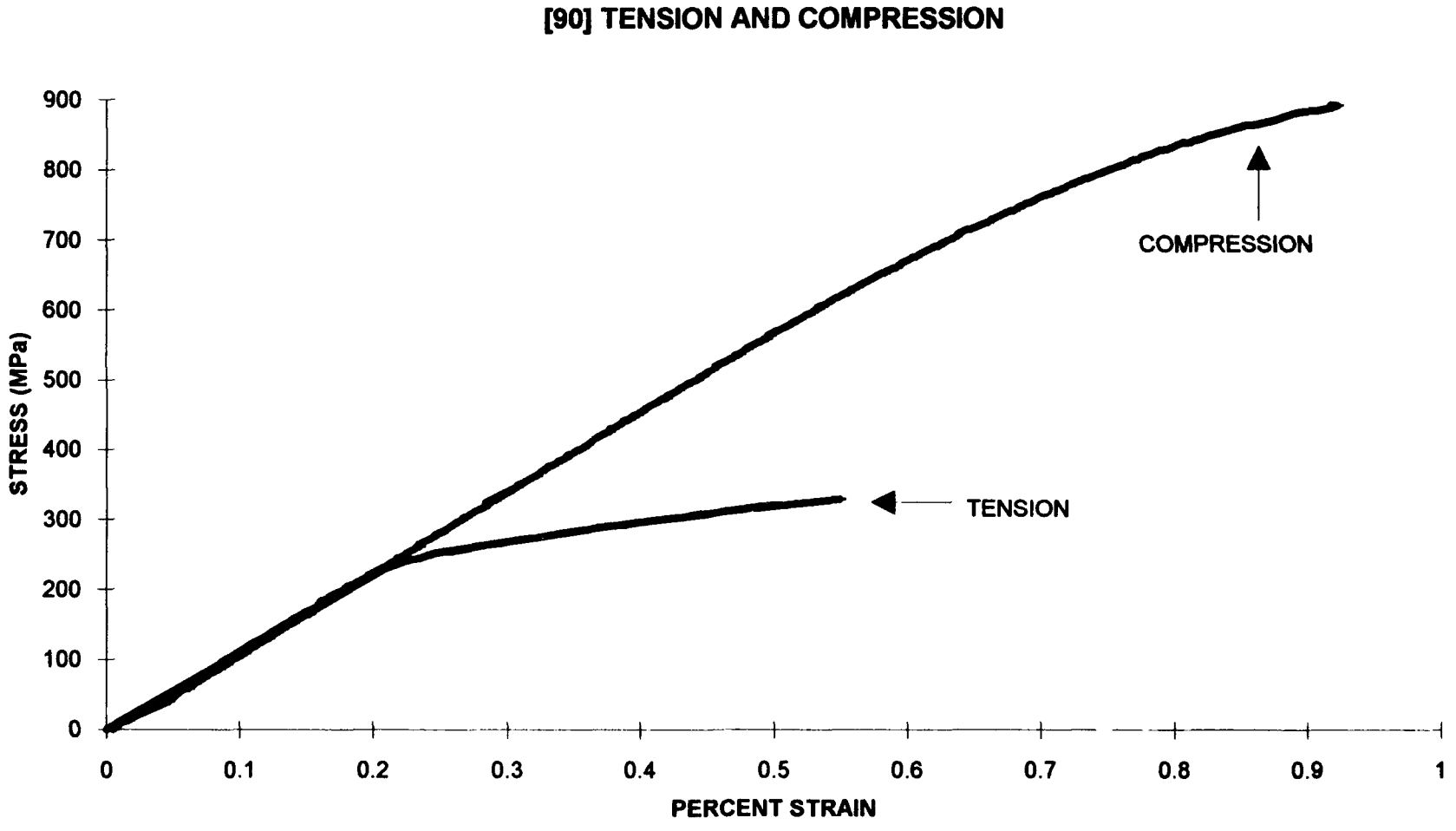
[90] TENSION AND COMPRESSION
900
800
700
600
500
400
300
200
100
0
STRESS (MPa)
COMPRESSION
TENSION
0
0.1
0.2
0.3
0.4
0.5
0.6
0.7
0.8
0.9
1
PERCENT STRAIN

Figure 52

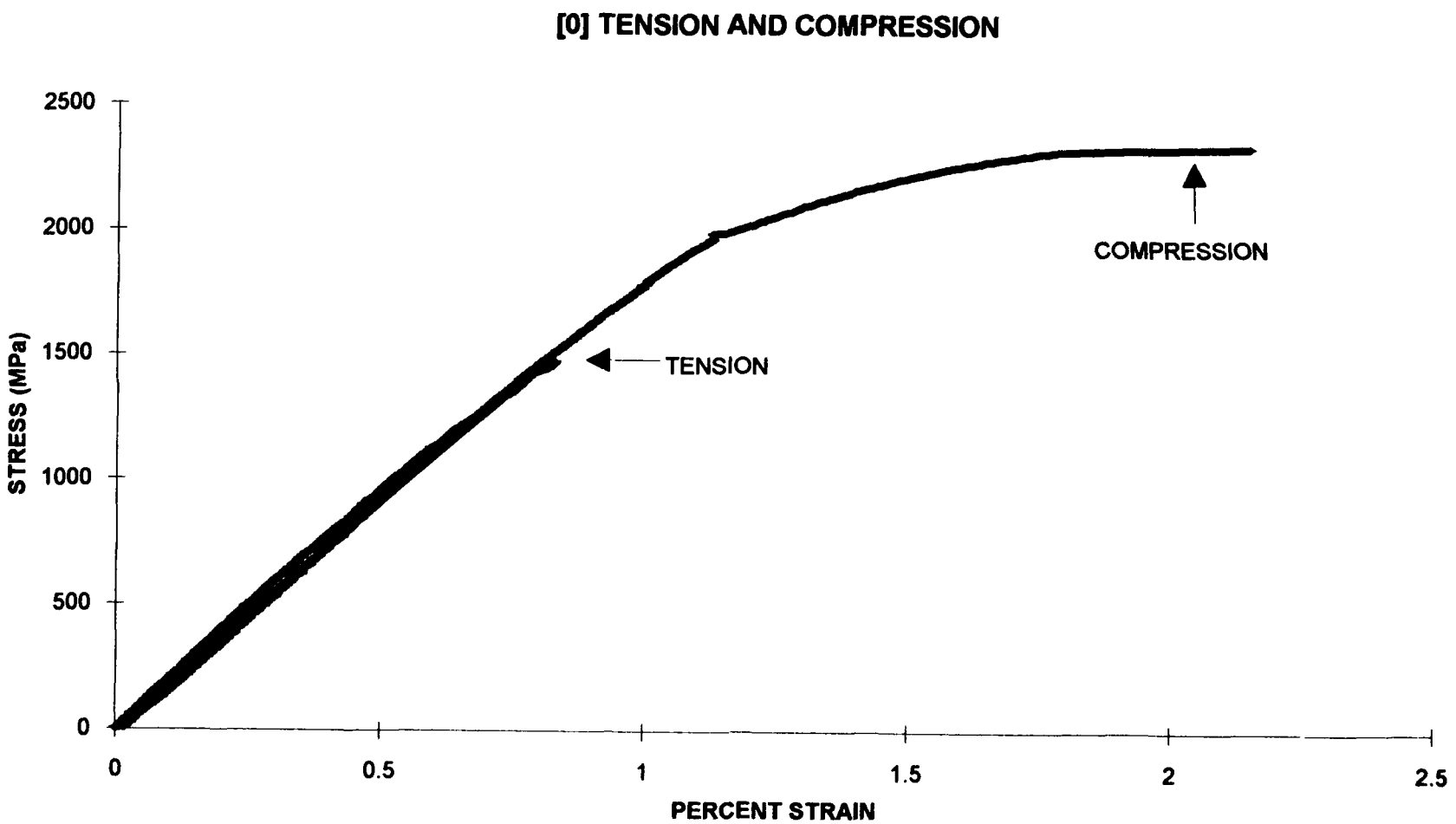
[0] TENSION AND COMPRESSION
2500
2000
1500
1000
500
0
STRESS (MPa)
0
0.5
1
1.5
2
2.5
PERCENT STRAIN
TENSION
COMPRESSION

Figure 53

5.4 Tensile and Compressive Failure Surfaces. Tensile and compressive experiments showed very different failure surfaces.

5.4.1 $[90]_{16}$ Tensile Failure. The ninety degree tension specimen failed due to matrix failure. The fracture was basically flat, with ductile fracture of the matrix between fibers. The flat fracture surface is shown in Figure 54, and the ductile matrix failure is shown in Figure 55. Ductile fracture is determined by the dimples seen in the matrix.

5.4.2 $[0]_{16}$ Tensile Failure. The zero degree laminate failed due to brittle fracture of the fibers and ductile fracture of the matrix. This resulted in the irregular shape of the fracture. This is shown in Figure 56. Figure 57 shows the ductile matrix failure and the brittle fiber failure with some fiber pull out. Brittle fiber failure is shown by the flat surface of the failed fiber.

5.4.3 $[90]_{16}$ Compressive Failure. The ninety degree laminate failed in shear under compression. This shear failure is shown in Figure 21 of the Results section. The failure surface showed the matrix to be plastically sheared over the fibers. The shear fracture surface is illustrated in Figure 58. This figure illustrates how the matrix "slid" over itself and the fibers.

5.4.4 $[0]_{16}$ Compressive Failure. The zero degree laminate also failed due to shear. This shear failure is shown in Figure 22 of the Results section. The fracture surface was torn up when the specimen failed. The shear failure is still evident, but when the specimen failed, the two failure surfaces collided with the IITRI fixture and were actually forced up inside the grips.

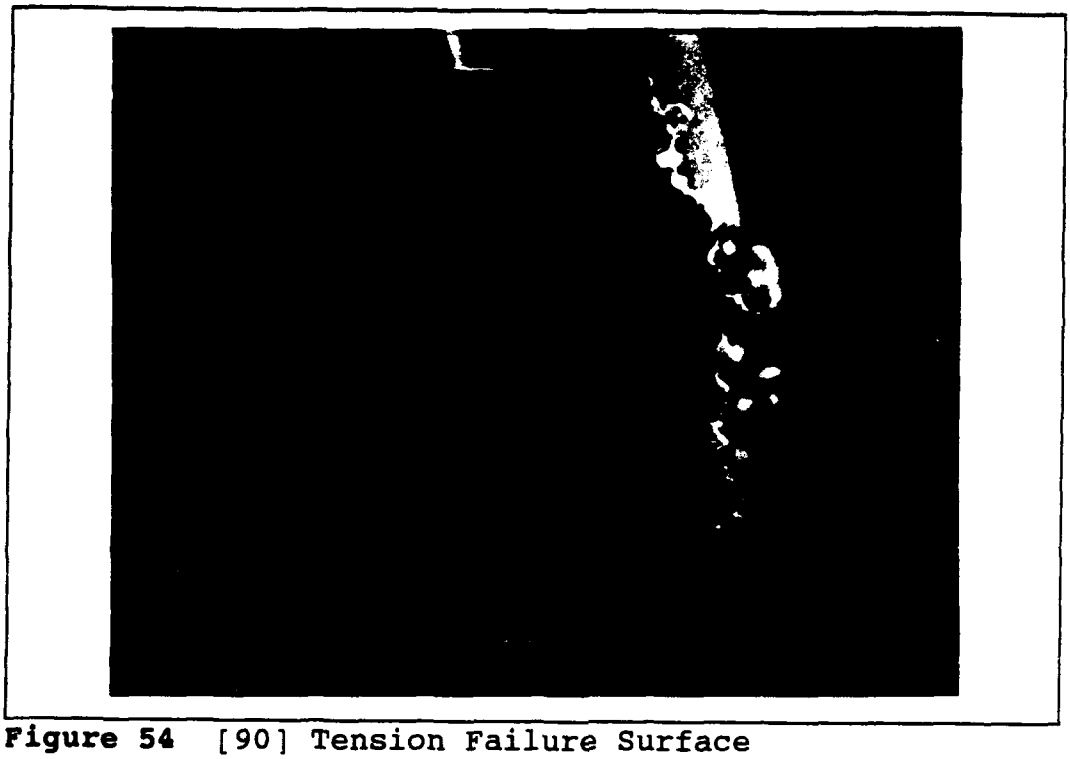

Figure 54 [90] Tension Failure Surface

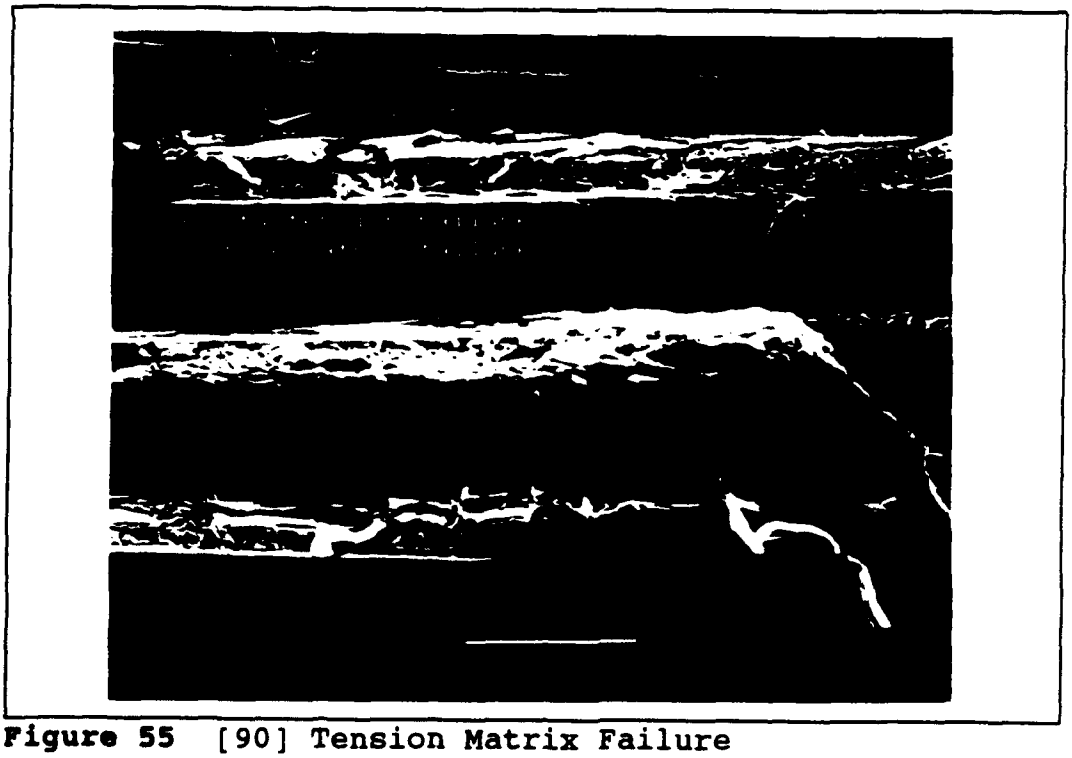

Figure 55 [90] Tension Matrix Failure

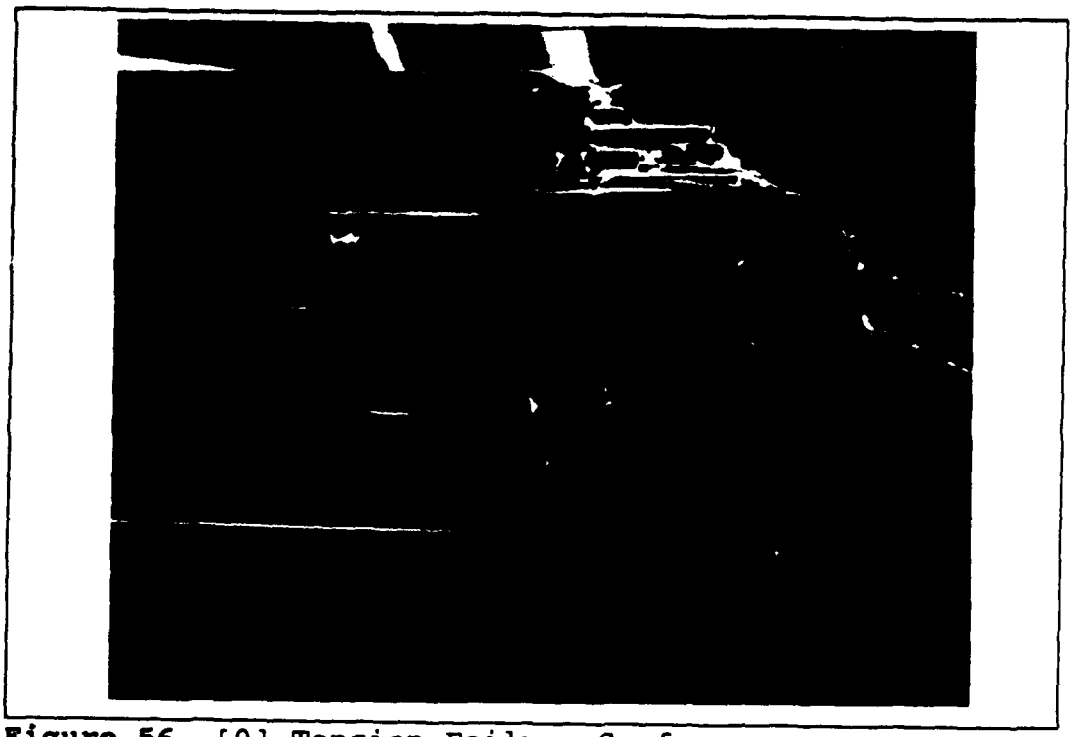

Figure 56 [0] Tension Failure Surface

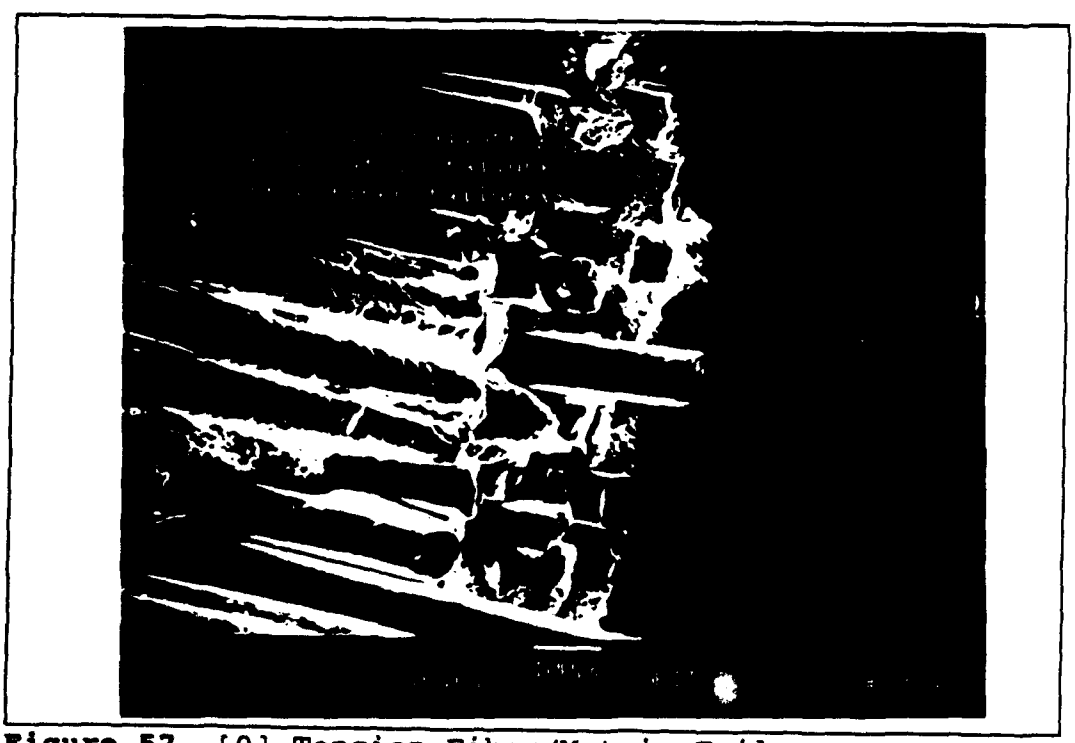

Figure 57 [0] Tension Fiber/Matrix Failure

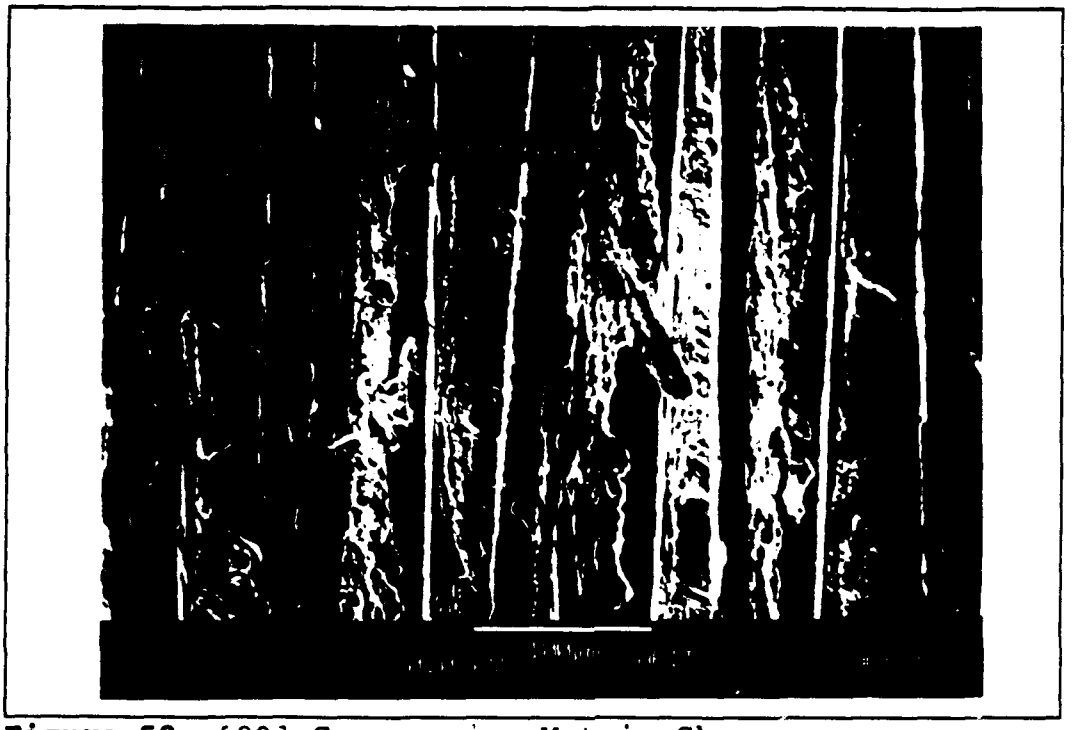

Figure 58 [90] Compression Matrix Shear

5.5 Comparison of Initial Modulus with Theoretical Modulus. The Halpin-Tsai Equations and the Rule of Mixtures were used to calculate the theoretical modulus of this material.

5.5.1 $[90]_{16}$ Initial Modulus. Both the initial tensile and compressive moduli for this material were the same. The average initial modulus was 115.4 GPa.

The Halpin-Tsai Equations were used to calculate the transverse modulus. This calculation is contained in Appendix A. The theoretical transverse modulus, E_2, for this material is 173.24 GPa. This is a 50.1 percent difference from the actual value. The Halpin-Tsai Equations do not predict transverse modulus very well. Therefore, it has to be assumed that the Halpin-Tsai Equations do not predict the shear modulus very well either, because it is also an off axis property. The Halpin-Tsai Equations can, however, be used to bound the transverse modulus, the 50.1 percent difference assumes a perfect fiber matrix bond. According to Jones, ξ is a measure of the effectiveness of the fiber reinforcement of the composite (Jones, 1975: 120). Therefore, for zero bond strength $\xi=0$ and the Halpin-Tsai equation reduces to the following:

$$\frac{1}{M} = \frac{V_f}{M_f} + \frac{V_m}{E_m} \qquad (6)$$

Which is the Rule of Mixtures for the off axis properties. Using this equation, E_2 is 151.4 GPa. This is still a 31.2 percent difference. Rattray has suggested that since the fibers have debonded, zero bond strength, they are not aiding the composite modulus and the stiffness of the fiber $E_f = 0$ (Rattray, 1991: 47). This results in the following Halpin-Tsai equation:

$$E_2 = \frac{E_m(1-V_f)}{1+\frac{1}{2}V_f} \qquad (7)$$

This assumption yields, E_2 = 55.9 GPa. This is 51.6 percent below the actual value obtained through testing. Therefore, E_2 can be bounded using the Halpin-Tsai equations, but a "good" prediction of the value for E_2 can not be acheived.

5.5.2 $[0]_{16}$ Initial Modulus. The tensile and compressive modulus for this material was also the same. The average initial modulus was 197.51 GPa.

The Rule of Mixtures was used to calculate the longitudinal modulus. This calculation is contained in Appendix A. The theoretical longitudinal modulus, E_1, for this material is 196.62 GPa. This is less than a 1 percent difference. The Rule of Mixtures is, therefore, a very effective was to predict the longitudinal modulus.

5.6 Manufacturing. During this thesis work, some manufacturing problems have been observed. The most prominent of these problems is that the molybdenum ribbon used to weave the fibers was breaking the fibers. A section of untested material was slowly dissolved with acid to reveal the first layer of fibers. This process revealed that nearly every fiber was fractured somewhere at the molybdenum weave. Figures 59 and 60 show the dissolved specimen, with a spacing of one molydenum weave. All but two fibers displayed in these figures are not broken. It can be assumed, however, that the unbroken fibers are in fact broken at another molybdenum weave in the material.

The broken fibers should be eliminated but as was seen above, the broken fibers

do not affect the initial modulus in the one direction. These broken fibers, however, may be able to explain why the Halpin-Tsai Equations do not predict the transverse modulus.

There is also a quality control issue that should be addressed. During the investigation of the microstructure, a rather interesting material was found in specimen number 14. This interesting material was one SCS-6 fiber held in the weave with the SCS-9 fibers. This fiber is shown in Figure 61. Foreign materials in the weave should be avoided, even though this fiber did not cause the specimen to fail prematurely or even to fail at its location.

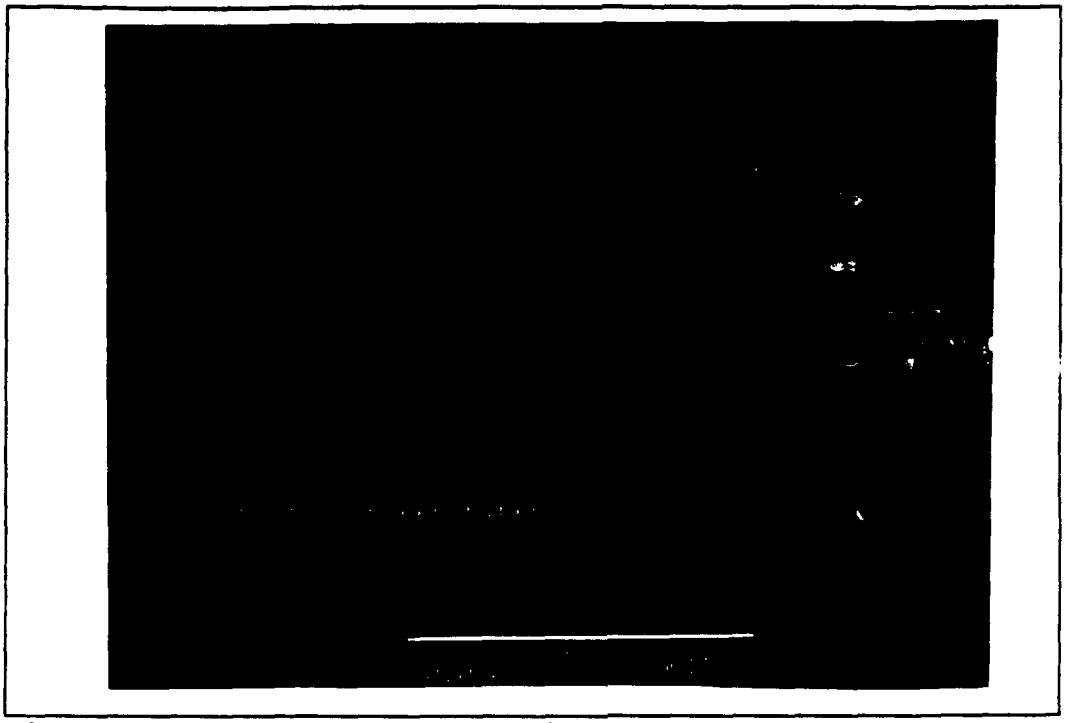

Figure 59 Untested Broken Fibers

Figure 60 Untested Broken Fibers

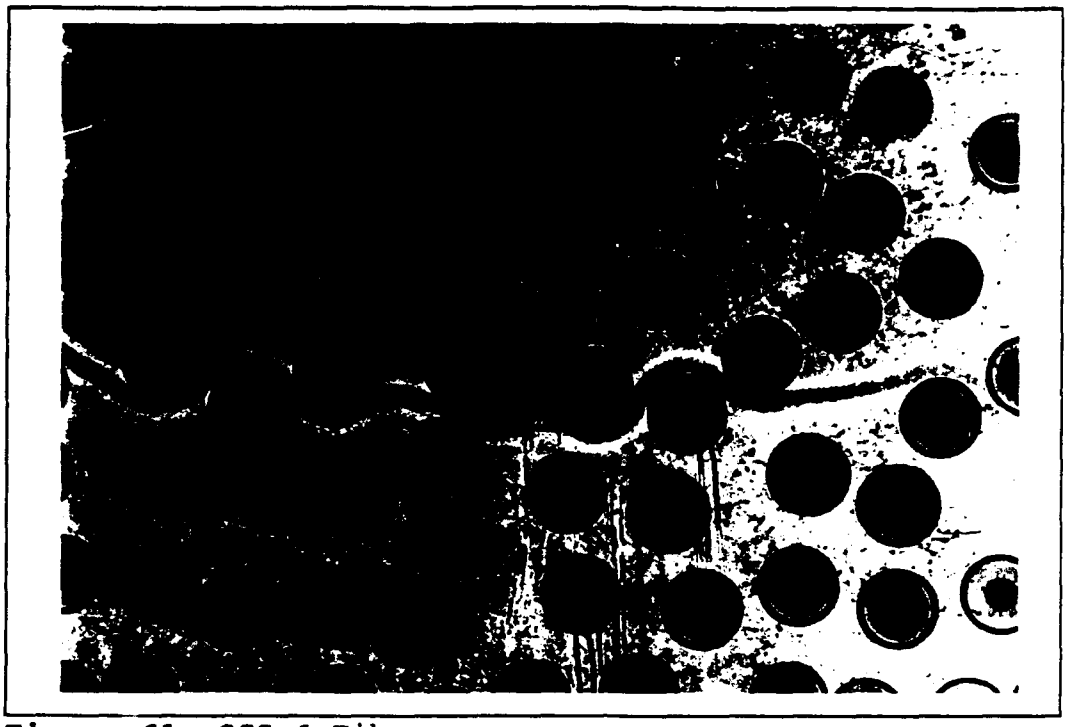

Figure 61 SCS-6 Fiber

VI. Conclusions and Recommendations

6.1 Conclusions. The experimentation and research conducted during this thesis has characterized the modulus for SCS-9/β 21S in both tension and compression as well as the primary deformation mode involved during each phase of the stress/strain curve. The following can be concluded:

1. The ninety degree laminate has the same initial modulus in tension and compression.

2. The zero degree laminate has the same modulus in tension and compression.

3. The ninety degree laminate has a three stage stress/strain response in tension. Stage I behaves as a linear-elastic solid. Stage II is dominated by damage with some plasticity. The damage in Stage II is fiber debonding and longitudinal matrix cracking. Stage III is dominated by plasticity with continuing damage. The plasticity in Stage III is seen as protruding fibers due to Poisson's effect.

4. The zero degree laminate has a two stage stress/strain response in tension. Stage I behaves as a linear elastic solid. Stage II is dominated by plasticity with some damage.

5. The ninety degree laminate has a two stage stress/strain response in compression. Stage I behaves as a linear-elastic solid. Stage II is dominated by plasticity with some damage. The damage in Stage II is seen as matrix cracks and fiber debonds. The plasticity is seen as plastic deformation in the matrix around the fibers.

6. The zero degree laminate has a two stage stress/strain response in compression.

Stage I behaves as a linear-elastic solid. Stage II is dominated by plasticity with damage. Damage is seen as fiber cracks and fiber debonding.

7. The ninety degree laminate has an ultimate strength 2.7 times as great in compression as in tension.

8. The zero degree laminate has an ultimate strength 1.7 times as great in compression as in tension.

The overall result of this work is illustrated in Figure 62. This figure shows the tensile and compressive stress/strain curves of the ninety degree and zero degree laminate with the tensile stress/strain curve for the matrix.

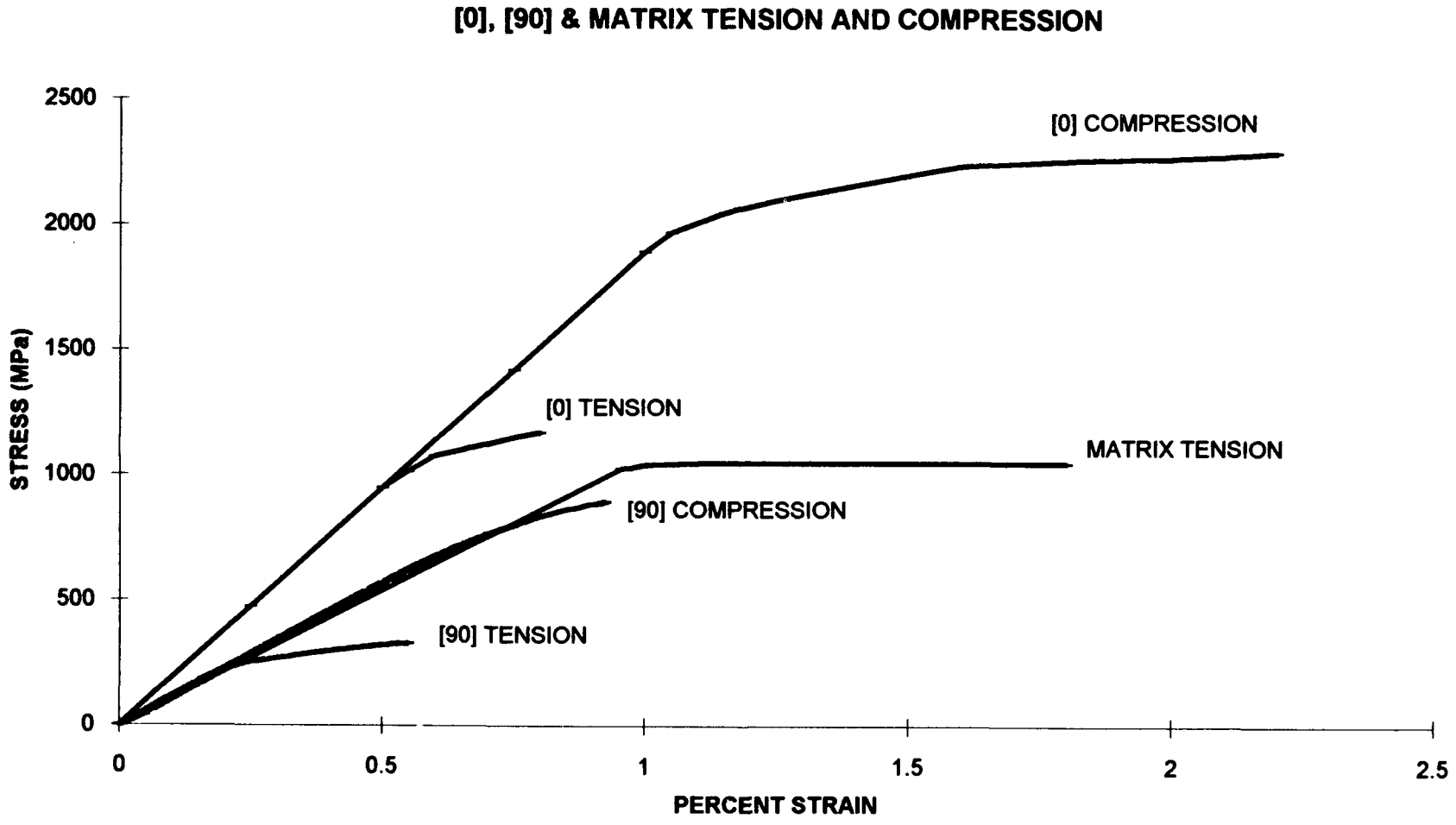
[0], [90] & MATRIX TENSION AND COMPRESSION
2500
2000
1500
1000
500
0
STRESS (MPa)
[0] COMPRESSION
[0] TENSION
MATRIX TENSION
[90] COMPRESSION
[90] TENSION
0
0.5
1
1.5
2
2.5
PERCENT STRAIN

Figure 62

6.2 Recommendations. This report fully characterized the room temperature tensile and compressive modulus of SCS-9/β 21S unidirectional composite. This leads directly to two more areas that need to be investigated. (1) Characterizing the elevated temperature unidirectional composite in tension and compression. (2) Characterizing a laminate in tension and compression at room and elevated temperature. The most likely laminate to choose is the [0/90] laminate. The [0/90] laminate will allow correlation with the work done here.

Bibliography

Agarwal, Bhagwan D. and Lawrence J. Broutman. *Analysis and Performance of Fiber Composites*. New York: John Wiley and Sons, Inc., 1990.

Ahmad, Jalees. NIC Meeting. "β 21S Material Characterization Data." 28 - 29 January 1992.

Brown, Alan S. "NASP Funds Titanium Composite Plant," *Aerospace America*, 66-67 (August 1992).

Hansen, J. G. LTC. WL/MLLN. Personal Interviews. May - Nov 1992.

Jones, Robert M. *Mechanics of Composite Materials*. New York: Hemisphere Publishing Corporation, 1975.

Kenaga, D. and others. "The Characterization of Boron/Aluminum Composite in the Nonlinear Range as an Orthotropic Elastic-Plastic Material," *Journal of Composite Materials, 21*: 516-531 (June 1987).

Majumdar, Bhaskar S. Personal Interview. UES WPAFB-WL/MLLM. 22 July 1992.

Majumdar, Bhaskar S. Personal Interview. UES WPAFB-WL/MLLM. 21 October 1992.

Majumdar, B. S. and G. M. Newaz. "Inelastic Deformation of Metal Matrix Composites: Plasticity and Damage Mechanisms," submitted to the *Philosophical Magazine*, (June 1991).

Majumdar, B. S. and G. M. Newaz. "Inelasitc Deformation of Metal Matrix Composites: Compression and Fatique," personal communication.

Marshall, D. B. and others. "Transverse Strengths and Failure Mechanisms in Ti_3AL/SiC Composites," submitted for publication, personal communication.

Newaz, G. M. and B. S. Majumdar. "Failure Modes in Transvers MMC Lamina Under Compression," submitted to the *Journal of Material Science and Letters*, (June 1992).

Newaz, G. M. and B. S. Majumdar. "Deformation and Failure Mechanisms in Metal Matrix Composites," personal communication.

Rattray, Jeffrey, Capt. *Tensile Strength Characterization of a Metal Matrix Composite with Circular Holes*. MS Thesis, AFIT/GAE/ENY/91D-24. School of Engineering, Air Force Institute of Technology (AU), Wright-Patterson AFB OH, December 1991

APPENDIX A

SCS-9-Beta 21S

Determine Lamina Properties

Material Properties of the Fiber:

Diameter: $D = 81.2 \cdot 10^{-6} \cdot m$

Density: $\rho = 2.685 \cdot 10^{3} \cdot \frac{kg}{m^3}$

Tensile Strength: $\sigma_1 = 3.44810^{3} \cdot MPa$

Modulus: $E_f = 3.24 \cdot 10^{5} \cdot MPa$

Volume Fraction: $V_f = .40$

Poisson's Ratio: $\nu_\phi = .214$ (Hansen, 1992)

Material Properties of the Matrix:

Density: $\rho = .178$

Modulus: $E_m = 1.117 \cdot 10^{5} \cdot MPa$

Tensile Strength: $\sigma_2 = 1.148 \cdot 10^{3} \cdot MPa$

Volume Fraction: $V_m = .60$

Poisson's Ratio: $\nu_\mu = .3$ (NIC Meeting Slides)

Determination of Modulus Parallel to the Fibers:

$$E_1 = E_f \cdot V_f + E_m \cdot V_m$$

Determination of Poisson's Ratio for the Lamina:

$$\nu_{12} = \nu_\phi \cdot V_f + \nu_\mu \cdot V_m$$

Determine Shear Modulus for Matrix and Fiber:
- Assume Matrix and Fiber are Isotropic

$$G_m = \frac{E_m}{\left[2 \cdot \left[1 + \nu_\mu\right]\right]}$$

$$G_f = \frac{E_f}{\left[2 \cdot \left[1 + \nu_\phi\right]\right]}$$

Determination of Lamina Shear Modulus and Modulus Perpindicular to the Fiber Direction:
- Use the Halpin-Tsai Equations (Jones, p114-115)

$$\xi_\Gamma = 1$$

$$\eta_\Gamma = \frac{\left[\left[\frac{G_f}{G_m}\right] - 1\right]}{\left[\left[\frac{G_f}{G_m}\right] + \xi_\Gamma\right]}$$

$$\xi_E = 2$$

$$\eta_E = \frac{\left[\left[\frac{E_f}{E_m}\right] - 1\right]}{\left[\left[\frac{E_f}{E_m}\right] + \xi_E\right]}$$

$$G_{12} = G_m \cdot \frac{\left[1 + \xi_\Gamma \cdot \eta_\Gamma \cdot V_f\right]}{\left[1 - \eta_\Gamma \cdot V_f\right]}$$

$$E_2 = E_m \cdot \frac{\left[1 + \xi_E \cdot \eta_E \cdot V_f\right]}{\left[1 - \eta_E \cdot V_f\right]}$$

Results of Calculations:

$$E_1 = 1.966 \cdot 10^5 \text{ MPa}$$

$$\nu_{12} = 0.266$$

$$E_2 = 1.732 \cdot 10^5 \text{ MPa}$$

$$G_{12} = 6.514 \cdot 10^4 \text{ MPa}$$

Let xi equal zero and determine E2:

$$E_2 = \frac{1}{\left[\frac{V_f}{E_f} + \frac{V_m}{E_m}\right]}$$

$$E_2 = 1.514 \cdot 10^5 \text{ MPa}$$

Let xi equal 2 and the fiber modulus equal zero:

$$E_2 = E_m \cdot \frac{\left[1 - V_f\right]}{\left[1 + .5 \cdot V_f\right]}$$

$$E_2 = 5.585 \cdot 10^4 \text{ MPa}$$

Calculate Euler Buckling

- Assumptions:
  1. Load in Fiber Direction
  2. Stress = Load/Area

Look at Geometry of the Specimen: 15.24 cm W x 1.27 cm T , 16 Ply Unidirectional

$$b = 12.7 \cdot 10^{-3} \cdot m$$

$$t = 114.3 \cdot 10^{-6} \cdot m$$

$$h = 16 \cdot t$$

$$A = b \cdot h$$

$$I = \frac{1}{12} \cdot b \cdot h^3$$

$$\sigma = \left[V_f \cdot \sigma_1 + V_m \cdot \sigma_2 \right] \cdot .82$$

$$P_{crit} = \sigma \cdot A$$

$$L = \left[\frac{\left[4 \cdot \pi^2 \cdot E_1 \cdot I \right]}{P_{crit}} \right]^{.5}$$

Length of Test Section:

$$L = 0.061 \cdot m$$

Vita

Keith Bearden was born 12 August 1965 in Aguadilla, P.R. He graduated from St. Xavier High School in Louisville, Ky. in 1983 and accepted an appointment to the United States Air Force Academy. He graduated from the Academy 1 June 1988 with a B.S. in Engineering Mechanics and was commissioned into the United States Air Force. From there, he went to Hanscom AFB as the Cheif Mechanical Engineer for a major imagery program. In June 1991, he entered the Air Force Institute of Technology as a student in the Graduate Aeronautical Engineering Program.

REPORT DOCUMENTATION PAGE

Form Approved
OMB No. 0704-0188

1. AGENCY USE ONLY (Leave blank)	2. REPORT DATE	3. REPORT TYPE AND DATES COVERED
	December 1992	Master's Thesis

4. TITLE AND SUBTITLE
Behavior of a Titanium Matrix Composite Under Quasi-Static Tensile and Compressive Loading

5. FUNDING NUMBERS

6. AUTHOR(S)
Keith L. Bearden, Capt, USAF

7. PERFORMING ORGANIZATION NAME(S) AND ADDRESS(ES)
Air Force Institute of Technology, WPAFB OH 45433-6583

8. PERFORMING ORGANIZATION REPORT NUMBER
AFIT/GAE/ENY/92D-07

9. SPONSORING / MONITORING AGENCY NAME(S) AND ADDRESS(ES)
James Hansen, LTC, USAF
WL/MLLN
Wright Laboratories
Wright Patterson AFB OH 45433

10. SPONSORING / MONITORING AGENCY REPORT NUMBER

11. SUPPLEMENTARY NOTES

12a. DISTRIBUTION / AVAILABILITY STATEMENT
Approved for public release; distribution unlimited

12b. DISTRIBUTION CODE

13. ABSTRACT *(Maximum 200 words)*

Quasi-Static tensile and compressive testing was performed on a unidirectional titanium matrix composite. The specific material was SCS-9/Beta 21S. The initial tensile and compressive modulus for both laminates was the same. The ninety degree laminate had a tensile and compressive modulus of 115.89 GPa. The zero degree laminate had a tensile and compressive modulus of 197.51 GPa. The ninety degree laminate exhibited a three stage stress/strain response in tension. The first stage is completely linearly elastic, however, partial debonding of the fiber from the matrix was observed. This partial debond did not effect the stress/strain response. The second stage is due to the complete debond of the fiber from the matrix. The ninety degree laminate in compression had a two stage stress/strain response, and the zero degree laminate had a two stage stress/strain response in tension and compression. Plasticity and damage were the main causes of deformation. Plasticity involved deformation of the matrix between the fibers and Poisson's contraction of the matrix from the fibers. Damage involved fiber matrix debond, matrix cracking and fiber cracking. All of these mechanisms were present, and they were related to the appropriate stress/strain characteristics.

14. SUBJECT TERMS	15. NUMBER OF PAGES
Titanium matrix composites, Compression, Tension, Damage, Plasticity	93
	16. PRICE CODE

17. SECURITY CLASSIFICATION OF REPORT	18. SECURITY CLASSIFICATION OF THIS PAGE	19. SECURITY CLASSIFICATION OF ABSTRACT	20. LIMITATION OF ABSTRACT
Unclassified	Unclassified	Unclassified	UL